5-2019

Analysis and Control of Socio-Cultural Opinion Evolution in Complex Social Systems

Farshad Salimi Naneh Karan
University of Tennessee, fsalimin@vols.utk.edu

To the Graduate Council:

I am submitting herewith a dissertation written by Farshad Salimi Naneh Karan entitled "Analysis and Control of Socio-Cultural Opinion Evolution in Complex Social Systems." I have examined the final electronic copy of this dissertation for form and content and recommend that it be accepted in partial fulfillment of the requirements for the degree of Doctor of Philosophy, with a major in Mechanical Engineering.

Subhadeep Chakraborty, Major Professor

We have read this dissertation and recommend its acceptance:

Michael Berry, Eric R. Wade, Xiaopeng Zhao

Accepted for the Council:

Dixie L. Thompson

Vice Provost and Dean of the Graduate School

(Original signatures are on file with official student records.)

Analysis and Control of Socio-Cultural Opinion Evolution in Complex Social Systems

A Dissertation Presented for the

Doctor of Philosophy

Degree

The University of Tennessee, Knoxville

Farshad Salimi Naneh Karan

May 2019

To my parents,

Behrouz and Zhila

and my sisters,

Elnaz and Sanaz

Acknowledgements

I would like to express my highest appreciation to Dr. Subhadeep Chakraborty for giving me the opportunity to work an learn under his supervision. Every single conversation with him has been a learning opportunity for me. His patience, trust, and encouragement have been crucial for me to have peace of mind during my program. I hope someday I can return the favor and add value to his life.

I would like thank my parents Behrouz and Zhila, my sisters Elnaz and Sanaz, and their husbands Bahram and Behzad for bearing the hardship of being contiuously separated from each other for the past five years. Without their love and support, my long and overwhelming path of PhD studies would have never been possible. I hope my accomplishments at the UTK make them proud and put a smile on their faces during my absense in Iran.

Furthermore, I would like to thank all my colleagues Aravinda Ramakrishnan Srinivasan, David M. Harris, Navneeth Kikkery, Christopher J. LaBord, and Russell Graves for providing a very warm and welcoming atmosphere for me in the office. They have helped me tremendously to get integrated into the American culture by answering numerous cultural questions of mine. I have learned so much from each of these individuals in different ways, and I am thankful for that. Additionally, I would like to thank all the friends (residing in Iran or the USA) who have always been there for me. We have lived through this together, supported each other in hardships, and celebrated accomplishments. Their friendships reside in my heart, and I feel blessed to have met them in my journey. Also, I would like to thank all my teachers during the last 27 years. I shall never forget Dr. Arthur Hatton's help.

Last but not least, I would like to thank my committee members, Dr. Eric R. Wade, Dr. Xiaopeng Zhao, and Dr. Michael W. Berry for their informative suggestions and guidance throughout my PhD program.

"I appreciate the teacher who taught me how to think,

instead of teaching me other people's thoughts!"

- Dr. Ali Shariati

Abstract

The overarching goal of this thesis is to further our understanding about opinion evolution in networked societies. Such insights can be used in a variety of fields such as economy, marketing, transportation, egress, etc. Three main subjects build up this interdisciplinary research: Sociology, Statistical Mechanics, and Network Sciences. In this thesis, for macro-level (or society-level) analyses, techniques from statistical mechanics have been borrowed to mathematically model the opinion dynamic on different network topologies based on different interaction models. Also, for micro-level (individual-level) analyses, Individual Decision Making Algorithms (IDMA) have been designed. To account for both macro-level and micro-level dynamics, these two regimes are combined resulting in a more accurate model for opinion propagation. Assessing the controllability of such dynamics through experiments in presence of actual humans is the part of this thesis.

Table of Contents

List of Tables

List of Figures

Chapter 1

Introduction and Literature Review

1.1 Introduction

Humans have always interacted with each other, either in small social groups such as a circle of close friends or larger social settings such as social media websites. Thus, they have likely always been attuned to the preferences and positions of others. At the same time, we have evolved sophisticated sensory systems and brains capable of reaching independent conclusions about the world. Therefore, in our efforts to function effectively, we have likely had to balance our own experiences, ideas, and beliefs with those of close and powerful others with whom we interact.

Through interactions, a specific idea, an opinion or a thought can initiate, develop, and in some cases, spread to the whole society. The study of such evolution trends traditionally falls into the field of social psychology, however, in recent years, borrowing techniques from the realm of statistical physics [1], mathematical sociologists [2] started investigating the emergence of consensus and divergence in networked nodes by constructing simplistic interaction models [3, 4]; however, the assumption in these simplistic interaction models is often, that every individual reacts the same way in response to different situations. These statistical methods are in the form of Differential Equations representing the time evolution of the probability of the system being at any point in the opinion space Fig. 1.1.

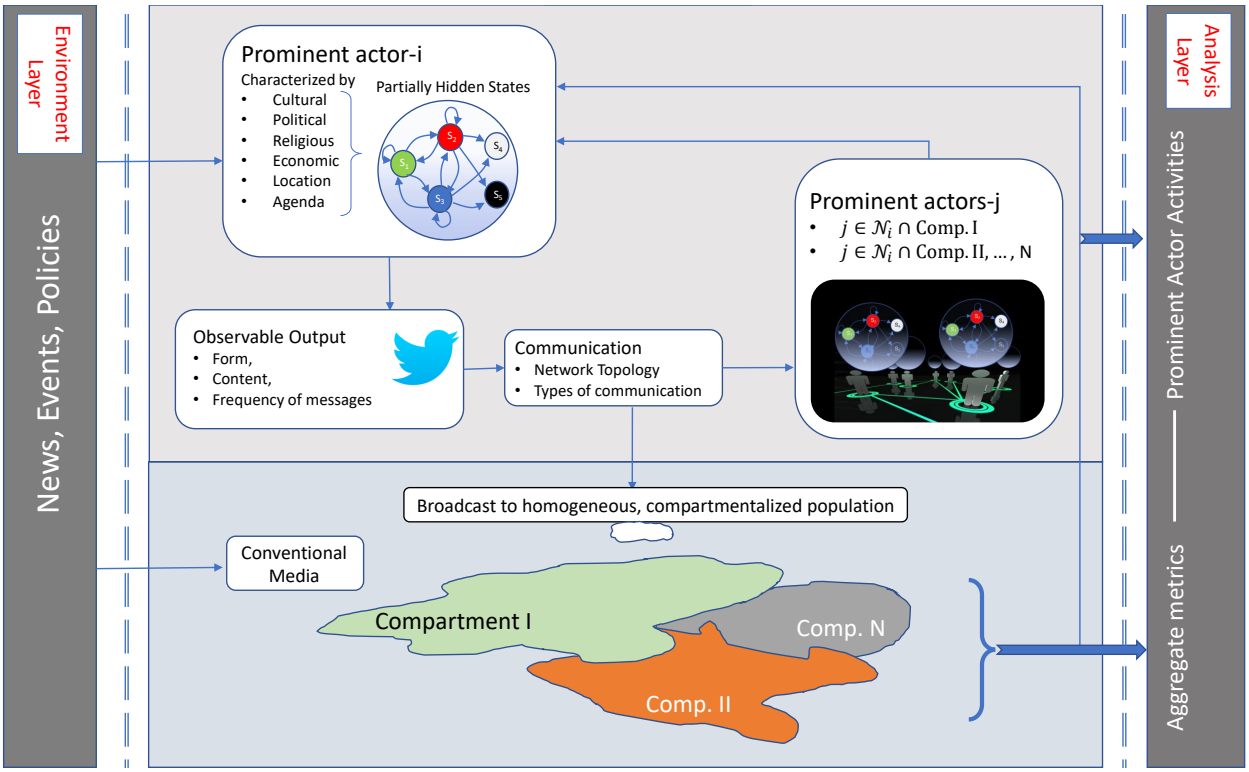

Figure 1.1: Graphical representation of people's social interactions, information resources, and decision making processes

1.1.1 Differential Equation Models (DE-Models)

Such differential equations are derived by using aggregate parameters of the society (e.g. the total number of people supporting a specific ideology in the society). As a result, the solutions of these differential equations explain the aggregate behavior of the society. But, they fail to include and explain individual level parameters and behaviors in the dynamics of opinion evolution. DE-Models have roots in the statistical analyses of order-disorder transitions in the paradigm of the Ising model.

Ising model is a mathematical model in statistical mechanics which studies ferromagnetism in alloys [5]. This model has discrete variables that represent magnetic spins. The spins can be in one of the two states ($+1$ or -1). Each spin can also get aligned with the neighboring spins. Ising model studies the transition from an initial disordered state (of spins) to an ordered state (where the spins are aligned) as an outcome of the interactions between spins. As a result of the available similarities between equations related to the Ising model and those of social interactions, statistical physics tools have been often used

to study social interactions [6, 7]. A statistical physics approach investigates the ways local interactions between agents can lead to order starting from a disordered initial condition [8, 9]. Direct outcomes of this approach are several elegant theories of emergent social behaviors, such as evolution of opinions, consensus formation, properties of elections, and formation of a common language.

The Ising model, based on a macroscopic approach, uses a master equation for global variables to study the main characteristics of ordering processes in such complex networks. The Master Equation is a set of first-order differential equations describing how the probability of finding the system in a specific state (m) at time t changes with time:

$$\frac{dP(m,t)}{dt} = \sum_{m' \neq m} T(m|m')P(m',t) - \sum_{m \neq m'} T(m'|m)P(m,t) \tag{1.1}$$

where, the quantity $T(m|m')$ is the transition rate from state m' to state m, and is only defined for $m \neq m'$.

1.1.2 Agent Bast Models (AB-Models)

Although DE-Models are capable of predicting the opinion dynamic in the society, they ignore individual level parameters. People affect each others' mental states through interactions, but this does not mean every person changes opinions as a result of his/her interactions. Individual's perceptions, past experiences, and background (cultural, political, religious, etc.) are some of the important factors in this process. Individual decision making abilities help the person to analyze all the information acquired (from conventional media, social media, different events, etc.), and then conclude whether or not s/he should change her/his opinion.

Decisions can be described in terms of three essential components: alternatives, anticipated consequences, and uncertainty. Despite vast diversity in the field of judgment and decision-making, its boundaries and major theoretical concerns are mostly related to the historically dominant expected utility family of theories made popular by Von Neumann & Morgenstern [10] and Savage [11, 12]. The heart of the theory, sometimes called the rational expectations principle or expectancy-value model [13], proposes that each alternative course

of action or choice option should be evaluated by weighting its global expected satisfaction-dissatisfaction with the probabilities that the component consequences will occur and be experienced. For example, in the Logit model, the relative frequency of usage of a strategy is proportional to the number of times it was successful. In mathematical terms, this law of relative effect [14] reads $p(i) = N(i)/(\Sigma_{i'} N(i')) = \frac{e^{U(i)/T}}{\Sigma_{i'} e^{U(i')/T}}$, where for any parameter T (sometimes called the 'social temperature'), $U(i) = T \ln N(i)$ is the utility function, somewhat arbitrarily defining a preference scale.

However, although expectancy-value theory has been very successful in explaining central concepts in uses and gratifications research, other factors have been recognized that influence the process. For example the social and psychological origins of needs, which give rise to motives for behavior, may be guided by beliefs, values, and social circumstances into seeking various gratifications through media consumption (Fig. 1.1) and other non-media behaviors. In a network setting, such as Twitter, one's estimate of rewards are not absolute quantities, but are influenced by opinions of friends and neighbors. Social scientists, for many years have developed theories of group position [15], social identity [16], and system justification [17]. Now, such theories can be validated quantitatively by analyses of "retweets", "via", "hat tip" and "mention" conventions which have been shown to be analogous to broadcasting one's position, and helps explain how virality, meme propagation, and opinion formation occur on social networks [18].

In reality, not everyone responds the same way in different situations. To demonstrate this non-deterministic behavior, different models for individual decision making have been proposed [19, 20, 21]. In different studies, Agent-Based Modeling (ABM) techniques are used to simulate individual decision making. In ABM, the idea is to construct computational entities (known as agents) with some properties. These agents function in parallel to simulate real phenomena. Agent based modeling has been applied in various fields such as molecular dynamics [22, 23], cellular automata [24], and population biology [25]. In social dynamics, the goal is to address the problem of emergence from the lower levels of the social system to the higher levels of such social systems. In this thesis, agents will be given decision making abilities.

1.1.3 Influence

Although interactions among society members might lead them to change their opinions, there are individuals in the society who never change their ideas. However, they are able to affect other people's perceptions through interactions. To explain such behavior, the concept of non-conformity was introduced to the field of opinion evolution; in essence, these agents do not conform with the opinions of other agents. These non-conformists are also called "influences" or "zealots" in the literature. Presence of influences has proven to be effective in dramatically changing the dynamic of opinion evolution. In some studies, influences are used (as control inputs) to control the dynamic of opinion evolution [26, 8, 27].

With the rapid improvement in the accessibility of computing resources, social scientists have been able to practice their models on larger scales to represent a more realistic behavior of the entire society [22]. Such simulations can also be used as a means of assessing the accuracy of assumptions and analytical analyses of quantitative sociology. In social dynamics, Monte Carlo (MC) simulation techniques are used because of the random nature of social interactions.

The main contributions of this thesis are:

1) Systematically studying the idea of exposing a society to influences (or inflexible agents) who never change opinions but do alter the dynamics of the system. The main research hypothesis of this part is that group level diffusion of opinions and ideology can be modeled and analyzed using discrete choice models for individuals interacting via "gossip", and this opinion diffusion process can be controlled or at least contained using strategically placed "influences". It was shown that by using such moderating agents the system can be forced to approach desired global behavior [8]. Nevertheless, so far, the placement of these control inputs has been random. We believe that a more methodical approach is very much needed to deal with this problem.

2) Addressing the gap between methods from quantitative sociology (DE-Models) and methods related to individual decision making (AB-Models) to develop a platform which is able to take advantage of both methods in predicting opinion evolution in a society.

In the remainder of this chapter, first, a brief literature review on different aspects of social dynamics is provided. Then the observed scientific gaps in the preceding studies are listed. At the end, the objectives of this thesis addressing the scientific gaps are described.

1.2 Literature Review

1.2.1 Interaction Models

In the study of large scale order as a result of local interactions, the Voter model [28, 29], the Sznajd-Weron model [30, 31], and the Bounded Confidence model [32, 33] have received considerable attention. These interaction models, their similarities and differences, and their related literature are provided below.

The Voter Model

Denoting the opinion of a node by s, in the Voter dynamics, a node i and one of its neighbors j are randomly selected, and s_i is set equal to s_j (or, $\uparrow\Downarrow\longrightarrow\uparrow\Uparrow$). It has been proven that the Voter model tends to increase the order of the system [34]. Slanina et.al. [27] show that on a complete graph, the mathematical model has the form of a Fokker-Planck equation and can be solved analytically. Watts and Strogatz [35] considered the Voter model on a small-world, and they found out that the initial dynamic is similar to a one-dimensional lattice. Voter dynamic includes only two agents and ignores the concept of social validation. Sznajd model, addresses this shortcoming by including three or four agents.

The Sznajd Model

Although the Sznajd-Weron model is similar to the Ising or Voter models in spirit, it describes a decision making mechanism in a closed community based on social validation. Sznajd model suggests that at each time step, a pair of neighbors in the same state, convinces their neighbor to join them ($\uparrow\uparrow\Downarrow\longrightarrow\uparrow\uparrow\Uparrow$) [36]. In the Sznaid model, two types of steady states are always reached, either complete consensus (ferromagnetic) or stalemate (anti-ferromagnetic).

The Sznajd model has been studied on different networks. One such work by Elgazzar [37] studies the Sznajd model on a small world network and observes that the stalemate situation disappears by including short-cutting neighbors. This work also considers the effects of including leaders (influences) in the behavior of the society. Further research by Schulze [38] investigates the effects of long-range interactions on opinion spread and phase transition through the Sznajd model. Slanina et.al. have proposed the analytical results for the Sznajd model [27] on a complete graph. They have witnessed sharp phase transitions in their simulations.

It is important to note that Voter model and Sznajd model are defined over a discrete opinion space; i.e. $+1$ vs -1 (or up spins vs down spins). These models fail to model opinions in between the two extremes. This shortcoming in interaction models was addressed by introducing a continuous opinion space. Bounded Confidence interaction model is based on a continuous opinion space.

The Bounded Confidence Model

In bounded confidence, connectivity is not the only condition for interaction. For two connected agents with opinions $x(t)$ and $x'(t)$, the difference between the opinions has to be less than a specific threshold ($|x(t) - x'(t)| < d$) to interact. After the interaction is complete, agents get closer to each other in the opinion space by a fraction, μ (convergence parameter) [32]. Bounded confidence can be best described by mathematical representation: if $|x(t) - x'(t)| < d$, then:

$$x(t+1) = x + \mu.(x'(t) - x(t)) \tag{1.2}$$

$$x'(t+1) = x' + \mu.(x(t) - x'(t)) \tag{1.3}$$

Fortunato et al. have shown that on complete graph, regular lattices, and scale-free networks for $d > \frac{1}{2}$ complete consensus happens (all the agents have the same opinions) [39]. Ben-Naim et al. have mathematically modelled and solved the bounded confidence on a complete graph [40]. Leguna et al. and Porfiri et al. have done extensive numerical simulations on bounded confidence and have proven that the number of clusters in the society in the steady state depends on the threshold d. They also show that the time to

reach stationary state (the convergence time) depends on the convergence parameter, μ [41, 42].

1.2.2 Individual Decision Making Algorithms

Individual Decision Making Algorithms (IDMAs) have been designed with different levels of accuracy and complexity. It has been concluded that in order to investigate the global behavior of a society, simpler IDMAs are more suitable and computationally cost-efficient [43]. However, to study the behavior of an individual or a small group, higher levels of complexity are needed to demonstrate and explain decision making patterns. According to Gilbert [44], this complexity of agents might range from "production system architectures" (i.e. agents that follow simple IF-THEN rules) to agents with sophisticated "cognitive architectures" which take into account emotions and feelings of the agent too. In the previous section, the theory of expected utility and related studies were explained.

1.2.3 Influence

In the past few years, the effect of "influences", "sharply opinionated agents", "zealots" or "committed agents" has been the main subject of numerous studies in agent-based modeling on almost all kinds of networks [45, 46]. The idea is exposing the society to the agents whose ideas never change [47]. Galam [48] and Mobilia [49] studied the role of "influences" on the breaking of democratic opinion dynamics. Xie [50, 51] investigated the consensus in the presence of competing committed groups. Also, Yildiz [52] explains binary opinion dynamics with stubborn agents.

1.2.4 Networks

Among elements of social dynamics, topology (the structure determining which agents can interact, with which frequency and intensity) carries a lot of importance [53, 54]. In a network, agents are placed on nodes (vertices), and the links between nodes represent a possibility to interact. A few of the important network structures are briefly explained in the following.

Random Graph

The Erdős Rényi random graph $G(N, p)$ is defined as N labeled nodes connected by n edges which are chosen randomly from $(N(N-1))/2$ possible edges [55]; i.e. every pair of nodes is connected with probability $p = \frac{n}{[(N(N-1))/2]}$. Since there are $C^n_{[(N(N-1))/2]}$ ways to construct such a graph, a probability space is formed in which every realization of the random graph owns an equal probability of happening. The probability of constructing a specific realization of a random graph such as G_0 with the specifications mentioned above is $P(G_0) = p^n(1-p)^{[N(N-1))/2]-n}$.

These graphs are static graphs; i.e. the number of vertices in the network is constant. Isolation of vertices could happen, Fig. 1.2. Most importantly, different graphs with the same set of nods (**N**) and edges (**E**) are possible to be formed. In the limit $p \longrightarrow 1$, ER graph becomes the Complete Graph where all nodes are connected to each other.

Small World

Small World is a well-known network structure in which the average distance between two agents is small [56]. Also, unlike the ER graph, many triangles are available, Fig. 1.3. In [35], authors characterize a SW network by two parameters: the characteristic path length $L(p)$, defined as the number of edges in the shortest path between two vertices, averaged over

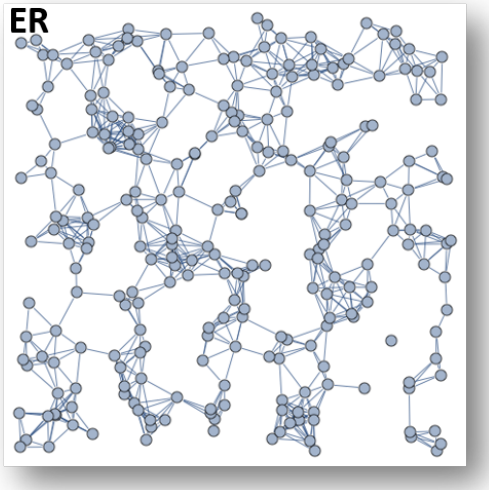

Figure 1.2: The Erdős Rényi random graph

all pairs of vertices, and the clustering coefficient $C(p)$, defined as follows. If a node i has k connections, then at most $\frac{k(k-1)}{2}$ edges can exist between its neighbors (this occurs when every neighbor of i is connected to every other neighbor. The clustering coefficient $C(p)$ denotes the fraction of these allowable edges that actually exist, averaged over all nodes. Small-world networks feature high values of $C(p)$ and low values of $L(p)$.

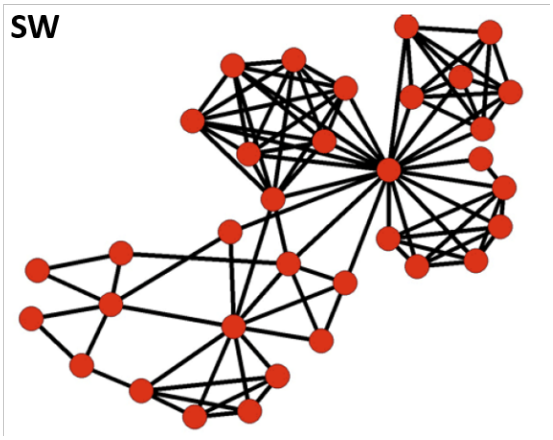

Figure 1.3: The Small World (SW) network topology

Barabási-Albert

In reality, most networks are not static but evolving with new agents entering the network and making connections with the already existing ones. The Barbasi-Albert (BA) model [57, 58] is one of the most famous models for growing networks, and it is constructed as follows: starting from a small set of m fully interconnected nodes, new nodes are introduced one by one. Each new node selects m older nodes according to the preferential attachment rule, i.e., with probability proportional to their degree, and creates links with them. The procedure stops when the required network size N is reached, Fig. 1.4.

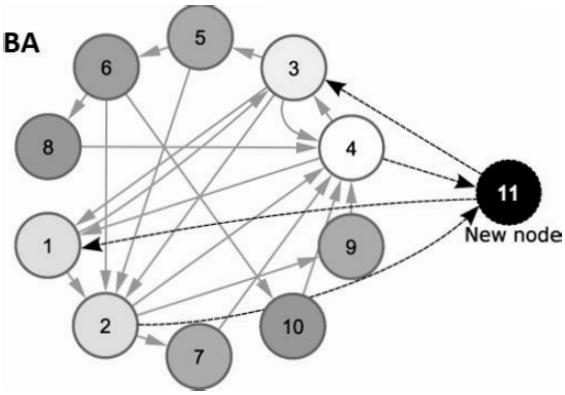

Figure 1.4: The Barabási-Albert network topology

1.3 Scientific Gaps and Objectives

1.3.1 Scientific Gaps

Gap 1. Some of the interaction models have not been mathematically modelled on all of the available network topologies. In addition, in some of the already studied interaction models, the effect of influences has not been accounted for. Developing mathematical models for opinion evolution based on different combinations of interaction models and network topologies in presence of influences can provide answers on progression of opinion, convergence time, and final distribution of opinions in the society. Also, these mathematical models can be used in studying the controllability of such dynamics.

Gap 2. As mentioned in previous sections, quantitative sociology studies social dynamics

only on societal levels without taking into account any individual decision making. On the other hand, studies on decision making mostly consider the individual without taking into account effects of the society. Augmenting these two techniques could provide information on their mutual effects on each other. Such augmented systems can also predict the opinion evolution more accurately. Again, manipulation of perception by incorporating influences can potentially lead to the control of opinion evolution.

Gap 3. Current state of the art involves control of opinion propagation by randomly introducing influences to a community. However, the authors believe the placement of these influences in the network, their strength, their density, and their activation time are important factors in maximizing their influence. Understanding the role each of these parameters play in the dynamics of opinion evolution could potentially lead to an optimal, cost-effective, and time-effective control strategy.

1.3.2 Research Objectives

The following objectives attempt to address the scientific gaps mentioned above:

Objective 1 (*addressing Gap 1*). **Mathematical modeling of opinion evolution (DE-Models).** In this section of the thesis, mathematical modeling of various combinations of interaction models and network topologies will be performed in the framework of the Master Equation (ME). ME is a stochastic differential equation describing how the population is distributed over the opinion space and how such distribution changes with time. All the analyses will be performed accounting for the presence of influences (control inputs) in the society. Analytical solutions are expected to cast light on different aspects of the system such as convergence time, equilibrium state opinion distribution, progression of the opinion dynamics, controllability of the system, etc.

Objective 2 (*addressing Gap 1*). **Numerical simulations of the systems from *Objective 1*.** This part will be devoted to extensive Monte Carlo simulations of the systems indicated in Objective 1. These simulations will be used to validate the precision of modeling procedures and accuracy of analytical solutions. Also, these simulations will serve as a guide

towards appropriate time scaling procedures of the systems. Effects of control inputs on the final state of the society can be investigated with such simulations.

Objective 3 (*addressing Gap 2*). **Decision making (AB-Models).** So far, only the objectives related to the study of the aggregate behavior (macro-level parameters) of the society have been mentioned. This section of the thesis will concentrate on the decision making processes of individuals (designed in the framework of a Probabilistic Finite State Automata (PFSA)). The decision making algorithm will be able to model the behavior of agents when they are exposed to external events, and also when they interact with other people. This part of the study combines micro-level and macro-level parameters of opinion evolution. Such combination can be instrumental in understanding the mutual effects that the society and the individual have on each other; or, how influences can alter an individual's decisions and cognitive states.

Objective 4 (*addressing Gap 3*). **Assessing controllability of collective human behaviors in presence of actual humans.** This part of the thesis will be devoted to studying the controllability of collective behavior of people in an experimental setup in presence of actual humans. Different influence scenarios will be developed with the purpose of maximizing the influence of control inputs.

Chapter 2

Modeling and Numerical Simulations of the Influenced Sznajd Model

2.1 Objective

Various studies in the field of opinion evolution consider mathematical modeling of interaction models on different network topologies; [59] is one of the studies in which the Voter interaction model is mathematically modelled on a complete graph to investigate the effect of biased nodes on the conrollability of the dynamic. Fig. 2.1 shows the composition of the society including the influence groups.

At first, [59] derives the Master equation on a complete graph which can be characterized by defining the magnetization parameter $m = \frac{N_+ - N_-}{N}$, where at a certain instant, there are N_+ nodes in state $+1$, N_- nodes in state -1. $N = N_+ + N_-$ nodes make up the vertices of the graph. At each time step, a node i and one of its neighbors j is randomly selected, and s_i is set equal to s_j. In addition to the N sites, there are $I = I_+ + I_-$ external agents with respective pre-conceived allegiance to states $+1$ and -1.

Defining the control variable $u = \frac{I_+ - I_-}{I}$, the master equation is composed as [59]:

$$\dot{P}_m = r_{m+\frac{2}{N}} P_{m+\frac{2}{N}} + g_{m-\frac{2}{N}} P_{m-\frac{2}{N}} - (r_m + g_m) P_m \tag{2.1}$$

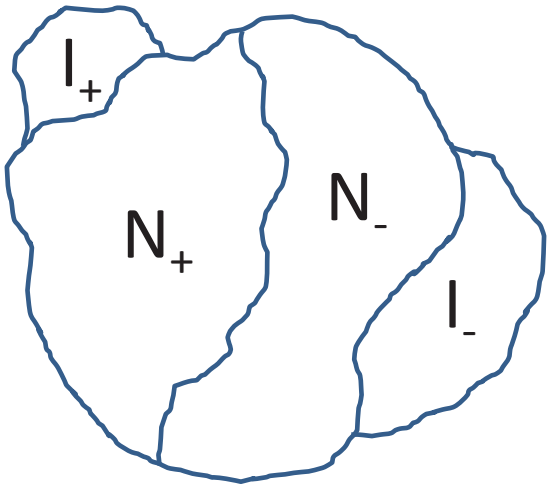

Figure 2.1: Population composition and external influence groups [59]

where,

$$
\begin{aligned}
r_m &= P(m \to m - \frac{2}{N}) = \left(\frac{N_+}{N}\right)\left(\frac{N_- + I_-}{N + I - 1}\right) \\
g_m &= P(m \to m + \frac{2}{N}) = \left(\frac{N_-}{N}\right)\left(\frac{N_+ + I_+}{N + I - 1}\right) \\
r_{m+\frac{2}{N}} &= \left(\frac{N_+ + 1}{N}\right)\left(\frac{N_- - 1 + I_-}{N + I - 1}\right) \\
g_{m-\frac{2}{N}} &= \left(\frac{N_- + 1}{N}\right)\left(\frac{N_+ - 1 + I_+}{N + I - 1}\right)
\end{aligned}
\tag{2.2}
$$

Using Eqn. 2.2 in Eqn. 2.1,

$$
\begin{aligned}
\dot{P}_m = &\left(\frac{N_+ + 1}{N}\right)\left(\frac{N_- - 1 + I_-}{N + I - 1}\right) P_{m+\frac{2}{N}} \\
&+ \left(\frac{N_- + 1}{N}\right)\left(\frac{N_+ - 1 + I_+}{N + I - 1}\right) P_{m-\frac{2}{N}} \\
&- \left[\left(\frac{N_+}{N}\right)\left(\frac{N_- + I_-}{N + I - 1}\right)\right. \\
&\qquad \left. + \left(\frac{N_-}{N}\right)\left(\frac{N_+ + I_+}{N + I - 1}\right)\right] P_m
\end{aligned}
\tag{2.3}
$$

In the limit $N \to \infty$, assuming that $I \ll N$, $I_- P_{m+2/N} + I_+ P_{m-2/N} \approx I P_m$, with proper scaling of time as $\tau = t/N^2$ and noting that $N_+ I_- - N_- I_+ = \frac{NI}{2}(m - u)$, the master equation

is simplified to its final form as,

$$\frac{\partial P_m}{\partial \tau} = \frac{1}{2}\frac{\partial^2}{\partial m^2}\left[B(m)P_m\right] - \frac{\partial}{\partial m}\left[A(m)P_m\right] \tag{2.4}$$

$$\text{where,} \quad B(m) = 2\left(1 - m^2\right) \tag{2.5}$$

$$A(m) = I\left(u - m\right) \tag{2.6}$$

Then, the authors continue to solve the derived differential equation, and assess the controllability of the dynamics. [59] is a thorough example of using the master equation to model opinion evolution on a network (DE-Models).

The Voter model is considered one of the simplest interaction mechanisms, and since only two agents are present in the interaction mechanism, the social validation concept is ignored in the Voter model. Sznajd model is an interaction mechanism which brings in the social validation concept. Sznajd model in presence of influences is the focus of the this chapter. First, a review of the most recent studies on the Sznajd model is provided. In section 2.3, the Sznajd model is mathematically modelled on a complete graph in presence of influences. In section 2.4, the modelled system is analyzed and interesting behaviors of the system are presented and discussed. In section 2.5, a summary of all the findings of this chapter is presented and the chapter is concluded.

2.2 Recent Studies on the Sznajd Model

In recent years, nonconformity has been a focal point for a large number of studies on the Sznajd model. In these studies, two types of nonconformity are usually considered: anti-conformity and independence. In a study by Nyczka et al., the authors investigate the effect of two types of social responses: conformity and anti-conformity in the dynamics of the Sznajd model on a complete graph [60]. In this dynamic, conformists choose the opinion of the group with probability p_1 (i.e. $\uparrow\uparrow\Downarrow \longrightarrow \uparrow\uparrow\Uparrow$ with probability p_1, no change with probability $1 - p_1$), and anticonformists choose the opposite opinion of the group with probability p_2

(i.e. $\uparrow\uparrow\Uparrow \longrightarrow \uparrow\uparrow\Downarrow$ with probability p_2, no change with probability $1 - p_2$). In another study by the same group, authors expand this idea to investigate the qualitative and quantitative differences of the two types of nonconformity under the framework of the q-voter model [61] on a complete graph. In this dynamic, anticonformists choose the opposite opinion of the group, and the independent agents do not follow the group; they act independently and choose the opposite opinion of the group with probability $\frac{1}{2}$.

Jędrzejewski [62], expanded these studies with the Pair Approximation methodology to study the behavior of a q-voter model with stochastic noise characterized as Independence on several complex networks. In this model, with probability p, a chosen agent acts independently and adopts the opposite opinion or preserves the old one with equal chances. Otherwise, with probability $1 - p$, the agent will be a conformist.

A special class of independent agents are "zealots" (sometimes called "inflexibles" or "influences"). These are agents who do not change their state throughout the progression of the dynamics. Mobilia uses Mean-Field approximation method to analytically model the nonlinear q-voter model in presence of zealots [63]. In this work, for simplicity, repetition in choosing agents is allowed. The derived transition probabilities are used for bifurcation analysis and finding critical zealotry density. Analyses presented in this work relate to special cases of symmetric and parameterized asymmetric zealotry distributions.

In this chapter, we model and investigate the effects of influences and initial conditions on the dynamics of the Sznajd model. The problem setup is closely linked to [63], but in contrast to Mobilia's work, it does not allow repetitive agent choices. Disallowing repetitive agent choices is not only more realistic, but surprisingly, leads to a new master equation which can be solved under specific conditions. Also, we do not observe rapid phase transitions in this dynamic. Here, influences are nonconformists of the Independent type, who never change their opinions (as opposed to [62]) but affect other agents' decisions. It is worth mentioning that influences of this study are different from what have been used in [60, 61]. In [60, 61], the nonconformists are **Anticonformists**, however in our study, we have chosen **Independents** as nonconformists.

2.3 Influenced Sznajd Model

In this study, a complete graph is considered. A complete graph can be characterized by a "magnetization parameter" defined as $m = \frac{N_+ - N_-}{N}$, where, N_+ represents the number of agents in state $+1$, and N_- represents the number of agents in state -1 at any instant. $N = N_+ + N_-$ nodes make up the vertices of the graph [64]. The system also includes $I = I_+ + I_-$ influences, in which I_+ represents the number of influences in state $+1$, and I_- represents the number of influences in state -1.

In the original Sznajd Model [65], the idea of *social validation* is used to introduce a spin dynamic with ± 1 alignments:

- In each time step a pair of spins S_i and S_{i+1} is chosen to change spins of their nearest neighbors, namely S_{i-1} and S_{i+2}.
- If $S_i = S_{i+1}$ then $S_{i-1} = S_i$ and $S_{i+2} = S_i$ (*social validation*).
- If $S_i = -S_{i+1}$ then $S_{i-1} = S_{i+1}$ and $S_{i+2} = S_i$.

In this chapter, a simplified Sznajd model dynamics, modified for a complete graph, rather than a one-dimensional lattice, introduced in [27], is used which inherits the *social validation* concept, but has slightly different update rules:

- In each time step a pair of nodes (i and j), respectively in states S_i and S_j are chosen at random and attempt to change the state S_k of a randomly chosen common nearest neighbor, $k \in \mathcal{N}_i \cap \mathcal{N}_j$, where $\mathcal{N}_i$ is the set of neighbor nodes of node i.
- If $S_i = S_j$ then $S_k = S_i$ (*social validation*).
- If $S_i = -S_j$ then nothing happens.

Due to the stochastic process of spin flips, Master Equation (ME) is used to formulate this model. ME represents the time evolution of the probability of a system having any configuration of ± 1 spins defined by m. Eqn. 2.7 represents the general form of the ME which includes in/out-flow rates calculated as probabilities [64].

$$\dot{P}_m = r_{m+\frac{2}{N}} P_{m+\frac{2}{N}} + g_{m-\frac{2}{N}} P_{m-\frac{2}{N}} - (r_m + g_m) P_m \tag{2.7}$$

where, in/out-flow rates are derived based on the Sznajd model as:

$$\begin{aligned}
r_m &= P(m \to m - \frac{2}{N}) = \left(\frac{N_- + I_-}{N+I}\right)\left(\frac{N_- + I_- - 1}{N+I-1}\right)\left(\frac{N_+}{N+I-2}\right) \\
g_m &= P(m \to m + \frac{2}{N}) = \left(\frac{N_+ + I_+}{N+I}\right)\left(\frac{N_+ + I_+ - 1}{N+I-1}\right)\left(\frac{N_-}{N+I-2}\right) \\
r_{m+\frac{2}{N}} &= P(m + \frac{2}{N} \to m) = \left(\frac{N_- + I_- - 1}{N+I}\right)\left(\frac{N_- + I_- - 2}{N+I-1}\right)\left(\frac{N_+ + 1}{N+I-2}\right) \\
g_{m-\frac{2}{N}} &= P(m - \frac{2}{N} \to m) = \left(\frac{N_+ + I_+ - 1}{N+I}\right)\left(\frac{N_+ + I_+ - 2}{N+I-1}\right)\left(\frac{N_- + 1}{N+I-2}\right)
\end{aligned} \tag{2.8}$$

By substituting Eqn. 2.8 in Eqn. 2.7, after some manipulations, and by defining the control variable as $u = \frac{I_+ - I_-}{I}$, for large but finite population sizes N, the master equation can be expressed as:

$$\begin{aligned}
\dot{P}_m = \frac{1}{N^4}\Bigg[&\left(Nm^2 - N + \frac{N^2}{2} - \frac{N^2m^2}{2} + \frac{I^2}{2} + \frac{I^2u^2}{2} + IN - I^2mu - Im^2N\right)\frac{\partial^2 P_m}{\partial m^2} \\
&+ \Bigg(10mN + INu - INm - \frac{N^3m}{2} - I^2uN - N^2Iu - 2N^2m + \frac{N^3m^3}{2} \\
&+ \frac{I^2mN}{2} + \frac{I^2u^2mN}{2} + N^2Ium^2 - 4ImN - 2I^2u + 4Iu\Bigg)\frac{\partial P_m}{\partial m} \\
&+ \left(4N - 3IN - N^2 - \frac{N^3}{2} + \frac{3N^3m^2}{2} + 2N^2Imu + \frac{I^2N}{2} + \frac{I^2u^2N}{2}\right)P_m\Bigg]
\end{aligned} \tag{2.9}$$

Assuming that a steady state density function exists, $\lim_{t\to\infty} \frac{dP_m}{dt} = 0$ [66], the steady state density $P_{ss}(m)$ has to satisfy:

$$\left(Nm^2 - N + \frac{N^2}{2} - \frac{N^2m^2}{2} + \frac{I^2}{2} + \frac{I^2u^2}{2} + IN - I^2mu - Im^2N\right)\frac{d^2P_{ss}(m)}{dm^2} + \left(10mN + INu - INm - \frac{N^3m}{2} - I^2uN - N^2Iu - 2N^2m + \frac{N^3m^3}{2} + \frac{I^2mN}{2} + \frac{I^2u^2mN}{2} + N^2Ium^2 - 4ImN - 2I^2u + 4Iu\right)\frac{dP_{ss}(m)}{dm} + \left(4N - 3IN - N^2 - \frac{N^3}{2} + \frac{3N^3m^2}{2} + 2N^2Imu + \frac{I^2N}{2} + \frac{I^2u^2N}{2}\right)P_{ss}(m) = 0 \tag{2.10}$$

which is a homogeneous second order linear differential equation. The terms can be rearranged to a more compact form:

$$\frac{d}{dm}\left[\left(\Sigma_{i=0}^{3}a_im^i\right)P_{ss}(m) + \left(\Sigma_{i=0}^{2}b_im^i\right)\frac{dP_{ss}(m)}{dm}\right] = -4mN\frac{dP_{ss}(m)}{dm} \tag{2.11}$$

Integrating the same equation and using the identity $\int_{-1}^{1}P_{ss}(m)dm = 1$, the general form of a first order ODE is obtained:

$$B(m)\frac{dP_{ss}(m)}{dm} + A(m)P_{ss}(m) = 4N \tag{2.12}$$

The coefficients of this equation are presented in Table 2.1.

Table 2.1: Coefficients of Eqns. 2.11 and 2.12

Coefficient	Quantity
a_0	$4Iu - I^2u - N^2Iu - NI^2u + NIu$
a_1	$8N - 3NI - N^2 - \frac{N^3}{2} + \frac{NI^2}{2} + \frac{NI^2u^2}{2}$
a_2	N^2Iu
a_3	$\frac{N^3}{2}$
b_0	$-N + \frac{N^2}{2} + \frac{I^2}{2} + \frac{I^2u^2}{2} + IN$
b_1	$-I^2u$
b_2	$N - NI - \frac{N^2}{2}$
A	$a_3m^3 + a_2m^2 + a_1m + a_0$
B	$b_2m^2 + b_1m + b_0$

The analytical solution of such equations has the general form of:

$$P_{ss}(m) = \frac{1}{v(m)} \left(\int v(m) \frac{4N}{B(m)} dm \right) + C, \tag{2.13}$$

where $v(m) = e^{\int \frac{A(m)}{B(m)} dm}$. $P_{ss}(m)$ after normalization, provides the steady state distribution of the population starting from an initial distribution m_0. In the simplified setting of $I = 0$ and $N \to \infty$, the population almost surely converges to either all $+1$ or all -1 states, the two attractors for that dynamics, i.e. $P_{ss}(m) = \delta(m \pm 1)$ where δ is the Dirac delta function. Which direction the population converges to depends on the initial starting condition, i.e. whether m_0 is greater or less than 0. However, for all these cases, it is observed that $P_{ss}(m = 0) = 0$, i.e. at steady state the probability of the population being equally divided between $+1$ and -1 states is almost surely 0, which stems from $m = 0$ being an unstable equilibrium and the stochastic nature of the process.

Keeping these in mind, the ODE is solved separately over two ranges, P_{ss_l} solved over $-1 \leq m \leq 0$ and P_{ss_h} solved over $0 \leq m \leq 1$ with $P_{ss}(m = 0) = 0$, as the boundary condition for both. It will be shown later that the entire span $[-1, 1]$ of possible starting values for m_0 can be divided into two distinct regions,

- a *convergence zone (Z_C), starting from which the population consistently converges toward a particular attractive state - consequently, the steady state PDF matches either P_{ss_l} or P_{ss_h}, and*
- *an indeterminate zone (Z_I), starting from which the population can, by chance converge toward any of the two attracting states, thus $P_{ss}(m)$ has a bimodal distribution which is a combination of P_{ss_l} and P_{ss_h}.*

It may be noted, that for the simple case of $I = 0$ and $N \to \infty$, Z_I is a singleton set, with $Z_I = \{0\}$.

2.4 Results

Using a variable-step Runge-Kutta method, Eqn. 2.12 is numerically solved and plotted for different population sizes. Then, results from the Monte Carlo (MC) simulations are overlayed on it.

Figure 2.2 includes numerical solution of Eqn. 2.12 (solid lines) as well as data points from MC simulations for different population sizes (N). Larger populations are characterized by higher peak values and lower variances. Additionally, the assumption of large but finite N lower bounds the population size. This can be seen in the $N = 50$ plot, where results from numerical simulations are not in accordance with the numerical solution of the mathematical model. High degree of fidelity between MC simulations data and numerical solutions of the model is observed for $N > 100$.

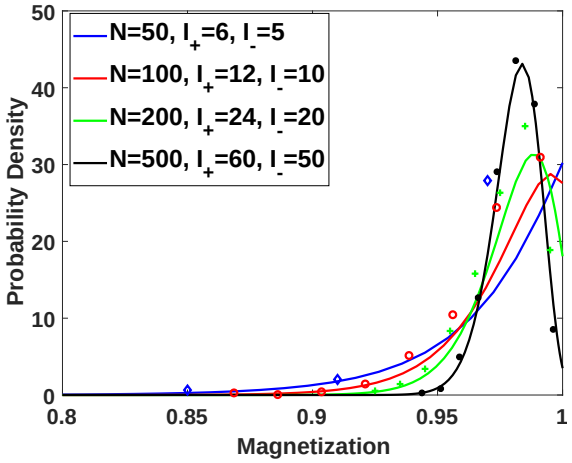

Figure 2.2: Effect of the population size N on the steady state density $P_{ss}(m)$

A caveat on the assumption of large population size should be mentioned here. Realistically, N cannot be unbounded, since there is a cognitive limit to the number of people with whom one can maintain social relationship - this is known as the Dunbar number [67]. It is true that influence in the world of social network is not completely dictated by relationships in which an individual knows the identity of each person and how s/he relates to every other person. For example, the Pew Research Center puts the average number of friends for a Facebook user at 338 [68]. However, these kinds of social networks rarely

ever assume a complete graph topology, but can be more realistically modelled as a scale-free network. Keeping this in mind, and since the derivations in this study rely on the complete graph assumption, all subsequent results are for an intermediate population size ($N = 100$) which is large enough for numerical accuracy, but smaller than the permissible Dunbar number limit ($N_{limit} = 150$).

2.4.1 Convergence and Indeterminate Zones

This section aims to elaborate on the effect of initial magnetization (m_0) on the steady state of the system. Each result is from 1000 runs of Monte Carlo simulations in which the magnetization parameter m is treated as a random variable. The rescaled histogram of the random variable is used to estimate the probability density function of the system at steady state. Different population sizes are considered and simulated with all the possible initial conditions (m_0 varies with steps equal to $\frac{2}{N}$).

For ease of representation, the mean magnetization $\langle m_{ss} \rangle$ estimated from the steady state PDF, $P_{ss}(m)$, for each simulation is plotted. Although, not the most comprehensive representation, Fig. 2.3 provides a visual representation of the convergence and indeterminate zones by representing the behavior of the mean steady state magnetization of systems as initial magnetization varies.

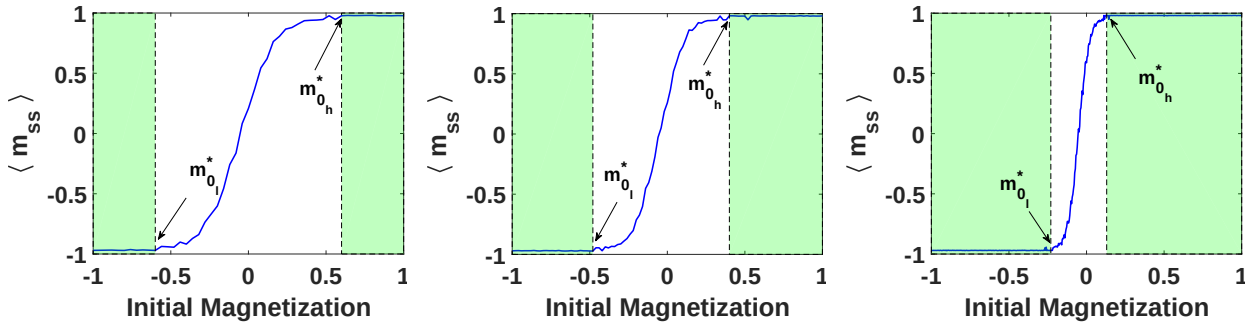

(a) $N = 50, I_+ = 6, I_- = 5$ (b) $N = 100$, $I_+ = 12$, $I_- = 10$ (c) $N = 500, I_+ = 60, I_- = 50$

Figure 2.3: Dependency of the mean steady state magnetization on initial magnetization.

Figure 2.3 depicts the two regions, convergence and indeterminate zones. The convergence zone is again composed of two regions - $Z_C = Z_{C_l} \cup Z_{C_h}$, where

$$\begin{aligned} Z_{C_l} &= \left\{ m_0 \leq m_{0_l}^* | P_{ss}(m) = P_{ss_l}(m) \right\} \\ Z_{C_h} &= \left\{ m_0 \geq m_{0_h}^* | P_{ss}(m) = P_{ss_h}(m) \right\} \end{aligned} \tag{2.14}$$

The indeterminate zone

$$Z_I = \left\{ m_{0_l}^* < m_0 < m_{0_h}^* | P_{ss}(m) = C_l P_{ss_l}(m) + C_h P_{ss_h}(m) \right\}$$

where $C_l > 0,\ C_h > 0$. For different configurations of population size and influences, Z_{C_l} and Z_{C_h} are represented by green with boundaries denoted by $m_{0_l}^*$ and $m_{0_h}^*$.

It can be observed that as population size increases, the convergence zone covers larger intervals of m_0. In addition, with linear scaling of simulation parameters, systems starting from their respective convergence zones converge to the same mean steady state magnetization value. In other words, for two generic systems α and β, with a scale factor of η, if $(m_{0_\alpha} = m_{0_\beta}) \leq m_{0_l}^*$ or if $(m_{0_\alpha} = m_{0_\beta}) \geq m_{0_h}^*$, then $\langle m_{ss}(N, I_+, I_-) \rangle = \langle m_{ss}(\eta N, \eta I_+, \eta I_-) \rangle$, $\eta = 2, 3, 4, \ldots$.

It may be noted that although the results presented so far are illustrated with the help of the mean of the stationary distribution, in fact, the hypothesis is that for each α, the sequence, $P_n^\alpha(m)$ converges in distribution to $P_{ss}(m)$, i.e., $\lim_{n\to\infty} P_n^\alpha(m) = P_{ss}(m)$.

To prove this, denoting a system configuration as $sys = \{N, I_+, I_-, m_0\}$, the following null and alternative hypotheses are constructed:

- **Null Hypothesis (H_0):** For sys_α and sys_β with $N_\alpha = N_\beta,\ I_{+_\alpha} = I_{+_\beta},\ I_{-_\alpha} = I_{-_\beta}$, if $(m_{0_\alpha} \neq m_{0_\beta}) \leq m_{0_l}^*$ or if $(m_{0_\alpha} \neq m_{0_\beta}) \geq m_{0_h}^*$ then $P_{ss}^\alpha(m) \sim P_{ss}^\beta(m)$.
- **Alternative Hypothesis (H_1):** For sys_α and sys_β with $N_\alpha = N_\beta,\ I_{+_\alpha} = I_{+_\beta},\ I_{-_\alpha} = I_{-_\beta}$, if $(m_{0_\alpha} \neq m_{0_\beta}) \leq m_{0_l}^*$ or if $(m_{0_\alpha} \neq m_{0_\beta}) \geq m_{0_h}^*$ then $P_{ss}^\alpha(m) \nsim P_{ss}^\beta(m)$.

Simulation data with different m_0's are tested at $\alpha = 0.01$ significance level using the two-sample Kolmogorov-Smirnov (KS) test. Results of the testing do not reject the null hypothesis; thus, the null hypothesis stands true with 99% certainty.

Figure 2.4 illustrates steady state PDF's of a system with different initial conditions (marked by red stars in Fig. 2.4a) for visual verification. It may be noted that when initial conditions are chosen from Z_{C_h}(Figs. 2.4f, g, h), or from Z_{C_l} (Figs. 2.4c, d, e), the steady state PDFs each time converge respectively to $P_{ss_l}(m)$ and $P_{ss_h}(m)$.

For $m_{0_l}^* \leq m_0 \leq m_{0_h}^*$ (Fig. 2.4b), the PDF is a mixture of two PDFs. K-S tests reveal that the rescaled PDFs of these modes are the same as P_{ssl} and P_{ssh} proving that the solution of Eqn. 2.10 contains both specific solutions; or equivalently, $C_l \neq 0$ and $C_h \neq 0$.

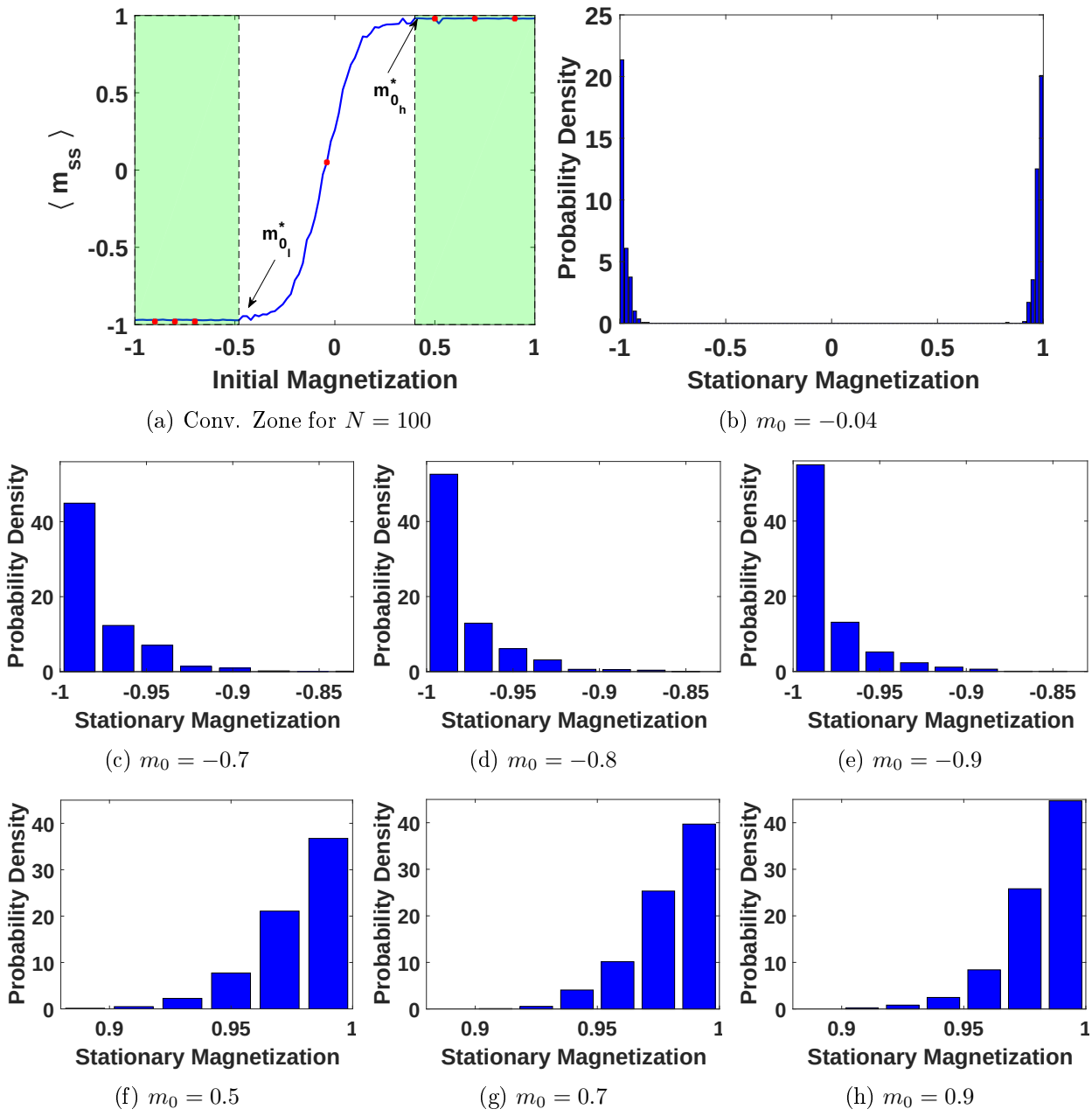

(a) Conv. Zone for $N = 100$ (b) $m_0 = -0.04$

(c) $m_0 = -0.7$ (d) $m_0 = -0.8$ (e) $m_0 = -0.9$

(f) $m_0 = 0.5$ (g) $m_0 = 0.7$ (h) $m_0 = 0.9$

Figure 2.4: Conv. zone and stationary PDF's of a system with $N = 100, I_+ = 12, I_- = 10$.

2.4.2 Convergence Zone with Varying Control Inputs

In section 2.4.1, a fixed control input is used to find the convergence zones related to different population sizes. The objective of this section is to investigate whether there exist convergence zones for other values of u. Also, how such convergence zones depend on the control input is studied.

To do this, control input u is treated as an independent variable in Fig. 2.5. Similar to section 2.4.1, MC simulations are performed for all possible combinations of m_0 and u. Then, mean magnetization of the system at the steady state is calculated and plotted.

A specific control input can correspond to different combinations of I_+ and I_-; for e.g., $I_+ = 8, I_- = 2$ and $I_+ = 16, I_- = 4$ both represent $u = 0.6$. To fully specify the problem, we define *influence ratio*, $\lambda = \frac{I}{N}$, as a simulation parameter, where $|I| = |I_+| + |I_-|$. Somewhat arbitrarily, we focus on the range $0 \leq \lambda \leq 1$ for λ, which regulates the total number of influences in the system to be at most the same size as the population. In Fig. 2.5, the control input changes with steps equal to $\frac{2}{I}$ to cover all possible discrete values in $[-1, 1]$.

Existence of convergence zones: Fig. 2.5 depicts that for different combinations of λ and u, region(s) ($m_0 \leq m^*_{0_l}$ or $m_0 \geq m^*_{0_h}$) exist, where the mean steady state magnetization $\langle m_{ss} \rangle$ loses its dependency on the initial magnetization, and all systems converge to a unique PDF.

To determine boundaries of convergence zones, a new set of figures are presented. Fig. 2.6a represents the case with $\lambda = 0.2$ with markers for $m^*_{0_l}$ and $m^*_{0_h}$. Fig. 2.6b is the two dimensional location of the same markers on the $m_0 - u$ plane. As it can be seen, for most values of the control input, both $m^*_{0_l}$ and $m^*_{0_h}$ are present. However, in extreme cases of control input one of them is absent. For example, $u = -1$ and $u = 1$ lack $m^*_{0_h}$ and $m^*_{0_l}$ respectively. Same analysis can be applied to systems with other values of λ.

Exit probability, i.e. the probability that the system ultimately reaches consensus as a function of the initial composition of the population, is a very important first-passage property [69]. In this work, the concept of exit probability is not completely applicable since the influenced system never reaches consensus. However, the proof of our Null Hypothesis

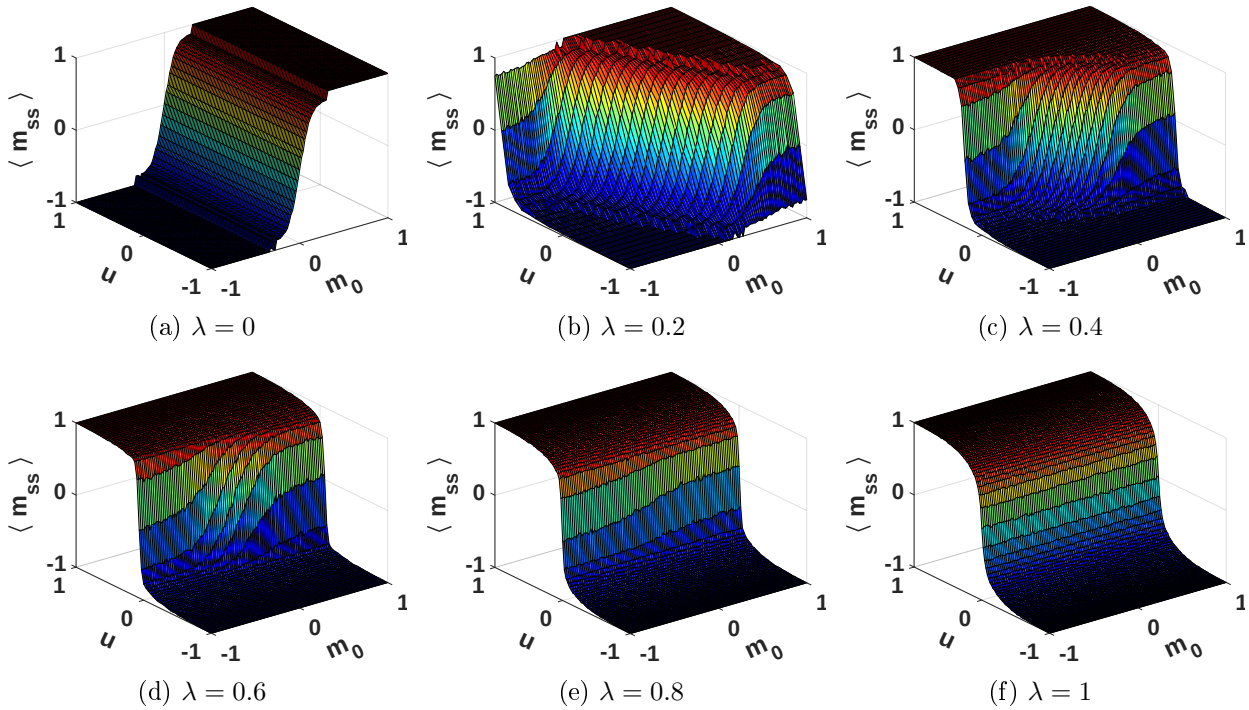

(a) $\lambda = 0$ (b) $\lambda = 0.2$ (c) $\lambda = 0.4$

(d) $\lambda = 0.6$ (e) $\lambda = 0.8$ (f) $\lambda = 1$

Figure 2.5: Dependency of mean steady state magnetization on initial magnetization and control input for $N = 100$.

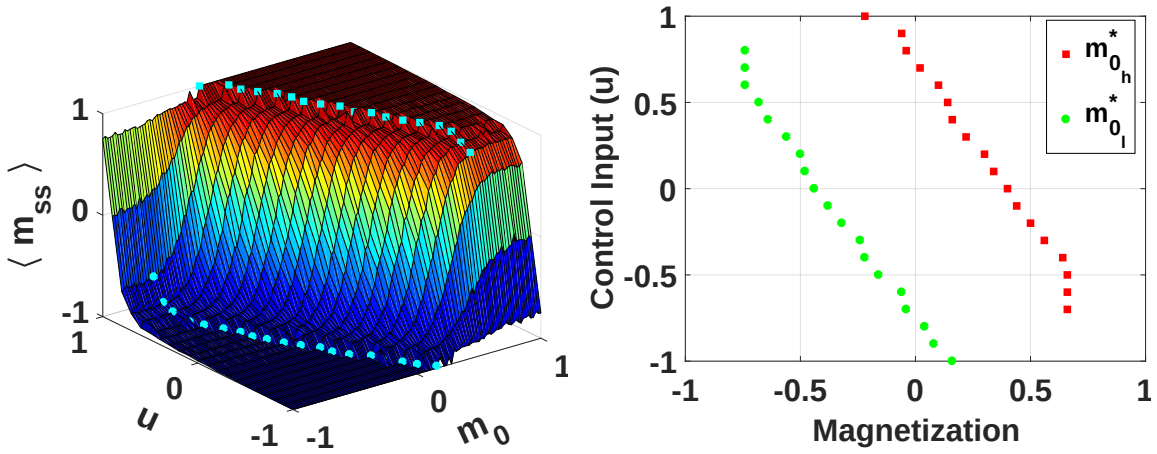

(a) (b)

Figure 2.6: (a) $m^*_{0_l}$ and $m^*_{0_h}$ marked on the 3D graph related to $\lambda = 0.2$ for all possible values of u. (b) 2D representation of the boundaries on the $m_0 - u$ plane.

does show some similarities with the concept of exit probability. Here, we have shown that two similar systems with initial conditions belonging to the same convergence zone will converge to the same probability distribution in their stationary states. The limits of convergence zones depend on N, λ, and u.

Effect of influence ratio (λ): Fig. 2.5a represents an uninfluenced society. $\langle m_{ss} \rangle$ is only a function of m_0, and boundaries of convergence zone are clear on both sides. However, as soon as influences are added to the society ($\lambda = 0.2$), the behavior of the $\langle m_{ss} \rangle$ starts to change, and dependency on u is noticeable. For instance, on plane $u = -1$, the $\langle m_{ss} \rangle$s for positive m_0s decrease since all of the influences are focused on the negative side. Also, on plane $u = 1$, the $\langle m_{ss} \rangle$s for negative m_0s increase because all the influences are focused on the positive side.

More importantly, at $\lambda = 0.2$, number of influences is not high enough to make the $\langle m_{ss} \rangle$ flatten as m_0 changes on planes $u = \pm 1$. This is the reason why there is neither a $m^*_{0_h}$ on plane $u = -1$ nor a $m^*_{0_l}$ on $u = 1$. However, for higher values of λ, number of influences is high enough to overcome the effect of m_0 and make the $\langle m_{ss} \rangle$ flatten (Figs. 2.5c-f).

In Figs. 2.5c-e, as λ increases, the control input becomes the dominant parameter in changing the behavior of $\langle m_{ss} \rangle$, and $\langle m_{ss} \rangle$ completely loses its dependency on m_0 as $u \longrightarrow \pm 1$. In addition, when $u \longrightarrow 0$, m_0 is the dominant parameter in the behavior of $\langle m_{ss} \rangle$. Interestingly, Fig. 2.5f, $\langle m_{ss} \rangle$ is a function of u only. It is interesting to note that when the influence size (I) exactly matches the population size (N) the steady state PDF completely loses its dependency on the initial condition.

Comparison to previous studies: In the study by Slanina and Lavička [27], it is proven that for a simplified Sznajd model dynamic on a complete graph, there exists a phase transition at $m_0 = 0$. However, in our simulations this phase transition is absent in Fig. 2.5. In the case of $\lambda = 0$, this is due to the fact that, in their analyses, Slanina and Lavička assume the population size is infinite, $N \to \infty$; however, in our simulations we assume the population is large but finite. In cases where $\lambda \neq 0$, the absence of a phase transition is partly because of the large but finite N assumption, and in part because of the presence of

influences.

Linear scaling property: In section 2.4.1, the linear scaling property with a fixed control input is mentioned. In this section, we investigate if this property holds true for other values of control input. Fig. 2.7 compares the behavior of $\langle m_{ss} \rangle$ for two population sizes $N = 50$ and $N = 100$ ($\eta = 2$). From visual inspection, linear scaling of simulation parameters preserves the general trend of $\langle m_{ss} \rangle$.

However, point-to-point comparison of $\langle m_{ss} \rangle$ data shows that the relation $\langle m_{ss}(N, I_+, I_-) \rangle = \langle m_{ss}(\eta N, \eta I_+, \eta I_-) \rangle$ does not hold true for all values of u. To determine the interval of control input for which the scalability property stands, we study the point-to-point difference in $\langle m_{ss} \rangle$ data values. Fig. 2.7c represents $\delta = \langle m_{ss} \rangle|_{N=50} - \langle m_{ss} \rangle|_{N=100}$ calculated on planes $m_0 = -1$ (blue line) and $m_0 = +1$ (red line).

It can be seen that for some values of u, $\langle m_{ss} \rangle$ of the scaled system ($N = 100$) and the base system ($N = 50$) are exactly equal ($\delta = 0$); thus, for the corresponding m_0 scalability property stands. For instance, if $\lambda = 0.2$, for $\forall u \in [-1, 0.4], \delta = 0$ on plane $m_0 = -1$ (the green area). For a unique m_0, intervals of control input for which $\delta = 0$ will be referred to as the **Scalability Zone** of the base system for that m_0.

To study the existence of scalability zone for different values of initial magnetization, the same process has been applied to $\langle m_{ss} \rangle$ data on other available m_0 planes. Fig. 2.8 presents $\delta(m_0, u)$ for different values of influence ratio. Interesting characteristics are observed for

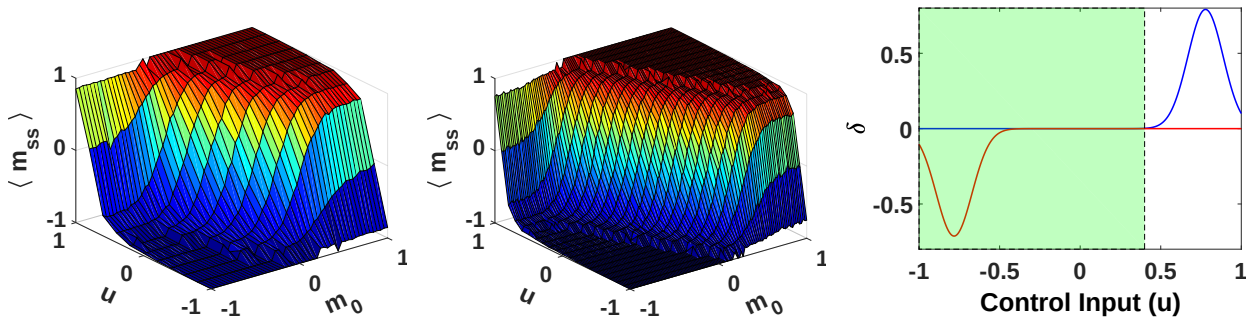

(a) $N = 50, \lambda = 0.2$ (b) $N = 100, \lambda = 0.2$ (c) Scalability zone for $m_0 = \pm 1$ with $\lambda = 0.2$

Figure 2.7: Three dimensional linear scaling property

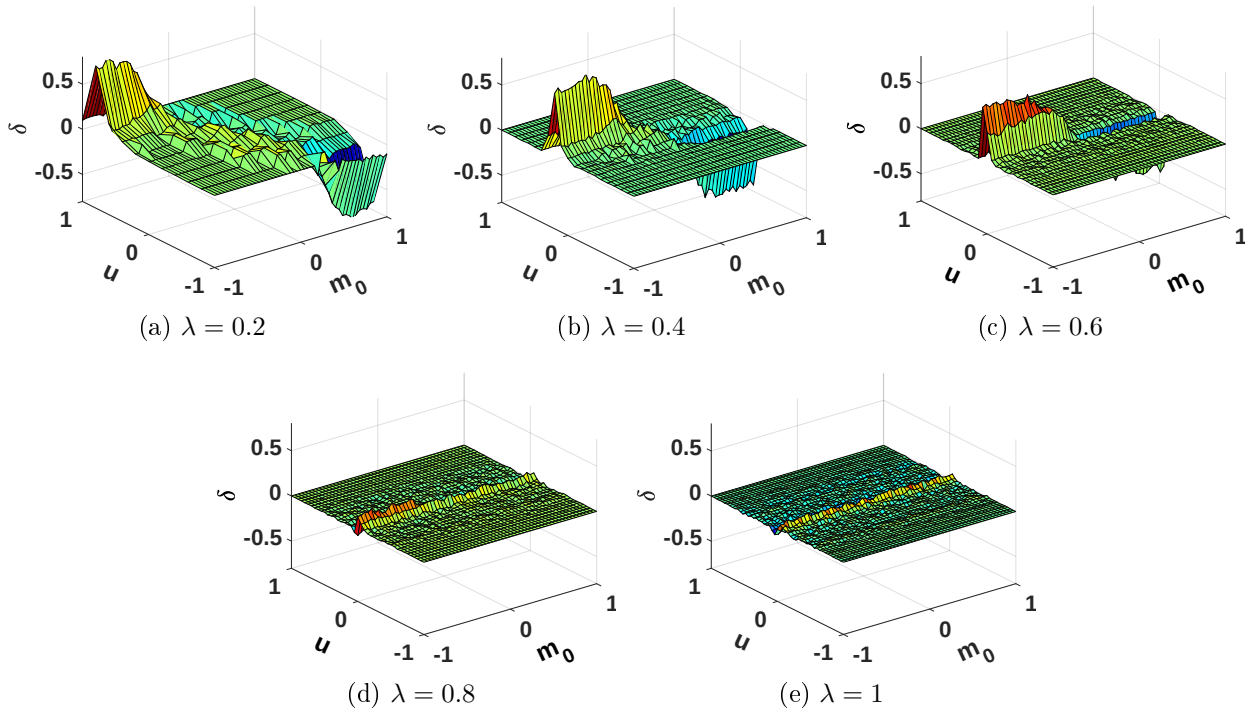

(a) $\lambda = 0.2$ (b) $\lambda = 0.4$ (c) $\lambda = 0.6$

(d) $\lambda = 0.8$ (e) $\lambda = 1$

Figure 2.8: Scalability zone for all m_0s for $N = 100$.

different values of λ regarding existence of scalability zone and its expansion, maximum difference values, and sign of δ.

It can be seen in Fig. 2.8a that for some values of m_0 close to zero $\delta \neq 0$. However, scalability zone appears and expands in the first and third quadrants of the $m_0 - u$ plane (where $sgn(m_0) = sgn(u)$) towards outer borders. In this figure, dependency of δ on m_0 is clear in a large area. Also, maximum difference happens in the second and fourth quadrants near the outer borders (where $sgn(m_0) = -sgn(u)$).

As λ increases, the dependency of δ on m_0 decreases; maximum differences decrease, and they happen close to $u = 0$ plane. The scalability zone is available for all values of m_0. When $\lambda = 1$, δ is a function of u only. Interestingly, $sgn(\delta) = sgn(u) = -sgn(m_0)$ for all values of λ. This means that for $m_0 \geq 0, \delta < 0 \Rightarrow \langle m_{ss} \rangle|_{N=50} < \langle m_{ss} \rangle|_{N=100}$ if $\delta(m_0, u) \neq 0$, or for $m_0 \leq 0, \delta > 0 \Rightarrow \langle m_{ss} \rangle|_{N=50} > \langle m_{ss} \rangle|_{N=100}$ if $\delta(m_0, u) \neq 0$.

So far, our findings are dominantly based on the mean of the probability distribution function of the system at its steady state; however, while calculating the mean, some information of the PDF is lost. For instance, although a family of Gaussian distributions

defined as $f(x) = \frac{1}{\sqrt{2\pi\sigma^2}} e^{\frac{-x^2}{2\sigma^2}}$ have a mean value of zero, their disorder or uncertainty cannot be explained by their mean. In information theory the concept of *Entropy* is used to study the uncertainty of PDFs. Next section is devoted to the study of system entropy at steady state.

2.4.3 Entropy Analysis

Entropy of a random variable X is defined as the expectation of the random variable $-\log P(X)$ with respect to the probability measure P [70, 71]:

$$H(X) = E_{P_X}\{-\log P_X(X)\} = -\sum_{x \in X} P_X(x) \log P_X(x) \tag{2.15}$$

where, E_P denotes the expectation with respect to probability distribution P. We use the steady state magnetization PDF of the systems in Fig. 2.5 to calculate entropy of each data point. Fig. 2.9 represents the entropy of the system for different values of influence ratio. It is worth noting that low entropy corresponds to higher certainty and high entropy represents lower certainty in the steady state.

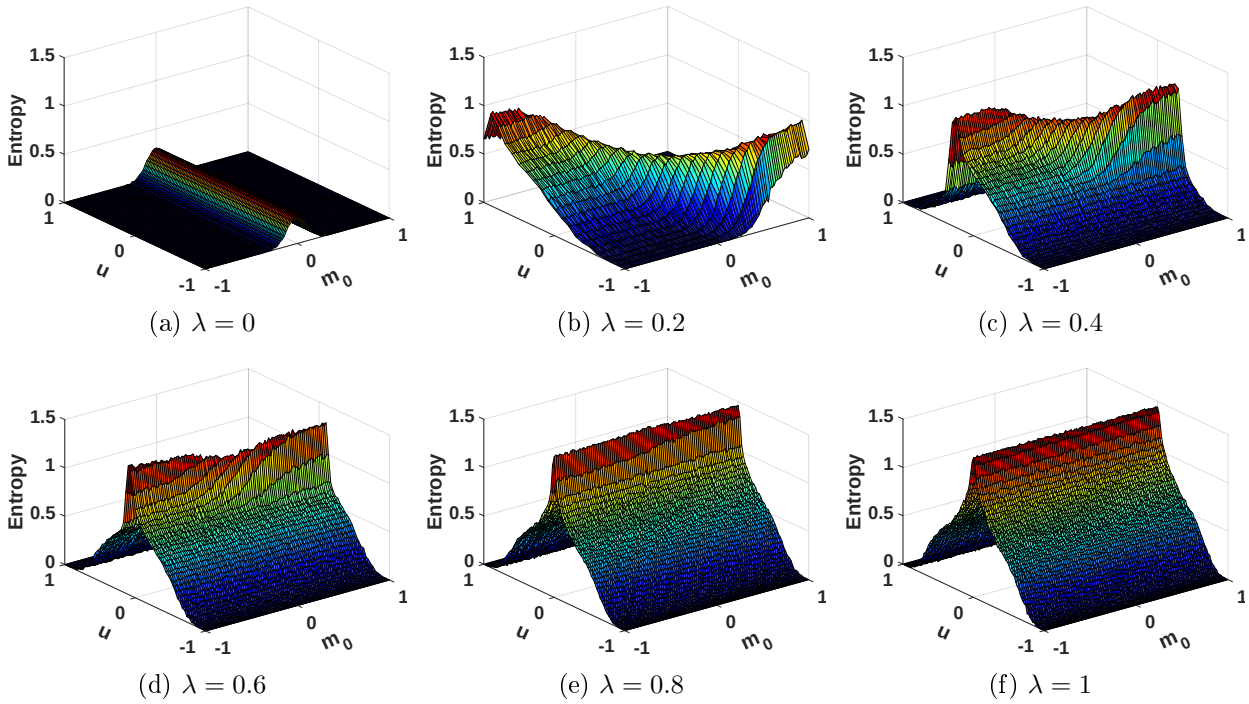

(a) $\lambda = 0$ (b) $\lambda = 0.2$ (c) $\lambda = 0.4$

(d) $\lambda = 0.6$ (e) $\lambda = 0.8$ (f) $\lambda = 1$

Figure 2.9: Entropy of distributions for different values of λ for $N = 100$.

For $\lambda = 0$, there are no influences in the population, and entropy of the system is a function of m_0 only. Entropy is zero for $m_0 \leq m^*_{0_l}$ or $m_0 \geq m^*_{0_h}$ because in these regions there are enough agents at the corresponding state to push the system PDF towards a Dirac delta function at either -1 for $m_0 \leq m^*_{0_l}$ or at $+1$ when $m_0 \geq m^*_{0_h}$. Also, entropy reaches its maximum at $m_0 = 0$, because in this region neither of the groups in ± 1 states are strong enough to completely attract the population towards themselves; this phenomenon results in a more distributed density function over the magnetization axis, and consequently higher entropy.

Figures 2.9b-f depict that adding influences to the population increases the entropy of the system. The reason is that although small in number, influences are capable of attracting agents to their state; as a result, the steady state magnetization of the system will have a different value from that of the uninfluenced population. So, the density function of the system becomes more distributed over the magnetization axis leading to higher entropy values.

For instance, $u = 0|_{\lambda=0.2}$ represents a system with influences equally divided between the two groups; this might imply that their effects on the steady state PDF will be eliminated by each other, and the resulted PDF will be the same as that of the uninfluenced system ($\lambda = 0$). However, by point-to-point comparison of data points we find that $\forall m_0$ on the $u = 0$ plane, the PDF of the influenced system is more distributed, and $H(m_0, u = 0)|_{\lambda=0} < H(m_0, u = 0)|_{\lambda=0.2}$.

In Fig. 2.9b, entropy is at its lowest levels when $sgn(m_0) = sgn(u)$. In this situation higher number of influences support the initially more populated state resulting in a sharp less-distributed magnetization density function close to one of the ends of the magnetization axis. The opposite happens when $sgn(m_0) = -sgn(u)$ since more influences are in the favor of the initially less populated state preventing the population from clustering at one of the edges of the magnetization axis; the resulting density function is nicely distributed causing higher entropy. This reasoning explains why the point $(m_0 = 0, u = 0)$ is similar to a saddle point. It is observed in Fig. 2.9b that entropy is more sensitive to the control input rather than the initial condition. Consider point $(m_0 = -1, u = -1)$ on the graph. Entropy starts to propagate from zero faster if $\{m_0 = const.$ and $u \uparrow\}$ compared to the situation where

$\{u = const.$ and $m_0 \uparrow\}$. The reason is that influences (even in small numbers) are always active in the process of changing agents' states to theirs. However, an agent is active in attracting other agents to its initial state till s/he changes to the opposite state; i.e. its effect is not ever-lasting. As a result, more agents are needed to have the same effect of a few number of influences on the PDF of the system and the entropy.

In Fig. 2.9b, as u increases on $m_0 = -1$ plane, entropy ascends till $u = 0.9$. This phenomenon is easy to comprehend since more influences in state $+1$ attract more agents from state -1, and the PDF of the system is more distributed. However, at $u = 1$, since all the influences are at the positive side, they are able to dramatically shift the PDF towards themselves and make it narrower resulting in lower entropy value. Here, the number of influences is not high enough to change the PDF into a Dirac delta function, so entropy does not reach zero.

On the contrary, in Figures 2.9c-f, number of influences is high enough to completely attract the population towards themselves on planes $u = \pm 1$; so, the entropy is zero. As λ increases, similar to $\langle m_{ss} \rangle$, for larger intervals of u entropy loses its dependency on m_0 and $sgn(m_0)$, and the saddle point disappears; for $\lambda = 1$, entropy depends on the control input only.

2.5 Chapter Summary

In this chapter, effects of external influences on the behavioral dynamic of a group of agents who interact with each other based on the Sznajd model are studied. The Sznajd model is formulated on a complete graph in presence of influences, and the governing differential equation for the population behavior at steady state is derived. The resulted ODE shows the dependency of $p_e(m)$ on population size N, control input $u = \frac{I_+ - I_-}{I}$, and total influence size I.

The mathematical model is numerically solved, and the results are compared with data from numerical simulations. Higher peak values and lower variances are observed for larger population sizes. We find good agreement between the results from numerical experiments and numerical solution of the mathematical model for network sizes exceeding $N = 100$.

Based on numerical simulations, regions (called convergence zone) are available where the steady state loses its dependency on the initial condition. By adopting Kolmogorov-Smirnov hypothesis testing method, it is proven with 99% certainty that steady state PDF's of systems with initial conditions belonging to the same convergence zone are equivalent. Different graphs are provided to display this phenomenon. A relationship based on these findings and the general solution of the stationary ODE is drawn for different ranges of m_0. Furthermore, results show that by increasing the population size, the convergence zone covers a larger area. Interestingly, it is observed that linear scaling of simulation parameters causes the same convergence value for the mean steady state magnetization.

Effect of the control input on convergence zones is studied on three dimensional graphs by defining a new parameter $\lambda = \frac{I}{N}$ named influence ratio. Results show that for different combinations of u and λ, convergence zone(s) exist. Figures are provided to show the boundaries of the convergence zones. It is shown that increase in the number of influences results in larger convergence zones. When $\lambda = 1$, the whole $m_0 - u$ plane is independent of m_0. In addition, the absence of a phase transition is explained by the large-but-finite population size assumption and presence of influences.

Linear scaling property is also investigated for all combinations of m_0 and u. It is shown that not for all values of the control input the mentioned property stands. Three dimensional figures are provided which show the dependency of the difference between the $\langle m_{ss} \rangle$'s of two linearly scaled systems for different λ's. In general, as influence ratio increases, δ decreases; and δ loses dependency on m_0. The reason behind high values of δ on the second and fourth quadrants of the $m_0 - u$ plane is discussed in detail. It is also shown that for negative initial conditions, the $\langle m_{ss} \rangle$ of the base system is higher than that of the scaled system.

Entropy study of the system reveals that higher influence (although small in number) equals higher entropy. Generally, entropy is a function of the initial magnetization and the control input, but as λ increases, the system loses its dependency on m_0. When $\lambda = 1$ the entropy is only a function of the control input.

Chapter 3

Dynamics of a Repulsive Voter Model

3.1 Objective

In literature, all of the interaction models are attracting models; i.e. after the interaction, the interacting agents become the same (Voter model and Sznajd model), or similar to each other in some sense (Bounded Confidence model). However, attracting interaction models are not capable of explaining all types of behaviors observed in the society. For example, anti-conformal behavior cannot be modelled using attracting interaction models. To model anti-conformal behaviors in the society, new types of interaction models, "repelling" models, are needed. This chapter introduces a new interaction model where similar agents repel each other instead of attracting each other.

3.2 Intorduction

In contrast to the rich and well-researched mode of conventional social interaction, in this chapter, we discuss a modified scenario where, each node is repelled, rather than attracted by its neighbors. Such anti-conformal behavior, though not nearly as wide-spread as 'herding' or mimicking behavior, is exhibited in a variety of social situations where there is a premium on novelty or on choices which can demonstrate an attitude of indifference or rebellion towards current trends. In the 1950s, a minimalist style described as 'anti-fashion' emerged with the advent of rock and roll, especially with young adolescent women [72]. Instead of the

standard dress or skirt, many young women wore jeans and plaid or T-shirts in rebellion with the gender roles and societal norms at that time. This fashion has the roots of many modern anti-fashion trends, such as Grunge [72], decades later.

A more recent example of anti-conformal behavior is observed by analyzing the beer drinking trend in America's young adults. Preference to beers in youths aged 18 to 29 has dropped from 75% to 40% in the last twenty years [73]. It is hypothesized that a cause of this shift in drinking preference is due to young people rebelling against the tastes of the generation before them - because what their parents drink isn't "cool".

We also draw inspiration from a behavioral demand model to trigger lane-changing maneuver of drivers in a multi-lane highway. When confronted with a slower car in the same lane, in the absence of other external factors, drivers tend to change to the other 'emptier' lane. This behavior exemplifies the repulsive Voter model dynamics that is introduced, described and analyzed in this chapter, albeit at a very low level of abstraction.

In this chapter, we introduce the simplest case, analogous to the Voter model, where at any time, each node has only two discrete states $+1$ and -1; thus, a single variable $s_i = \pm 1$ fully specifies the state of node i. This Ising model based approach is not intended to model any real phenomena, rather allow a mathematical treatment of a new emergent phenomena, where simple interactions among agents lead to complex global behaviors.

In this chapter, section 2 introduces the Repulsive Voter Model (RVM), and discusses it in the context of a complete graph. We derive the equilibrium solution of the Master equation related to our model formulated on a complete graph, which reveals some interesting facts about the role of the influencing nodes on the convergence state, time to convergence, etc. This is then validated by numerical simulations in section 3, the theoretical results are compared with numerical simulations, and several interesting characteristics of the system are pointed out. Section 4 presents the derivation of the Master equation for the Repulsive Voter model with biased nodes on a random graph with connection probability p. In this part also, numerical simulations are conducted not only to validate the mathematical modeling but also to perform a sensitivity analysis on the connection probability of p. Section 5 is dedicated to analytical solution of the Repulsive Voter model on a regular lattice. The analytical solution demonstrates some interesting results of the time evolution of the system.

In the final section of this chapter, the findings from this chapter are summarized and the chapter is concluded.

3.3 The Repulsive Voter Model Dynamics

In this section, a complete graph is considered. The complete graph, being a fully connected random graph $G(N, p)$ in the limit $p \to 1$, can be conveniently characterized by a single parameter, the magnetization factor, defined as $m = (N_+ - N_-)/N$, where, at any instant, N_+ represents the number of nodes (agents) in state $+1$, and N_- represents the number of nodes of the network in state -1. $N = N_+ + N_-$ nodes make up the vertices of the graph.

The Repulsive Voter model dynamics is a straightforward modification of the standard Voter model. At each time step, a node i and one of its neighbors j are randomly selected, and s_i is set equal to $-s_j$, i.e. node i chooses the opposite state as its neighbor. Several social behaviors find parallel in this anti-conforming tendency in a group, a typical example being lane selection in heavy traffic. Although not accurate at a fine level of granularity, an analysis of the dynamics can provide valuable information regarding the steady state equilibrium distribution, its dependence on group size and stabilization time.

Figure 3.1 demonstrates the instantaneous composition of the population which, in addition to N_+ and N_- nodes, comprises of $I = I_+ + I_-$ external agents with respective pre-conceived allegiance to states $+1$ and -1. In the repulsive interaction scenario, the influence groups represent decentralized control inputs which aim at repelling nodes away in

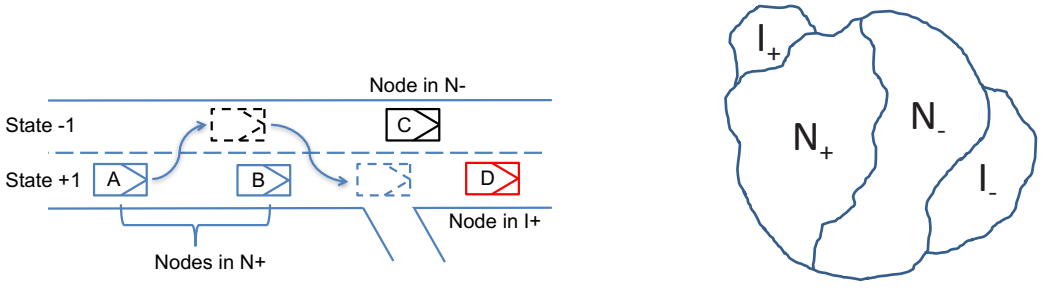

Figure 3.1: (a) An example demonstrating traffic flow modelled with the Repulsive Voter dynamics, (b) Population composition

order to attain a target state distribution. Natural examples of such repulsive influences in a traffic network are police vehicles stationed near accidents or construction sites in order to attain smooth uninhibited traffic flow [74, 75] through reduced number of lanes.

We use the same nomenclature as Slanina and Lavicka to develop the Master equation for the RVM dynamics. A Master equation is a set of first-order differential equations describing how the probability of finding the system in state m at time t changes with time:

$$\frac{dP(m,t)}{dt} = \sum_{m' \neq m} T(m|m')P(m',t) - \sum_{m \neq m'} T(m'|m)P(m,t) \tag{3.1}$$

where, the quantity $T(m|m')$ is the transition rate, and is only defined for $m \neq m'$. It may be noted that, in our case, the system performs a random walk over a $[-1, +1]$ range of the magnetization parameter m with a discrete step size of $\pm 2/N$. For such a one step process, the master equation takes the simpler form:

$$\begin{aligned} \frac{dP(m,t)}{dt} &= T(m|m+\frac{2}{N})P(m+\frac{2}{N},t) \\ &+ T(m|m-\frac{2}{N})P(m-\frac{2}{N},t) \\ &- [T(m-\frac{2}{N}|m) + T(m+\frac{2}{N}|m)]P(m,t) \end{aligned} \tag{3.2}$$

We can now proceed to compose the master equation as:

$$\dot{P}_m = r_{m+\frac{2}{N}} P_{m+\frac{2}{N}} + g_{m-\frac{2}{N}} P_{m-\frac{2}{N}} - (r_m + g_m)\, P_m, \tag{3.3}$$

where,

$$\begin{aligned} r_m &= T(m-\frac{2}{N}|m) = \left(\frac{N_+}{N}\right)\left(\frac{N_+ + I_+ - 1}{N + I - 1}\right) \\ g_m &= T(m+\frac{2}{N}|m) = \left(\frac{N_-}{N}\right)\left(\frac{N_- + I_- - 1}{N + I - 1}\right) \\ r_{m+\frac{2}{N}} &= T(m|m+\frac{2}{N}) = \left(\frac{N_+ + 1}{N}\right)\left(\frac{N_+ + I_+}{N + I - 1}\right) \\ g_{m-\frac{2}{N}} &= T(m|m-\frac{2}{N}) = \left(\frac{N_- + 1}{N}\right)\left(\frac{N_- + I_-}{N + I - 1}\right) \end{aligned} \tag{3.4}$$

Using Eqn. 3.4 in Eqn. 3.3, we get:

$$\begin{aligned}\dot{P}_m =& \left(\frac{N_+ + 1}{N}\right)\left(\frac{N_+ + I_+}{N+I-1}\right) P_{m+\frac{2}{N}} \\ &+ \left(\frac{N_- + 1}{N}\right)\left(\frac{N_- + I_-}{N+I-1}\right) P_{m-\frac{2}{N}} \\ &- \left[\left(\frac{N_+}{N}\right)\left(\frac{N_+ + I_+ - 1}{N+I-1}\right)\right. \\ &\left. + \left(\frac{N_-}{N}\right)\left(\frac{N_- + I_- - 1}{N+I-1}\right)\right] P_m\end{aligned} \tag{3.5}$$

Defining the control variable as $u = \frac{I_+ - I_-}{I}$, for large N, after simplification, the Master equation can be expressed as:

$$\begin{aligned}\dot{P}_m =& \frac{1}{N(N+I-1)}\left[(1+m^2)\frac{\partial^2 P_m}{\partial m^2}\right. \\ &+ (2mN + 2m + Iu + Im)\frac{\partial P_m}{\partial m} \\ &\left. +2NP_m + IP_m\right]\end{aligned} \tag{3.6}$$

With the proper time scaling as $\tau = t/N$, the final form of the influenced Repulsive Voter model can be expressed as:

$$\frac{\partial P_m}{\partial \tau} = \frac{\partial}{\partial m}\left[(1+m^2)\frac{1}{N}\frac{\partial P_m}{\partial m} + 2mP_m + \frac{I}{N}P_m(m+u)\right] \tag{3.7}$$

If we assume that an equilibrium density function exists, then $\lim_{\tau\to\infty}\frac{\partial P_m}{\partial \tau} = 0$, and by assuming that constants of integration are equal to 0, the equilibrium density $P_e(m)$ has to satisfy:

$$(1+m^2)\frac{1}{N}\frac{\partial P_e(m)}{\partial m} + 2mP_e(m) + \frac{I}{N}P_e(m)(m+u) = 0 \tag{3.8}$$

whose solution is:

$$P_e(m) = \frac{1}{C}\frac{e^{-Iu\tan^{-1}(m)}}{(1+m^2)^{(N+I/2)}} \tag{3.9}$$

where C is the constant that ensures proper normalization of the probability density function.

The effect of influences is apparent both in the exponential term in the numerator and in the power of the denominator. Putting $I = 0$ results in the solution of the Repulsive Voter model without influence.

3.4 Discussion and Numerical Results

We can estimate the probability density functions at each time (decision) point simply with a rescaled histogram by performing Monte Carlo simulations and treating the magnetization parameter m as a random variable. We expect Eqn. 3.9 to accurately represent the density estimates at the steady state and provide us with insights into some characteristics of this interesting system such as the expected equilibrium magnetization, effect of N, I, u, etc.

3.4.1 The Equilibrium Density

It may be noted that $P_e(m)$ from the analytical solution is not independent of N for large but finite population sizes. Thus, for bigger populations to reach similar expected magnetization levels, more control (bigger u) has to be exerted. This is in stark contrast to the regular Voter model with influence, where the mean magnetization was shown to be independent of the population size [8].

To investigate the dependence of $P_e(m)$ on N, we plotted probability densities for a variety of population sizes. Numerical results from 1000 Monte Carlo simulations are overlayed on the analytical solutions for each N in Fig. 3.2a. Larger populations are characterized by lower variance and mean magnetization close to 0. The assumption of large N lower bounds the population size. This may be observed in the $N = 10$ plot where the data points from MC are not in accordance to the theoretical result obtained in Eqn. 3.9. High degrees of fidelity between MC simulation data and analytical result is observed for $N > 100$.

Expected Magnetization

The effect of size of different influence groups on the equilibrium density is shown in Fig. 3.2b along with the expected magnetization $\langle m \rangle$ plotted as vertical lines. It is observed that the Repulsive Voter model is extremely stable in the sense that even high values of u and I

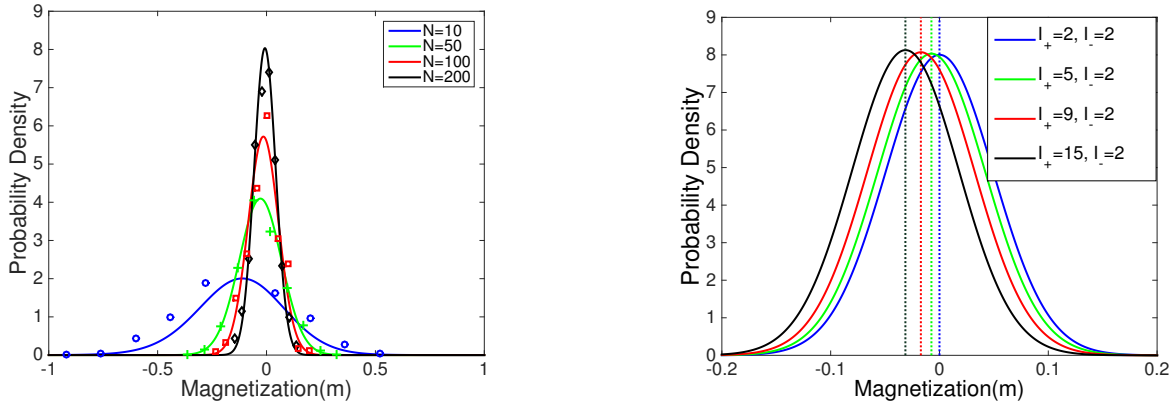

Figure 3.2: (a) Effect of the population size (N) on the equilibrium density $P_e(m)$, and (b) Effect of size of influence groups on $P_e(m)$

are not be able to cause noticeable shifts in $\langle m \rangle$. In smaller populations, however, the effect is much more pronounced. Recalling the significant shift in the beer drinking preference in youths, we may observe that this is one case, where the influencing set (parents) is similar in size to the target population. Without such large influence, significant shifts in the mean magnetization is impossible to achieve.

An interesting behavior for the system is observed if the influences I_+ and I_- are scaled proportionally with the population size. Figure 3.3 shows the effect of the scale factor α. Interestingly, $\langle m \rangle$ is independent of α, i.e.:

$$\langle m(N, I_+, I_-) \rangle = \langle m(\alpha N, \alpha I_+, \alpha I_-) \rangle$$

This result may have practical use in planning traffic management strategies in congested highways using police vehicles. The results suggest that if $I = 5$ police cars were sufficient to achieve the mean target lane distribution for a $N = 100$ car capacity section of a highway, in a $N' = 5 \times 100 = 500$ car capacity highway section, $I' = 5 \times 5 = 25$ police cars would achieve the same mean lane distribution. However, the variance monotonically decreases with scale.

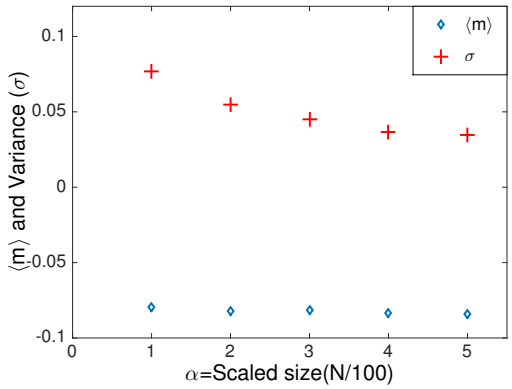

Figure 3.3: Effect of scale factor on the mean and variance of $P_e(m)$

3.4.2 Progression of the Density Function

So far, only aspects of the system at its equilibrium point have been presented. Now, we investigate the dynamic characteristics of the probability density function; specifically, the effect of the influence groups I_+ and I_-.

Figure 3.4a plots the progression of the PDF for such a numerical experiment with simulation parameters $N = 200$, $I_+ = 1$ and $I_- = 9$. Starting from a delta distribution $p(m)|_{\tau=0} = \delta(m-0.8)$, the figure gives a snapshot of the distribution at time instants spaced in a geometric sequence. The choice of the time instants displayed are purely based on aesthetic considerations. The plots with the empty circles are scaled histograms from 1000 simulation runs at the corresponding scaled time points, while the solid lines are the normal distributions fit to the data. An important observations from these plots is that starting from a delta, the distribution at each instant quickly assumes and remains in the Gaussian form, which should help policy making by providing suitable confidence bounds for achieving target distributions within a certain time frame.

Figure 3.4b plots the expected magnetization trajectory $\langle m \rangle$ with τ. It can be readily seen that the convergence time is independent of the population size N if time is scaled as $\tau = t/N$. This implies that the number of interactions it takes for the Repulsive Voter dynamical system to reach equilibrium is proportional to the size of the population. This means that for $N = 20$, if the time (number of decisions) to convergence is $t = 60$, then for $N' = 200$, the convergence time is simply $t' = 600$. Even at this very low level of fidelity,

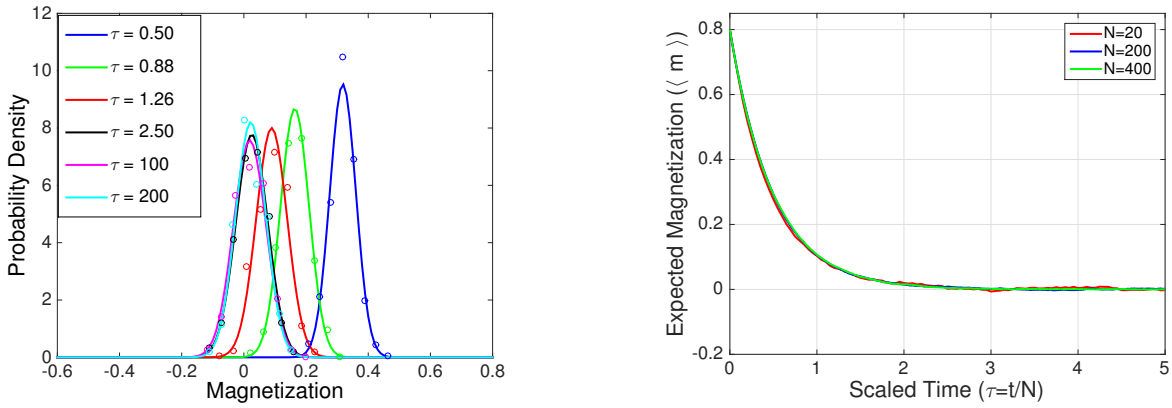

(a) (b)

Figure 3.4: (a) Progression of the PDF with time for $N = 200$, $I_+ = 5$ and $I_- = 2$, (b) Effect of N on the time to convergence

this information can be potentially useful in a variety of situations including the design of merge sections in highways.

3.5 RVM on a Random Graph

In this part, behavior of the RVM on a random graph is investigated. The Erdős Rényi random graph $G(N, p)$ is defined as N labeled nodes connected by n edges which are chosen randomly from $(N(N-1))/2$ possible edges [55]; i.e. every pair of nodes is connected with probability $p = \frac{n}{[(N(N-1))/2]}$. Since there are $C^n_{[(N(N-1))/2]}$ ways to construct such a graph, a probability space is formed in which every realization of the random graph owns an equal probability of happening. The probability of constructing a specific realization of a random graph such as G_0 with the specifications mentioned above is $P(G_0) = p^n(1-p)^{[N(N-1))/2]-n}$.

3.5.1 Model Formulation and Analytical Solution

In order to formulate this system, elements of the Master equation do not need to be composed again. Intuitively, every interaction happens with probability p, so all parts of the Master equation are going to be the same as the case involving complete graph with the only exception that they will incorporate a probability coefficient. Here, only one representative

transition rate is presented to clarify the effect of connection probability of the random graph:

$$r_m = T(m - \frac{2}{N}|m) = \left(\frac{N_+}{N}\right)\left(\frac{N_+ + I_+ - 1}{N + I - 1}\right).p \tag{3.10}$$

By substituting new rates in Eqn. 3.3 and after following the same steps as before, the Master equation becomes:

$$\begin{aligned}\dot{P}_m = \frac{p}{N(N+I-1)}\Bigg[&(1+m^2)\frac{\partial^2 P_m}{\partial m^2} \\ &+ (2mN + 2m + Iu + Im)\frac{\partial P_m}{\partial m} + 2NP_m + IP_m\Bigg]\end{aligned} \tag{3.11}$$

The final form of the influenced Repulsive Voter model on a random graph can be expressed in an exactly similar form as Eqn. 3.9; the only difference is that the time needs to be differently scaled as $\tau = t/(N/p)$:

$$P_e(m) = \frac{1}{C}\frac{e^{-Iu\tan^{-1}(m)}}{(1+m^2)^{(N+I/2)}} \tag{3.12}$$

3.5.2 Numerical Results and Discussion

Since effects of population size N and different combinations of influences I_+ and I_- have already been considered in the complete graph scenario, this part will solely be devoted to demonstrating the effects of connection probability p on the behavior of the system in the equilibrium state as quantified by Eqn. 3.12. Figure 3.5 illustrates results of Monte Carlo simulations for different population sizes N and for two different values of the connection probability p. The results are overlayed on the analytical solutions associated with each system.

In Fig. 3.5a, p is greater than $p_c = \frac{\ln(N)}{N}$ for $N = 50, 100$ and 200, the random graphs in these cases are almost surely connected and consequently, the analytical solutions and numerical results represent high degrees of similarity. However, for $N = 10$, $p < p_c$ leading to development of isolated nodes which cause the equilibrium density to deviate from the analytical solution. In Fig. 3.5b, for each N, the connection probability is smaller than

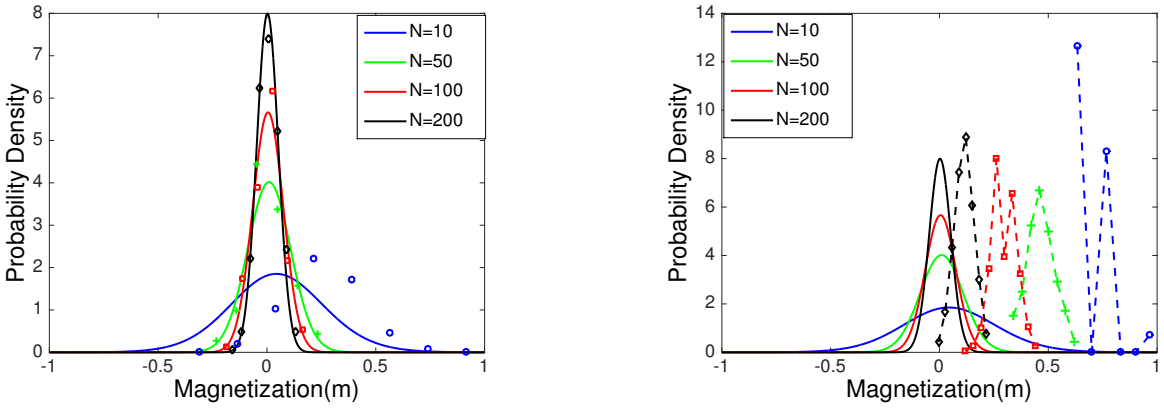

(a) $p = 0.1$ (b) $p = 0.01$

Figure 3.5: Effect of connection probability p on the equilibrium density for different N

the threshold leading to large deviations. This indicates the presence of a critical connection probability (p_c) and possible phase transition in the expected equilibrium magnetization $\langle m \rangle$, which we hypothesize should coincide with the phase transition related to the emergence of fully connected random graphs at $p \xrightarrow{\epsilon \to 0} (1+\epsilon)\frac{lnN}{N}$.

Figure 3.6 is the result of such investigation where the equilibrium magnetization $\langle m \rangle$ is plotted against the average degree of the graph $\langle k \rangle \approx pN$. We may point out that in this case, influence size is $I = 0$ and consequently, the analytical solution would predict the expected equilibrium magnetization $\langle m \rangle = 0$. It can be inferred from the graph that there exists a $\langle k_c \rangle \approx \ln N$ above which the mean equilibria of the systems do reach $\langle m \rangle = 0$ mean magnetization, and they are perfectly aligned with the analytical results. For $N = 50,\ 100$ and 200, the critical degree $\langle k_c \rangle = 3.9,\ 4.6$ and 5.3 respectively, which qualitatively match the critical average degree observed in Fig. 3.6; beyond these critical values the expected equilibrium magnetizations converge to $\langle m \rangle = 0$.

The significant difference of analytical solution on a random graph and a complete graph is the way the time parameter is scaled. It has already been shown that on a complete graph if the time is scaled as $\tau = t/N$, the convergence time is independent of the population size. On a random graph, with time scaled as $\tau = t/(N/p)$ the convergence time is independent of p as well as N. Figure 3.7 demonstrates this behavior. For the case with $p = 0.01$, since

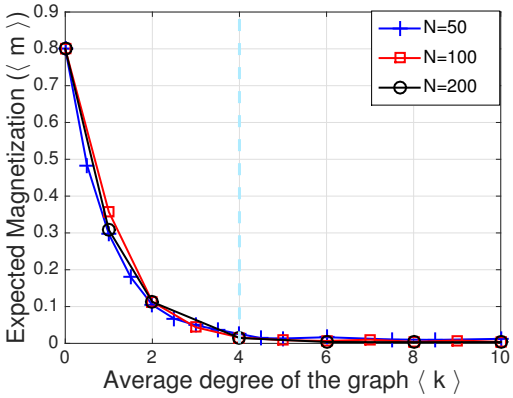

Figure 3.6: Effect of average degree $\langle k \rangle$ on the mean equilibrium density for different population sizes

the connection probability of the graph is lower than p_c, the system converges to a finite non-zero value of expected magnetization.

Essentially, this exercise and the preceding results provide us with the means of analytically predicting the mean value of magnetization with which the RVM system will stabilize and the convergence time when the network existing between the participating nodes can be modelled as a random graph. More importantly, we can determine the range of parameters where this analysis is meaningful. The random graph is a step closer to real networks between individuals.

3.6 RVM on a Lattice

Lattices are regular arrangements of points in the Euclidean space, and their applications are found in the analyses of various phenomena related to networked environments such as crystal formation, opinion evolution in societies, etc. Considerable attention has been given to the study of the Voter model on lattices and how such systems tend to organize into a single-opinion state in the absence of inflexible agents (or influences) [76]. In this section, first, the RVM is formulated and solved analytically on a one-dimensional lattice without the presence of influences. Then the solution is extended to the case of a general multi-dimensional lattice.

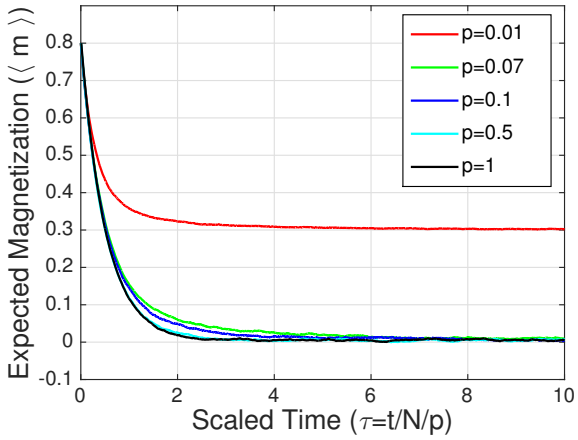

Figure 3.7: Effect of connection probability on convergence time of a system with $N = 100$ and $\tau = t/(N/p)$

On a regular lattice, based on the RVM, the rate at which the state of agent x changes to $-s(x)$ can be written as:

$$w(s(x)) = \frac{1}{2}\left(1 + \frac{s(x)}{z}\Sigma_{y:n.n.x}s(y)\right) \tag{3.13}$$

in which the sum is done over the nearest neighbors of site x. This rate is simply the probability of state transformation based on an agent's nearest neighbors' states. z is the coordination number of the graph and is assumed to be constant; i.e. periodic boundary conditions apply.

Clearly, transition rate of agent x is a linear function of the fraction of the agreeing neighbors. For instance, when an agent and all his neighbors agree, the transition rate is one, conversely, if all the neighbors disagree, the transition rate is zero. In contrast to previous sections where we studied the whole system using a magnetization factor, in this part, mean spin of an agent at point x namely $S(x) = \langle s(x)\rangle$ is studied to represent the individual behavior throughout the interaction process.

If a change of opinion happens at x, based on RVM, $s(x, t+1) = -s(x, t)$; as a result, the opinion at x changes by $s(x, t+1) - s(x, t) = -2s(x, t)$. Based on the previously obtained change rate, $w(s(x))$, the average opinion at x will evolve as:

$$\frac{dS(x)}{dt} = -2\langle s(x)w(s(x))\rangle \tag{3.14}$$

In the rest of the modeling, we will use $s(x)$ as a substitute to $s(x,t)$ for simplicity. By substituting Eqn. 3.13 in Eqn. 3.14 we will get:

$$\frac{dS(x)}{dt} = -S(x) - \frac{1}{z}\Sigma_i S(x+e_i) \tag{3.15}$$

in which e_i are the unit vectors of the lattice. The solution of this linear differential equation will reveal the temporal behavior of an agent at node x. This differential equation can be solved by introducing a one-dimensional Fourier transform considering x as the spatial variable and employing a generating function representation of the Bessel function $I_\nu(Z)$ for a part of the solution. The time evolution of the mean opinion of an agent at point x in one dimension becomes:

$$S(x,t) = I_x(-t)e^{-t} \tag{3.16}$$

For simplicity, the initial condition of $S(x, t = 0) = \delta(x, 0)$ is considered; that is, we start with a single $+1$ opinion (or spin) in a background population of undecided voters. It is important to note that the first agent is positioned at $x = 0$. The interested reader can refer to [76] for full details of the inspiration of this solution. For the general d-dimensional lattice, the rate equation becomes:

$$w(s(x)) = \frac{1}{2d}\left(1 + \frac{s(x)}{z}\Sigma_{y:n.n.x}s(y)\right), \tag{3.17}$$

Utilizing such a transition rate along with adopting a d-dimensional Fourier transform (one for each dimension), following the previous steps and assuming the same initial conditions, the time evolution of the mean opinion of an agent at point $x(x_1, x_2, ..., x_d)$ will be:

$$S(x,t) = \Pi_{i=1}^{d} I_{x_i}(-t)e^{-dt} \tag{3.18}$$

Analytical solutions have been plotted for nodes at sites $x = 0,\ x = 1$ and $x = 2$ on a one-dimensional lattice in Fig. 3.8. The results demonstrate how the mean opinion changes at the first 3 nodes in an infinitely long $1-d$ lattice. The blue plot for site $x = 0$ starts from 1 because the initial condition is assumed to be $S(x, t = 0) = \delta(x, 0)$. It starts decreasing immediately because of its interaction with node at $x = 1$. The node at $x = 1$ itself starts to

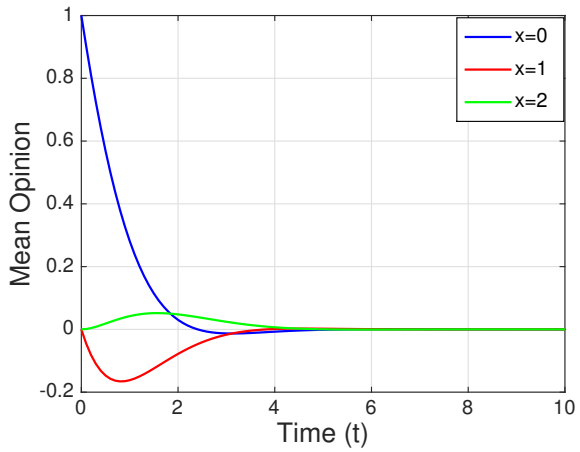

Figure 3.8: Evolution of mean opinion in nodes at sites $x = 0,\ x = 1$ and $x = 2$

dip below 0 because, out of its two neighbors, the node at $x = 0$ is more likely to be $+1$ and that interaction drives node at $x = 1$ opinion towards the -1 state. The effect is reversed for node at $x = 2$ and the oscillatory pattern continues for increasing node indeces.

The RVM on a lattice, as discussed above, can closely replicate the dynamics of traffic flow and lane change in a 2-lane highway. Before any interactions occur, the leading car (at node $x = 0$) has no reason to occupy the faster lane, hence almost surely, his state is $+1$. The rest of the cars (at nodes $2, 3, ...$ are equiprobably occupying either of the two available lanes (states ± 1). This gives rise to the initial condition, $S(x, t = 0) = \delta(x, 0)$. As soon as the cars start to interact, the mean choice for car at node 0 starts to shift towards an equilibrium value of 0, while that of node 2 dips below 0.

An interesting feature to note is that, the 'wave' for node 2 is phase-lagged from the wave for node 1, node 3 lags node 2 and so on. Also, the effect diminishes away from the seed node at site $x = 0$. The reason to this lagging behavior could be found in the initial condition and in the exponentially decaying behavior of the analytical solution.

To get a visual understanding of opinion evolution in lattices, a set of experiments were conducted on a two-dimensional lattice. Results of the experiments are presented in Fig. 3.9. White squares represent $+1$ state, and the black ones represent the -1 state. The system starts from the initial condition $m_0 = 0.8$ which is the reason there are more white squares than black ones in Fig. 3.9a. Through interactions the system is pushed towards its equilibrium state of zero magnetization. Eventually, a checkerboard-pattern is observed for

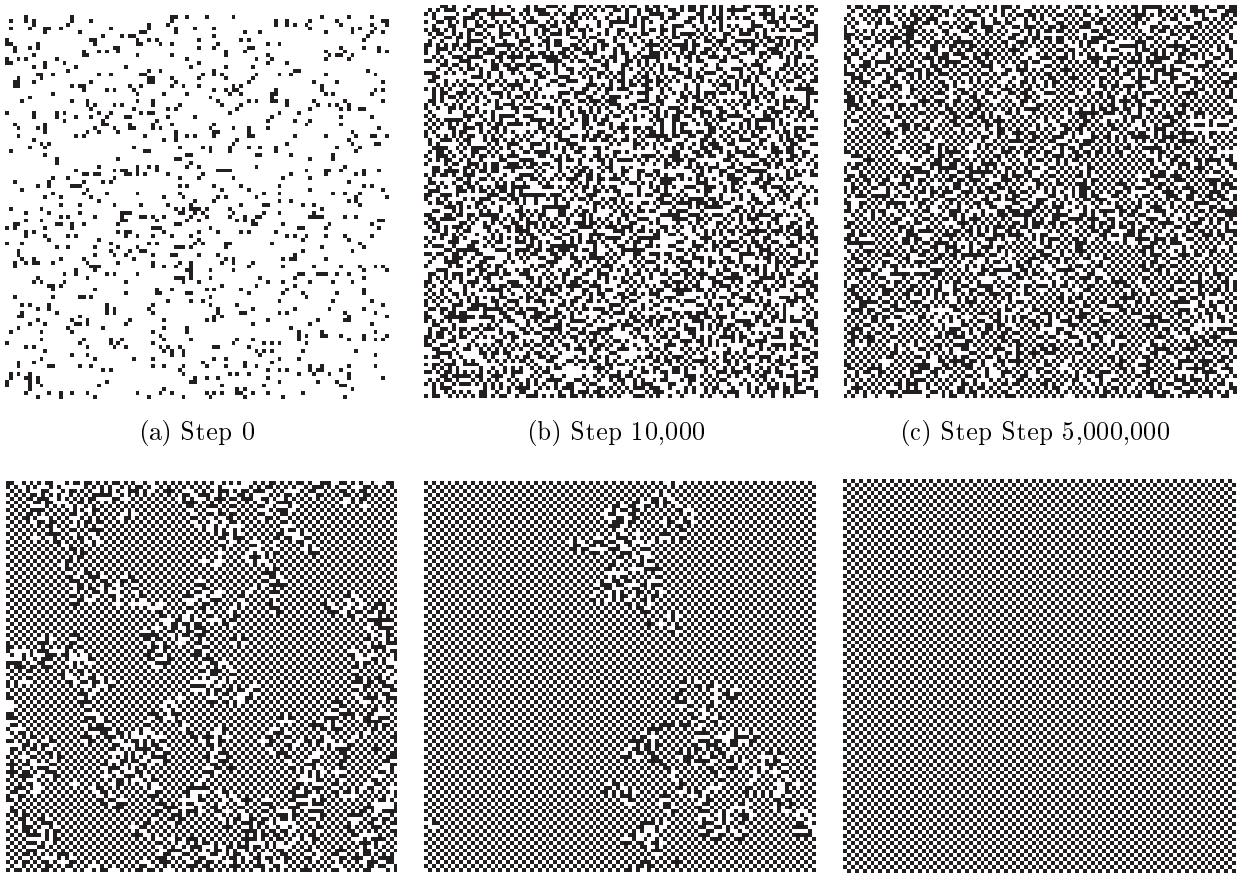

(a) Step 0 (b) Step 10,000 (c) Step Step 5,000,000

(d) Step 50,000,000 (e) Step 100,000,000 (f) Step 150,000,000

Figure 3.9: Opinion diffusion in a two-dimensional lattice

the converged system, as expected. Figure 3.10 show the progression of the magnetization factor of the system at different time steps.

3.7 Chapter Summary

In this chapter, a new interaction model has been introduced where each node repels rather than attracts its neighbors. First, the model is formulated on a complete graph and solved under the effect of influences at equilibrium. The equilibrium density $p_e(m)$ is derived as a function of the population size N, total influence size I and the control input $u = \frac{I_+ - I_-}{I}$. Then, the model is studied on a random graph with connection probability p. Analytical solutions for such a network is also derived at equilibrium point. Finally, the behavior of

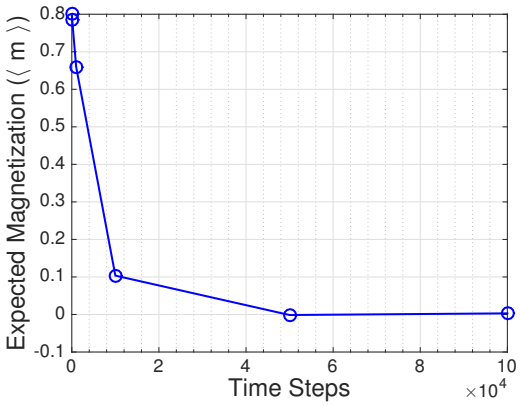

Figure 3.10: Magnetization versus time on the two-dimensional lattice

the model on a regular lattice is investigated which is followed by the analytical solutions for the system on a general d-dimensional lattice.

In the case of complete graph, even though the repulsive dynamics proved to be very stable around the zero magnetization state, some interesting characteristics were observed. The expected equilibrium magnetization is dependent on the population size as well as the size of the positive and negative influences, but it is invariant when all three are scaled identically. The distribution variance is a monotonically decreasing function of the population size. The time to convergence scales proportionately with the population size and is independent of influences. The validity of analytical results has been checked by means of extensive numerical simulations. We found good agreement between the results from numerical experiments and analytical results for network sizes exceeding $N = 100$.

For a random graph, it is shown that by modifying the time scaling, the same PDE may be obtained. On this network, too, the equilibrium density is dependent on the network size, number of influences, and the control input. However, the effect of connection probability is traceable only in the scaled time. Extensive Monte Carlo simulations verified that there exists a critical value of the connection probability p above which the existence of a fully connected graph facilitated the spread of opinion leading to a zero mean equilibrium magnetization. Finally, it is concluded that the convergence time of the model on a random graph is independent of both population size and connection probability only if the time is scaled as $\tau = t/(N/p)$.

Finally, analytical treatment of the Repulsive Voter model on a multi-dimensional lattice provided some interesting insight into the time evolution of mean opinion at every site in the lattice.

It is important to note that the nontrivial phenomenology we have witnessed in this chapter may lead to decision aids in design and policy making. However this is only valid under the strict assumptions of the Voter dynamics and simplified graph topology considered in this system. To address this issue and expand the applicability of the results, future studies should adopt the solution for more complex decision space and more realistic diffusion characteristics of opinions. Another important investigation area can be the application of the RVM dynamics on different network topologies, such as the configuration model, the small world topology and the scale free network.

Chapter 4

Effect of Zealots on the Opinion Dynamics of Rational Agents with Bounded Confidence

4.1 Objective

In the previous two chapters, we were able to mathematically model opinion evolution on different networks based on different interaction models (the Sznajd model and the Repulsive Voter model). These models have a few limitations:

- They are defined over a two-state opinion space (up vs down spins, or $+1$ vs -1).
- If interaction conditions are met, change of opinion in the agent is certain.
- Effects of environmental effects such as news and mass media cannot be included.
- Society level statistics are studied and individual level decision dynamics are ignored.

In this chapter, we try to develop a decision making algorithm which can include multiple states (instead of two) in the opinion space. Also, in this algorithm, change of opinion after interaction is not guaranteed. The algorithm can include effects of environmental stimuli. Additionally, the algorithm can track individuals' desire to change their opinions.

4.2 Introduction

To study the effect of social influence and interaction on emergent behavior, a statistical physics approach deals with a single basic question of social dynamics: how do local interactions between social agents create order out of an initial disordered situation? Much theoretical efforts have been devoted to clarify the implications on the macroscopic outcomes among other aspects of different interaction mechanisms (modelled by the Voter model [77], Sznajd model [27], Bounded Confidence model [78, 33, 79], as well as different topologies of the interaction networks (such as the complete graph, Erdős Rényi random graphs [55], the Watts-Strogatz small world network [80, 81], and the Barabási-Albert scale free topology [82]).

In all the above-mentioned models, opinions are modelized as numbers, integer or real. Each agent is initialized with a random number as their representative opinions. As interactions proceed, the agents rearrange their opinion variables, through mutual discussions. At some stage, the system reaches a configuration which is stable under the chosen dynamics; this final configuration may represent consensus with all agents sharing the same opinion, polarization with two main clusters of opinions ("parties"), or fragmentation where several opinion clusters survive. In all such evolutionary models of societies, the detailed behavior of each human, inherently the complex outcome of many internal processes, is largely overlooked. This gross simplification is justified by assuming that only higher level features such as symmetries, dimensionality, and topology of the interaction network are relevant for the global behavior of the society rather than microscopic details of individual motives, perceptions, and judgments.

In this chapter, we try to bridge this gap between microscopic and macroscopic studies of emergent behavior using an Agent-Based Model (ABM) in presence of influences. We incorporate individual judgment and decision mechanism parameterized as a Probabilistic Finite State Automata (PFSA) while observing the effect of interactions between these PFSA models and influences linked through a Barabási-Albert scale free network. The basic idea behind this PFSA-based discrete choice model (DCM) is that each decision maker chooses from a finite set of alternatives to maximize the potential cumulative reward s/he can collect

over several steps in the future, Fig. 4.1. The perceived reward for the different choices are negotiated by each individual through interaction with a subset of her/his neighbors whose reward values do not differ from hers/his by more than a chosen threshold (confidence bound).

To do so, we consider a society whose population are indecisive about supporting their government or opposing it by joining the rebellion group. The population includes a few influences who try to convince the population to join the rebellion group. We have created a setup which enables individuals to interact with other agents in their network, take into account different actions of the government, and then decide which of the two groups they should join or remain indecisive.

Section 2 discusses the PFSA-based discrete choice model used in this chapter. Section 3 explains elements of the social computation such as the interaction model and the network topology. Section 4 presents the results obtained from simulations along with necessary discussions. Finally, findings of this chapter are summarized and the chapter is concluded.

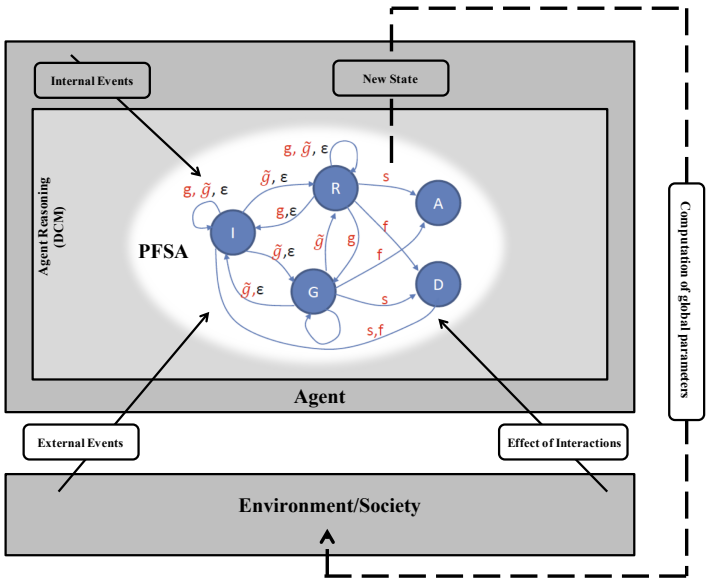

Figure 4.1: Schematic of the interaction between PFSA based individual logic mechanisms and the society. At each decision step, an individual chooses the most attractive state based on a utility maximization principle. This choice influences the reward estimates of each of his neighbors within his confidence bounds, who in turn choose the most attractive state. This cycle of interaction and reward update continues till equilibrium is reached.

4.3 Individual Decision Making Algorithms (IDMAs)

Assumption 1. Finite set of discrete choices

At each instant, every individual in the network is faced with the same set of finite discrete choices – for example, to vote for political candidate 'A' or 'B' or not to vote at all [83]. In Markov Decision Modeling [84] as well as in the current framework, the problem is posed as finding the optimal choice policy for maximizing the rewards gained as a result of one's own choices. It may be noted that this marks a departure from the usual setting in which the Krause and Hegselmann bounded confidence model is studied. To a degree, our model resembles the study of vector opinion dynamics such as those done by Axelrod [85] and several studies by Jacobmeier [86] and Fortunato et al. [87]. In vector opinion dynamics, the opinion has an integer number of components and the agents occupying the sites of a network communicate within the KH framework.

Assumption 2. Rational perspective

Individuals are assumed to be rational. This means they order the states into which they can reach, and they maximize something, reward function in the case of this chapter [83]. Subscription to the rational perspective does not suggest similar reactions from individuals under the same influence. But, it creates a rational structure for individuals' behavior. Since this behavioral logic will be encoded as a Probabilistic Finite State Automaton (PFSA) in the next section, rational perspective permits pairs of states without authorized transitions to exist.

Assumption 3. Probabilistic individual decisions

In the IDMA, decision making is not assumed to be a deterministic phenomenon, i.e. we assume that even when provided with the same conditions and reward vectors, different individuals may choose different decisions, and even the same individual can choose differently on different occasions [83]. The only constraint is that the choices should conform with the *rational perspective* (Assumption 2).

Assumption 4. Two kinds (external and internal (ε)) of events

External/global events simultaneously affect all individuals often resulting in uncontrollable large scale transitions in the society as a whole. In contrast, *internal/local* events represent the individuals' personal choices.

4.3.1 Normative Perspective Modelled as a Probabilistic Finite State Automata (PFSA)

The assumption of *rational perspective* allows individual behavior to be encoded as a PFSA. Even though the IDMA described in the last section is a generic mathematical structure which can be used to model various scenarios of emergent opinions, in this work, we study the specific case of a society in the cusp of a rebellion against the existing ruling power. In our simplified depiction of the situation, each individual faces the *internal* decision of supporting the existing government, supporting the rebelling group, or remaining in a state of indecision. Additionally, the individual can reach a state of political advantage, or disadvantage, but the uncontrollable transition to these two states can only occur through an *external* event, namely, the success or failure of the revolution. The five PFSA states and events are described in table 4.1.

Figure 4.2 gives a schematic of the assumed rational perspective encoded as a PFSA. It may be noticed that transitions such as $g : G \to R$ or $g : I \to R$ are unauthorized, since it is assumed that a favorable act by the government should not make anyone decide to join

Table 4.1: List of PFSA States and Events

States	Description	Events	Description
I	State of being undecided/neutral	g	A popular act by the government
R	State of supporting the Revolutionary group	$\tilde{g}$	An unpopular government act
G	State of supporting the Government	ε	An internal decision
A	State of political advantage	s	Success of the revolution
D	State of political disadvantage	f	Failure of the revolution

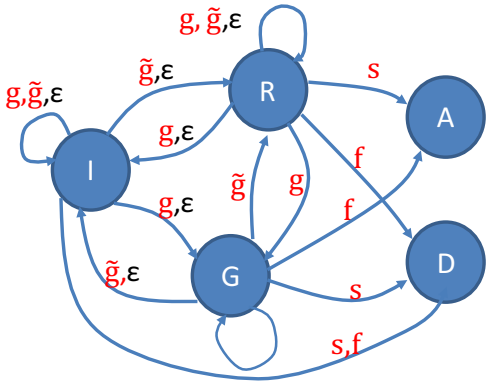

Figure 4.2: Schematic of normative perspective encoded as a PFSA

the opposing group. Also, the same event can cause alternate transitions from the same state; the actual transition will depend probabilistically on the measure of attractiveness of the possible target states. In the simplified model described, all events of the same type are clubbed together as g (popular) or $\tilde{g}$ (unpopular acts by the government). However, varying degrees of 'popularity' and 'unpopularity' of government acts can be encoded by creating separate groups $g_1, g_2, ..., g_n$ and $\tilde{g}_1, \tilde{g}_2, ..., \tilde{g}_m$ with different costs associated with these transitions.

4.3.2 Rewards, Transition Costs and Probabilities

The probability of transitioning from one state to another depends on three things - whether the target state is reachable from the current state, whether the current event acts as an impetus for state change, and whether the target state is relatively more attractive compared to the current state. The concept of *positive real measure of a sequence of events* is used to calculate the relative degree of attractiveness of states [88]. This is briefly explained next.

A finite state machine consists of states, inputs and outputs. The number of states is fixed; when an input is executed, the state is changed and an output is possibly produced. The probabilistic automaton is a generalization of the finite automaton structure and includes two probabilities: the probability P of a particular state transition taking place, and with the initial state q_0 replaced by a stochastic vector giving the probability of the automaton being in a given initial state.

With suitable definitions of the states, inputs and transition matrices, the PFSA structure is well-suited for quantifying the IDMA framework. Let the discrete choice behavior be modelled as a PFSA as:

$$G_i \equiv (Q, \Sigma, \delta, q_i, Q_m) \tag{4.1}$$

where $Q = \{I, R, G, A, D\}$ is the finite set of choices with $|Q| = 5$ and the initial state $q_i \in Q = I$; i.e. the whole society is neutral in the initial stage. The distribution of states may be represented as a coordinate vector of the form $\bar{v}_i$, defined as the $1 \times N$ vector $[v_1^i, v_2^i, ..., v_N^i]$, given by:

$$v_j^i = \begin{cases} 1 & \text{if } i = j, \\ 0 & \text{if } i \neq j. \end{cases} \tag{4.2}$$

$\Sigma = \{\varepsilon, g, \tilde{g}, s, f\}$ is the (finite) alphabet of events (inputs to the PFSA) with $|\Sigma| = 5$; the Kleene closure of Σ is denoted as Σ^*; the (possibly partial) function $\delta : Q \times \Sigma \times Q \to [0, 1]$ represents probabilities of state transitions and $\delta^* : Q \times \Sigma^* \times Q \to [0, 1]$ is an extension of δ; and $Q_m \subseteq Q$ is the set of marked (i.e. accepted) states. It may be noted that the parameters of the model introduced so far are a physical manifestation of the choices that each rational actor faces in an election scenario (as explored in [88]) - the choice set Q is well defined by the number of available options (parties to vote for, G and R in this case), and the initial state choice ($q_i = I$) allows the simulation to start from the same point every time. The effect of initial clustering of similar choices in regional and local neighborhoods can be an important factor. The transition probability δ signifies a parameter that the actors learn or estimate through their experience and understanding.

Definition. The reward from each state $\chi : Q \to [0, \infty)$ is defined as a characteristic function that assigns a positive real weight to each state q_i, such that

$$\chi(q_j) \in \begin{cases} [0, \infty) & \text{if } q_j \in Q_m, \\ \{0\} & \text{if } q_j \notin Q_m. \end{cases} \tag{4.3}$$

Definition. The event cost, conditioned on a PFSA state at which the event is generated, is defined as $\tilde{\pi} : \Sigma^* \times Q \to [0,1]$ such that $\forall q_j \in Q, \forall \sigma_k \in \Sigma, \forall s \in \Sigma^*$,

(1) $\tilde{\pi}[\sigma_k, q_j] \equiv \tilde{\pi}_{jk} \in [0,1)$; $\sum_k \tilde{\pi}_{jk} < 1$;

(2) $\tilde{\pi}[\sigma, q_j] = 0$ if $\delta(q_j, \sigma, q_k) = 0 \, \forall k$; $\tilde{\pi}[\epsilon, q_j] = 1$;

The event cost matrix, ($\tilde{\Pi}$-matrix), is defined as: $\tilde{\mathbf{\Pi}} = \begin{bmatrix} \tilde{\pi}_{11} & \tilde{\pi}_{12} & \dots & \tilde{\pi}_{1m} \\ \tilde{\pi}_{21} & \tilde{\pi}_{22} & \dots & \tilde{\pi}_{2n} \\ \vdots & \vdots & \ddots & \vdots \\ \tilde{\pi}_{n1} & \tilde{\pi}_{n2} & \dots & \tilde{\pi}_{nm} \end{bmatrix}$

The characteristic vector $\bar{\chi}$ is a numerical depiction of an individual's perception of expected benefits or "rewards" to be obtained by being in a particular state. For example, if the states represent various job choices, the remuneration from these jobs can serve as the characteristic vector. On the other hand, the event cost is an intrinsic property of the nominal perspective. The event cost is conceptually similar to the state-based conditional probability of Markov Chains, except $\sum_k \tilde{\pi}_{jk} = 1$ is not allowed to be satisfied. The condition $\sum_k \tilde{\pi}_{jk} < 1$ provides a sufficient condition for the existence of the real signed measure as discussed in [89].

Definition. The state transition function of the PFSA is defined as a function $\pi : Q \times Q \to [0, 1)$ such that $\forall q_j$, and $q_k \in Q$,

(1) $\pi(q_j, q_k) = \sum_{\sigma \in \Sigma : \delta(q_j, \sigma, q_k) \neq 0} \tilde{\pi}(\sigma, q_j) \equiv \pi_{jk}$

(2) *and* $\pi_{jk} = 0$ *if* $\{\sigma \in \Sigma : \delta(q_j, \sigma) = q_k\} = \emptyset$.

The state transition matrix, (Π-*matrix*), is defined as: $\mathbf{\Pi} = \begin{bmatrix} \pi_{11} & \pi_{12} & \dots & \pi_{1n} \\ \pi_{21} & \pi_{22} & \dots & \pi_{2n} \\ \vdots & \vdots & \ddots & \vdots \\ \pi_{n1} & \pi_{n2} & \dots & \pi_{nn} \end{bmatrix}$

4.3.3 Measure of Attractiveness of the States

A real measure ν_θ^i for state i is defined as:

$$\nu_\theta^i = \sum_{\tau=0}^{\infty} \theta\,(1-\theta)^\tau\, \bar{v}^i \Pi^\tau \bar{\chi} \tag{4.4}$$

where $\theta \in (0, 1]$ is a user-specified parameter and $\bar{v}^i$ is defined in Eqn. 4.2.

Remark. Physical Significance of Real Measure

Assuming that the state probability vector is $\bar{v}_i$ corresponding to the current state of the Markov process (i), at an instant τ time steps in the future, the state probability vector is given by $\bar{v}^i\Pi^\tau$. Consequently, the expected value of the characteristic function is given by $\bar{v}^i\Pi^\tau\bar{\chi}$. The measure of state i described by Eqn. 4.4, is the weighted expected value of χ over all time steps in the future for the Markov process that begins in state i. The weights for each time step $\theta\,(1-\theta)^\tau$ form a decreasing geometric series (sum equals to 1). The measure in vector form yields

$$\bar{\nu}_\theta = \theta\left(\mathbb{I} - (1-\theta)\,\Pi\right)^{-1}\bar{\chi} \qquad \text{and} \qquad \bar{\nu}_{norm} = \frac{1}{\sum_k \nu_k}\bar{\nu} \tag{4.5}$$

Remark. The effect of θ

The rate at which the weights decrease with increasing values of τ is controlled by θ. More importance is put on the states reachable in the near-future if parameter θ assumes large values (close to 1) because of the fast decay in the weights. The states through time are more uniformly weighted for small values of θ allowing the system to interact with a large neighborhood of the connected states.

The probabilistic decisions are made based on $\bar{\nu}_{norm}$. The discounted expected reward of a state is proportional to the measure of that state. Higher measure of a state corresponds to a higher discounted expected reward, hence the potential to make a transition to that state is higher.

4.4 Elements of Social Computations

The dynamics of the KH Bounded Confidence model is very simple: one of the agents is chosen at random; then, the agent adopts the average opinion of its compatible neighbors [90, 91]. Compatibility between two nodes is determined by the distance between the current opinions held by the two nodes. The procedure is repeated by selecting another agent randomly and so on. The type of final configuration reached by the system depends on the value of the confidence bound d. For a complete graph, consensus is reached for $d > d_c$, where $d_c \simeq 0.2$ or 0.5, depending on whether the average degree of the graph diverges or stays finite when the number of vertices goes to infinity.

In this chapter, it is assumed that the interaction is entirely through the characteristic function χ of the states [92]. This assumption is based on the insight that the anticipated reward from a state is the most well-discussed and well-broadcast quantity in a social network [93, 94]. The update rule for the reward vector of agent i due to interactions with its neighbors is as follows:

$$\bar{\chi}^i_{t+1} = \bar{\chi}^i_t + \mu.(\bar{\chi}^i_{t_{neighbors}} - \bar{\chi}^i_t) \tag{4.6}$$

where $\bar{\chi}^i_{t_{neighbors}}$ is the *mean reward vector* of the first-order neighbors in the network of agent i at time step t. Following the notion of bounded confidence, only those neighbors whose opinions are within $\chi(q_j) \pm d, \forall j$ contribute to the opinion update of agent i. Here, μ (or the convergence parameter) is the weight which determines how much an agent is influenced by the other one.

Since many networks in the real-world are conjectured to be scale free including the World Wide Web, biological networks, and social networks, in this study, a BA extended model network created by the Pajek software program is used. Table 4.2 presents the parameters of the network. In addition, one of the experiments is repeated on a complete graph topology for comparing the results related to different networks.

4.4.1 Numerical Simulations

In this chapter, a population of 100 people are initialized and assigned a random number drawn from a uniform distribution $U(0, 1)$, representing the time remaining before that

Table 4.2: List of parameters used for BA scale-free network

Number of vertices	100
Number of initial disconnected nodes	3
Number of added/rewired edges at a time	2
Probability to add new lines	0.3333
Probability to rewire edges	0.33335

person makes a decision. This imposes an ordering on the list of people in the network. As soon as someone makes a decision, the time to her/his next decision, drawn from $U(0,1)$, is assigned and the list is updated. Additionally, external events g and $\tilde{g}$ are also associated with a random time drawn from $U(a,b)$. Choosing a and b, the external events can be interspersed more or less densely.

At t_0, all 100 individuals are initialized at state I. Initial values of a mean reward vector $\bar{\chi}_m$ and the true event probabilities are fixed. Individuals receive a noisy estimate of the true probabilities and the rewards. At the time epoch t_k when it is the i^{th} person's turn to make a decision, s/he updates his personal estimate of the reward vector according to the influence equation (Eqn. 4.6). S/he then calculates the degree of attractiveness of the states based on the normalized measure using Eqn. 4.5. The transition probabilities are calculated as $P(q_{t_{k+1}} = q' | q_{t_k} = q, \sigma = \sigma') = \nu_{norm}(q') R(q, \sigma', q')$ where $R(q, \sigma', q') = 1$ if $\sigma' : q \to q'$ exists, otherwise 0. The only difference in the case of an external event such as $g, \tilde{g}, s$ or f is that everyone simultaneously updates their states rather than asynchronously, as in the case of internal events. Alg. 1 describes how numerical simulations of this study have been conducted.

4.4.2 Effect of Influencing Agents in Decision Making

In this chapter, the influences are treated as indistinguishable except for the fact that they never update or change their $\bar{\chi}$ values; moreover, they do not make decisions, and stay in the same state of mind during the entire simulation. Also, it is typical that the influences are serving a certain agenda, in this case, trying to mobilize forces to join the rebellion. But, this influence is exerted very passively, by advertising a higher value for $\chi(R)$ and lower values

Algorithm 1: Interactions and decision making

Data: N, μ, d, θ, Influence size, network

Initialization: Randomly order nodes and events;
while *Not converged* **do**
  for *Node* i **do**
    Update $\bar{\chi}^i_{t+1}$ from Eqn. 4.6;
    Update $\bar{\nu}^i_{norm}$ from Eqn. 4.5;
    Update state for Node i;
    Insert Node i randomly in the ordered list;
  end
  if *an external event occurs* **then**
    Update $\bar{\chi}^i_{t+1}$ $\forall i \in N$;
    Update $\bar{\nu}^i_{norm}$ $\forall i \in N$;
    Update state for all nodes;
  end
end

for all other states as:

$$\chi^I(q_j) = \begin{cases} \chi_m(q_j) - \Delta & \text{if } j = 1, 3, 4, 5, \\ \chi_m(q_j) + \Delta & \text{if } j = 2. \end{cases} \tag{4.7}$$

in which $\chi^I(q_j)$ represents the reward associated with state q_j for influence nodes, and $\bar{\chi}_m$ is an estimate of the reward values expressed by the whole society on an average. Δ is a parameter adjusting the strength of influences (control input). In a situation where influences have to favor other states, the corresponding element in the mean reward vector needs to be strengthened.

4.5 Results and Discussions

This chapter investigates the simultaneous interplay between two separate subsystems, namely a logical decision making subsystem, modelled by a PFSA and the interaction and influence subsystem, modelled by Bounded Confidence. Parameters of each subsystem is investigated separately. Moreover, each simulations is conducted in two phases. During the first phase (*decision epoch* ≤ 5000) the dynamics of the opinion evolution is studied without

introducing the effect of influences. In the second phase (*decision epoch* > 5000), a group of 10 influences is activated.

4.5.1 PFSA Parameters

External Events: in the first set of experiments, the ratio of occurrences of "good" and "bad" external events, $r = P(g) : P(\tilde{g})$ is varied to observe the effect of long term government policies on a population. Each simulation was run 30 times and the average of all the runs are showed in Fig. 4.3.

Effects of external events can be observed in the first phase (decision epoch≤ 5000) of each subfigure. When $r = P(g) : P(\tilde{g}) = 1 : 1$, the percentage of the population in states R and G are equal, and a large part of the population remains undecided (Fig. 4.3a). In the absence of any deadline for making a decision this result is only to be expected. As the government starts to push more and more unpopular policies, opinions bifurcate and the

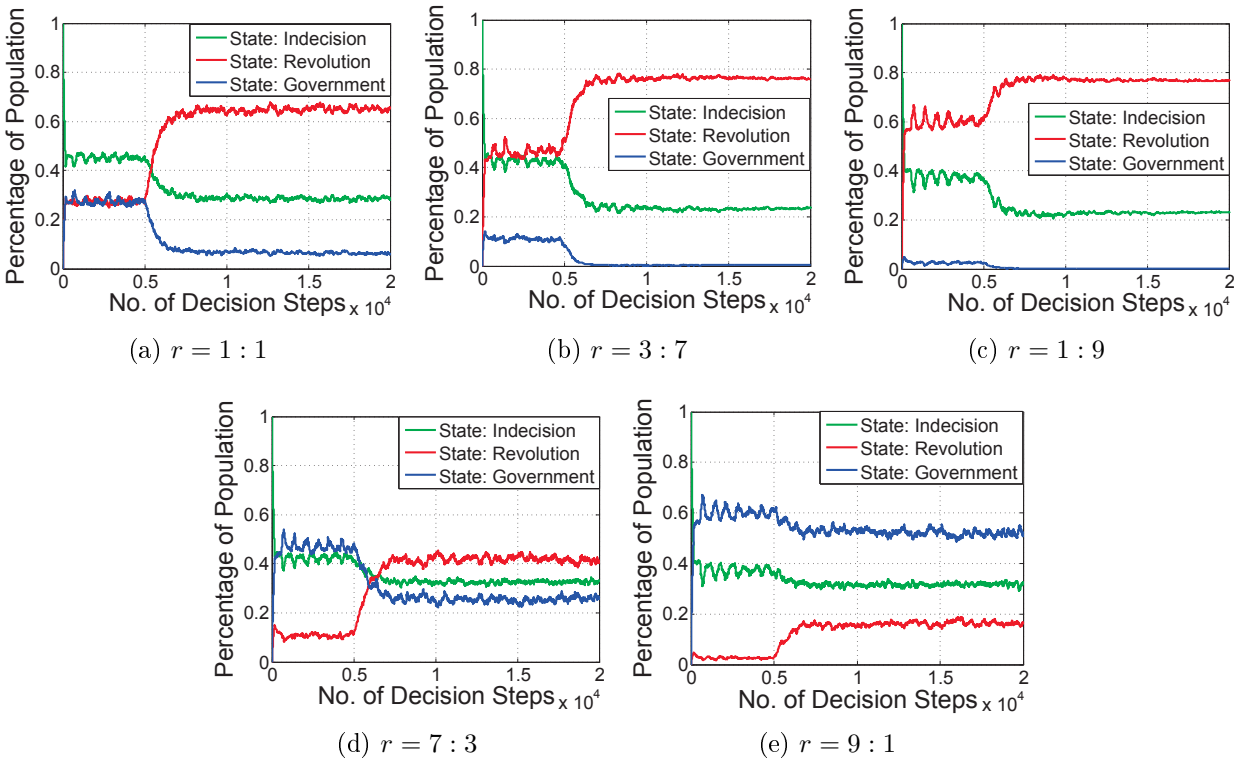

(a) $r = 1 : 1$ (b) $r = 3 : 7$ (c) $r = 1 : 9$

(d) $r = 7 : 3$ (e) $r = 9 : 1$

Figure 4.3: Effect of external events on the final state distribution of the society with $|I| = 10$ and $\Delta = 0.3$

rebellion group starts to become more popular. Distribution of the society between the 3 states varies monotonically with r.

Presence of influences in the second phase causes a dramatic change in system behavior. In each of the influenced cases (Fig. 4.3), the percentage of the population in state R starts to increase rapidly as soon as the influencing nodes are activated. Interestingly, the length of the transition phase between the initial (uninfluenced) distribution and the final steady state is independent of r (Table 4.3). The final steady state distribution, on the other hand is affected both by r, and I. In Fig. 4.3e, the number of popular policies by the government is high enough to overcome the effect of influences, and therefore, a smaller portion of people are converted to join the rebellion state. It may be noted that the quick transition period is a clear indication of the narrow window of opportunity available to intervene and prevent the society from transitioning into instability.

Table 4.3: Convergence time related to different ratios in Fig. 4.3

r	1 : 9	3 : 7	1 : 1	7 : 3	9 : 1
Convergence Time	6958	6940	6986	6856	6739

Comparison of IDMA with Standard Interaction Models: a focus on network structure and large scale dynamics rather than individual behavior have successfully put forward several elegant theories of emergent social behaviors such as evolution of opinions, consensus formation, properties of elections, and formation of a common language.

In order to gauge the relative expressive power of such a simple interaction dynamics with the IDMA framework developed in this study, we directly compare the results obtained by implementing the more complex IDMA framework with that of a well-established but simple model of social interaction, namely the Voter model where at each step, an arbitrarily chosen node imitates the state of an arbitrarily chosen neighbor. We use the same parameters to make the comparison reliable such as the same BA scale free network, and consider a population of indecisive people alongside a few influences who promote joining the rebellion group. In this setup, people can stay in the indecisiveness state, or they can join either the rebellion group, or the group which supports the government. Again, influences enter the simulations after the $5000th$ decision step, Fig. 4.4.

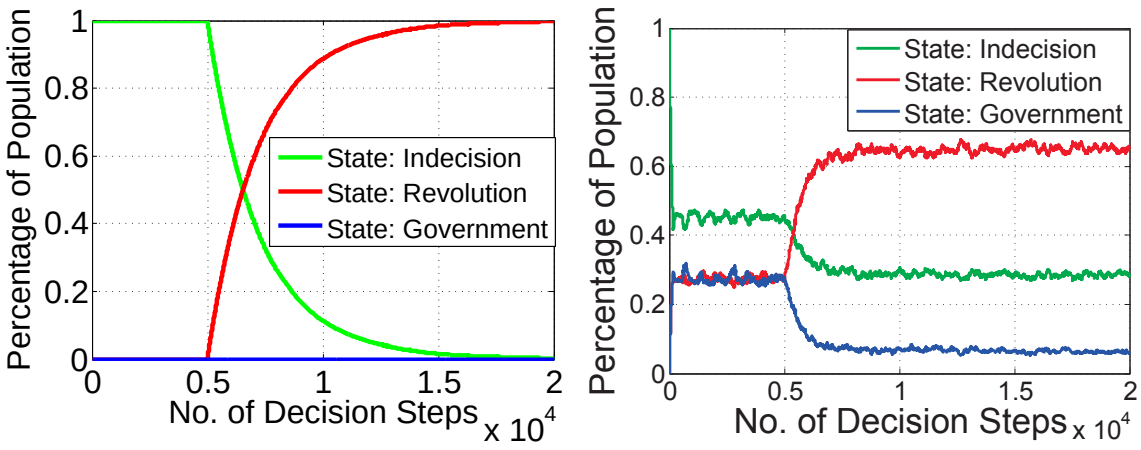

(a) Voter Model (b) $r = 3 : 7$

Figure 4.4: effects of incorporating an IDMA

One of the shortcomings of the Voter model becomes apparent from the first phase of the simulations; since the Voter model runs purely on imitation, starting from an initial condition where all agents are in the state of indecisiveness, none of them is able to change their state to another one. Conversely, when IDMA is included in the model, with the help of the reward vector, effects of external events can be taken into account resulting in opinion change of agents in this region.

Another drawback of the Voter model can be seen in the second phase of the simulations. As soon as influences are activated, the number of people supporting the revolution increases; and finally converges to one of the stable equilibria where all nodes cluster in the R-state. This phenomenon is rather unrealistic. However, in the model with IDMA, although this increase is seen, this is limited by the heterogeneity in the probabilistic decision making logic of individuals. Most importantly, this model can thus predict and converge to multiple equilibria, rather than just the three unrealistic pure states where the Voter model converges. Considering these factors, the benefits of incorporating rational decision making in opinion change models become apparent though it comes with added layers of complexity.

4.5.2 BC Model Parameters

Distance Parameter (d) and the Control Input Δ: the influences deliberately advertise biased reward values in an attempt to pull the population slowly towards the state of their choice (R, in this chapter). The amount of bias (Δ) is vitally important since too high of an offset would cause the influences to drift outside the confidence bound of the general population, and consequently they will not be able to enter into dialogues with the undecided nodes. On the other hand, a very low Δ will not have a pronounced effect on the dynamics of opinion evolution and will not be able to produce a substantial change on a global scale.

Since Δ may be thought of as an opinion bias adopted by the influencing group in order to "control" the final distribution of people over the different states, we call Δ the control input. d is the distance parameter that determines the bound in the Bounded Confidence model. For simplicity, the effect of d and Δ are presented here only with respect to the state R,Fig. 4.5. The results for other states are qualitatively equivalent. Higher values of Δ mean stronger influences exist in the society whose reward vectors have been altered significantly (Eqn. 4.7). Hence, for low values of d, agents do not interact with influences causing no change in the system behavior. However, for low values of Δ, although agents interact with influences, the influences are not strong enough to seriously affect the system behavior.

As an example, for an intermediate confidence bound ($d = 0.3$), agents can interact with strong influences resulting in noticeable changes in the behavior. However, if the control Δ is too high, influences lie out of the confidence zone of agents. So, although present,

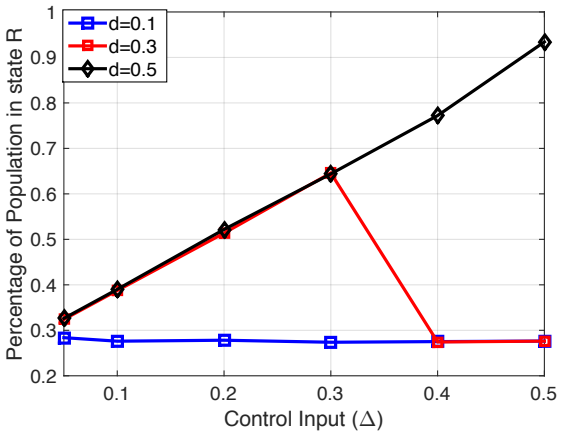

Figure 4.5: Dependence of the dynamics of the R state on d and Δ with $|I| = 10$

influences cannot affect the society. For $d = 0.5$, agents are able to interact with even stronger influences. Consequently, a higher percentage of the population is in state R. From a social psychology perspective, it is very important to estimate the bound of confidence for individual groups in order to be effective in bringing about positive change. The optimal approach when trying to impact an older population may not be similar to the control parameter suitable for younger demographics.

Convergence Parameter: based on Eqn. 4.6, the convergence parameter determines the influenceability of a node, i.e. to what extent a node adheres to his personal estimates of anticipated rewards from a choice as opposed to converging to the mean estimate gathered from his first-order neighbors. $\mu = 0$ implies complete self-reliance while making decisions, whereas $\mu = 1$ implies complete malleability. It may be conjectured that, larger μs might lead to fewer steps required for convergence for the population as a whole. This conjecture is validated in Fig. 4.6.

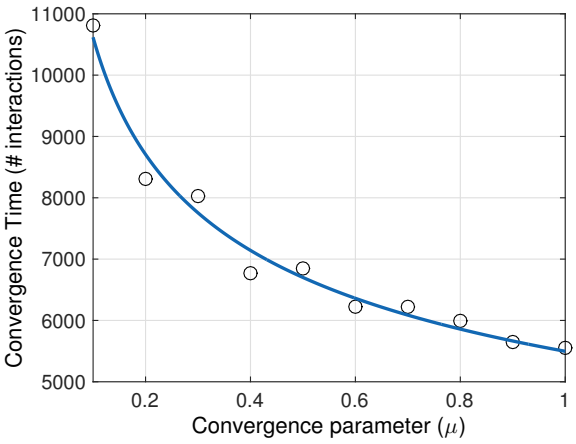

Figure 4.6: *Effect of μ on convergence time*

Clustering Behavior: formation of clusters is a typical behavior observed in the Bounded Confidence (BC) model. The distance parameter d determines the number of clusters in the equilibrium state of a system. Large values of d results in interactions among a large number of nodes, and consequently very few clusters emerge [78]. This phenomena is visualized in Fig. 4.7. As the distance parameter increases, the number of clusters decreases.

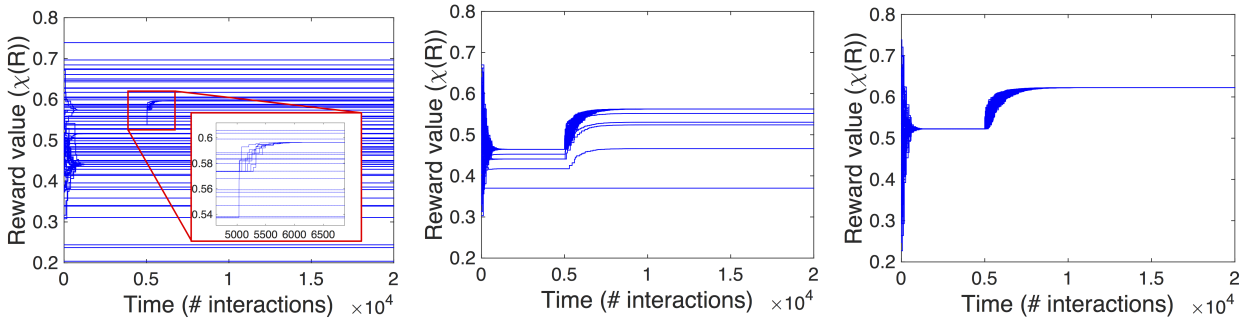

(a) $d = 0.1$ (b) $d = 0.3$ (c) $d = 0.5$

Figure 4.7: Clustering behavior of the BC model for different d's with $|I| = 10$

Addition of influences after 5000 decision epochs adds a layer of complexity to the clustering process. The influences effectively attract and cluster nodes, but in societies with low confidence bounds ($d = 0.1$), the effect is very local. Most clusters retain their identities and never enter into any interactions outside their own clique. This is demonstrated in Fig. 4.7a where the small effect of the influences is illustrated in the inset. Broadly speaking, this implies that societies which are highly clustered due to low confidence bounds are more difficult to influence, unless all the nodes are very homogeneous to begin with. An increase in d allows more agents to interact (with each other as well as with influences), and therefore a more populated cluster forms around influences ($d = 0.3$). Finally, when $d = 0.5$, the influences are reachable to all agents resulting in only one cluster around influences.

Varying Control Input $\Delta(t)$: so far, the influences have always been treated as static agents; i.e. the pro-revolution value of $\chi^I(q_2)$ was fixed and unchanged during the course of the simulation. The motivation behind studying varying control input (Δ) is to investigate whether a small group of influences can start from a popular stand-point, cluster the population around themselves, affect them continuously without getting out of population's confidence bound, and guide them to a different set of rewards ($\bar{\chi}$) which ultimately get filtered through the IDMA to support of a different state. To do so, a new set of experimentations have been conducted using the exact same model; however, the χ value of influences increases linearly as a function of time steps with a rate of r.

The results of these experiments are shown in Fig. 4.8. Results are presented based on the distance parameter d and the rate r. The red graph represents the χ value of influences at each time step. Fig. 4.8 depicts that for a specific distance parameter, there is a threshold for r after which the influences get strong so fast that the society looses its reach to influences. For example, in Fig. 4.8a, the increase rate is low resulting in a homogenous population clustered around influences. However, as r increases, clusters appear both in and out of the reach of influences, Fig. 4.8b. Finally, after the threshold, the whole society looses its reach to the influences, Fig. 4.8c, rendering their presence in the society obsolete. The same reasoning can be applied for Figs. 4.8d, e, f.

It can also be seen that the threshold for r depends on the distance parameter d. When $r = 0.0005$, $d = 0.3$ produces a cluster who do not get affected by the influences, but $d = 0.5$ produces a homogenous population grouped around influences. Or, in the case of $r = 0.001$, $d = 0.3$ results in a society which does not interact with influences, however, $d = 0.5$ results

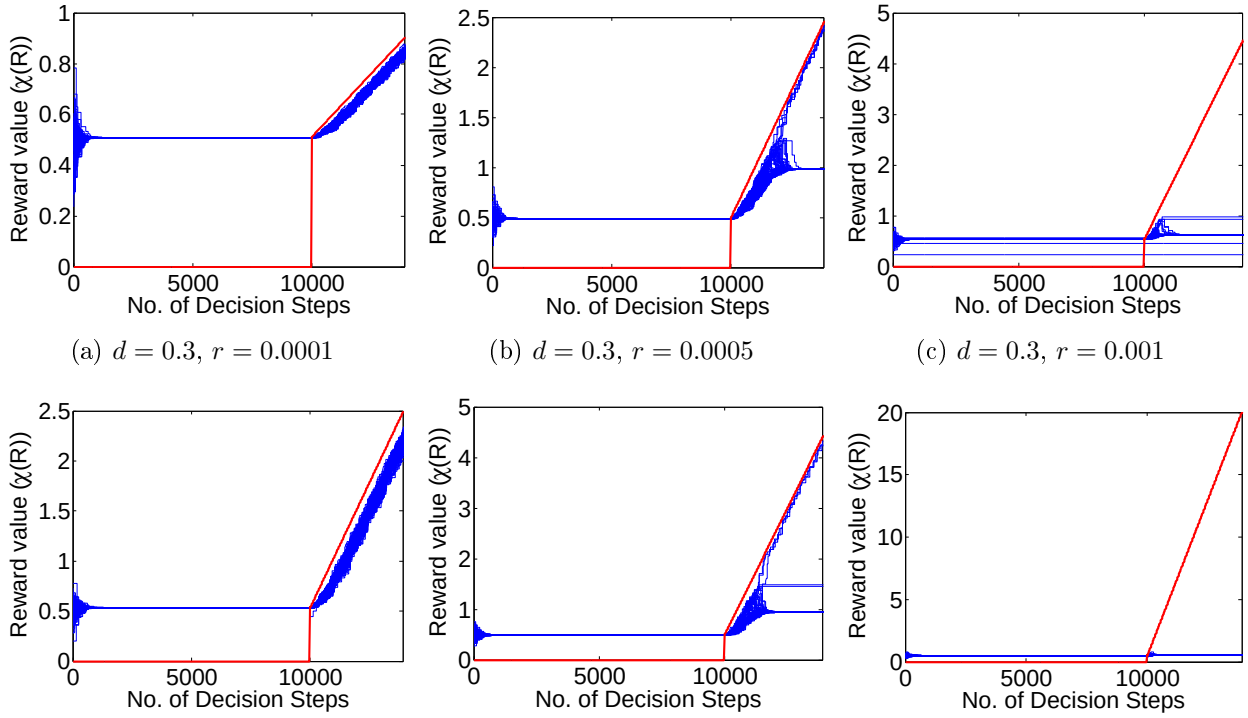

(a) $d = 0.3$, $r = 0.0001$ (b) $d = 0.3$, $r = 0.0005$ (c) $d = 0.3$, $r = 0.001$

(d) $d = 0.5$, $r = 0.0005$ (e) $d = 0.5$, $r = 0.001$ (f) $d = 0.5$, $r = 0.005$

Figure 4.8: Clustering behavior of a society in the presence of influences with variable control input

in a society with clusters both in and out of the reach of influences. This phenomenon is in line with the findings of the previous section.

The interesting finding of these experiments is the fact that although for some rates the influences get out of the reach of individuals very fast, in the time interval when they do interact with individuals, the whole society is affected by their presence. For example, in Fig. 4.8b, in the first few time steps, most of the society start lagging the influences, but they cluster again at a higher level of reward values. This means that the society is more inclined towards the rebellion state (although influences are out of reach) in comparison to the period when influences were absent.

Effect of Network Topology: figure 4.9 provides a comparison of the time evolution of the BC interactions deployed on a BA network and on a complete graph. Intuitively, the complete graph promises to have a faster dynamics since the average degree of each node is higher and influence should propagate faster. Conversely, results from numerical simulations indicate the opposite; influence propagation through the BA network is faster (measured by a smaller transition period between initial and final states). This can be qualitatively explained by the fact that the relative influence on each node from the influences is much lower when the nodes are connected through a complete network. The presence of many links from other regular nodes dilute the effect of the influencing nodes leading to a slower

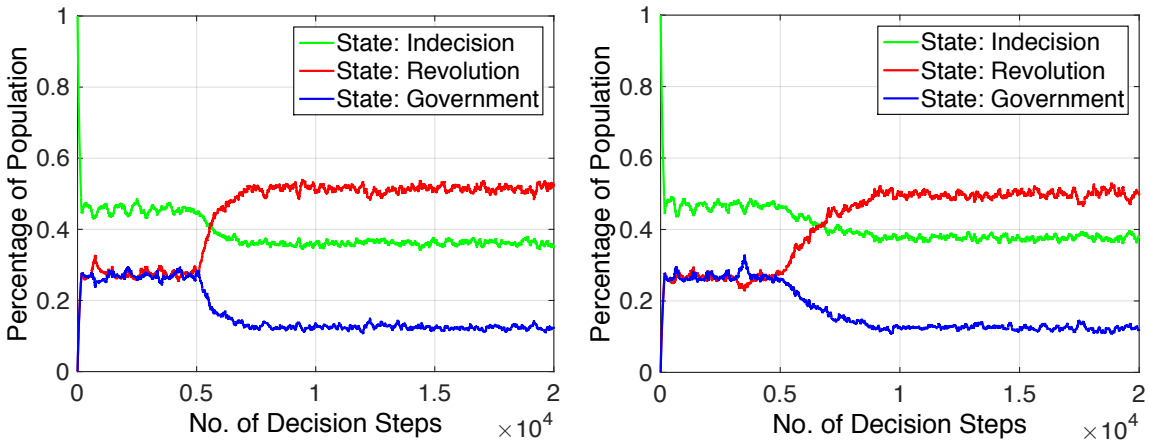

(a) BA Network (b) Complete Graph

Figure 4.9: Effect of different network types on the final state distribution with $|I| = 10$

change and a lower percentage of the population in state R at equilibrium. The convergence times for the two networks under discussion are reported in Table 4.4.

Table 4.4: Comparison of characteristics related to two different Networks

Network	Convergence Time	Percentage of population in R
BA	6624	51.51
Complete Graph	8156	49.98

4.6 Chapter Summary

This chapter attempts to incorporate a micro-level decision making paradigm along with a social interaction model (Bounded Confidence) in presence of influences (zealots). Every agent in the society is given a decision making ability (to choose from a fixed set of states). The decision making is based on maximization of accumulated rewards gained as a result of an individual's own choices in presence of different events.

The effects of interactions and events on the final distribution of decision states are studied with and without the presence of influences. Bounded confidence model parameters (the distance parameter and the convergence parameter) are used to study the final distribution of states and the time the society needs to reach its equilibrium (convergence time). Moreover, effects of network topology on the final distribution of states, convergence time, and dynamic of the society is presented.

It is observed that without influences, the final distribution of states is purely a function of the external events; more unpopular policies by the government result in higher percentages of people joining the rebellion group. However, presence of influences causes a rapid change in the behavior of the system in favor of the group they support (state R). A short transition period is required for the system to reach equilibrium after the influences are activated.

It is shown that no change in the final distribution of states takes place unless influences are in the confidence bound of the population and at the same time, have large enough offsets. The clustering behavior of the BC model is visualized for different values of the distance parameter. It is concluded that the time interval needed for a system to reach its equilibrium decreases as the convergence parameter increases. In addition, the effect of

varying inflenceability is studied. Results show that there is a limit for the influence rate so that the society can keep up with the influences, and that limit depends on the distance parameter.

Finally, simulations reveal that not only is influence propagation slower in the society when agents have higher number of links (complete graph network), but also their effect in the final distribution of state R is weaker too.

Chapter 5

An Experimental Study on the Controllability of Collective Human Behaviors in Networked Societies

5.1 Objective

In the preceding chapters, the main focus of this thesis was theoretical development of concepts related to opinion evolution and effect of influences in networked societies. To do so, mathematical models were developed, analytical solutions were derived, and numerical simulations were provided. However, both the literature and this thesis lack experimental studies on the effect of influences on collective behavior of groups. This chapter provides an experimental setup along with different experimental scenarios to study the effect of influences on collective human behaviors.

5.2 Background

Effect of influences (control inputs) on the behavioral dynamics of a group of people has been one of the focal points of social psychology studies for years - group psychology and attitude change being studied through small-scale group experiments. From word-of-mouth marketing studies and mathematical study of virality and meme propagation, it has been

shown that using influences is an effective way to change the behavioral dynamics of groups [64, 95, 96]. This chapter aims to expand on a series of experiments from 2006 performed by Kearns et al. [97] to gain a better understanding of the effect of influences on a group in collaboratively solving a puzzle.

Kearns et al. [97] studied the effect of different network structures on the behavioral dynamics of people by the use of the well-known "Graph Coloring Problem". In this game, every individual (player) is in charge of a node on the network, and the collective goal is for every player to select a different color for their node that is different from the colors of all of their network neighbors [98]. The number of available colors in the experiment is equal to the Chromatic Number of the network which is the minimum number of colors necessary to color the entire network without any conflicts. The graph is "solved" when there are no conflicts in the graph (no two nodes with the same colors are attached to each other). In this work, it is concluded that the higher the complexity of the network, the harder it is for the participants to solve the graph. The metrics of this study are the frequency of "successful" solutions, and the Average Solution Time (AST).

We have modified the graph coloring problem description to make it suitable to quantitatively study the effect of influences on this collective behavior. Additionally, the graph coloring problem mimics the dynamics of the Repulsive Voter Model introduced in chapter 3 when the chromatic number of the network is 2. We define influences as individuals who collectively select a unique solution to the particular network under consideration, assume the colors representative of that solution and never change their color during the experiment. These influences can be hidden or known. We have chosen only two types of the networks, from the previous study [97], small world and scale free. These networks are visualized in Fig. 5.1. The chromatic number of the small world network is 2, whereas the chromatic number of the scale free network is 3.

5.3 Experimental Setup

This section explains all the details of the experimental setup. In [97], the effect of parameters such as social status, level of friendship, people's feelings, etc. is eliminated by using an online

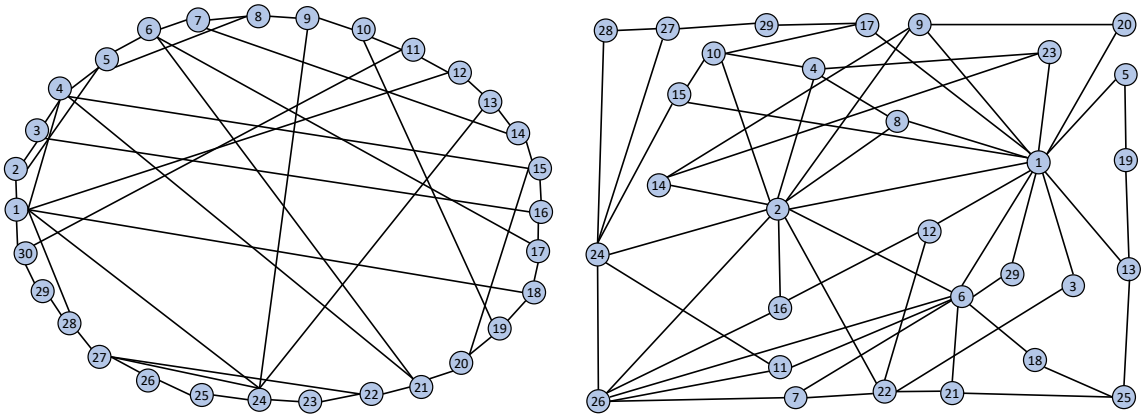

(a) Small World Network (b) Scale Free Network

Figure 5.1: Networks used in the experiments

network. Each participant is assigned the control of a node in the network, and they can interact only through the network. We have created our networked game on UnrealEngine4.

After everyone playing the game logs in, they are randomly connected to each other based on a pre-designed network representing which nodes are socially connected. As the participants click through their choices (colors), these choices are recorded for each user's identifier along with a time stamp corresponding to the time when each decision is made. The full set of information passed to each user in the game's interface is (Fig. 5.2):

1. The progression of the game.
2. The opinion of his/her anonymous network neighbors.
3. The conflicts between the participant and his/her neighbors.
4. The remaining time.

In our experiments, participants are university undergraduate and graduate students. In each experiment, depending on the scenario under study, there are approximately 30 students from a selection of different disciplines. Each experiment is programmed to stop when the graph is solved or otherwise at 5 minutes, and each scenario is conducted 6 times. Students have the option to not participate and are provided with an informed consent document. Figure 5.2 represents the physical setup of the experiments.

(a) User Interface (b) Physical Setup

Figure 5.2: Physical setup of the experiments and game's user interface

5.4 Experiment Scenarios and Results

In this section, different experiment scenarios and their results will be presented. The order of experiments and results does not necessarily follow the order of the actual experiments.

5.4.1 Scenario 1. Benchmark (BM)

In this scenario there are no influences present, and it is designed as a benchmark and a basis for comparison. We witness a lot of similarity between the results of our experiments and those of [97]; In our experiments, too, it is harder to solve the network with higher complexity (scale free). In our experiments, the small world network is solved 5 times, and the scale free networke is solved once. In [97], the small world network was solved 6 times, and the scale free networked was solved 2 times. The slight difference in the results of our experiments and those of [97] follow from the fact that the network sizes and consequently their structures are not exactly the same in these two studies.

Futhermore, our analysis shows that in most of the unsuccessful experiments, 98% of the graph is solved, and the only conflicting nodes are the nodes with high number of connections. If one of the nodes changes its color to resolve only one conflict, then up to 12 conflicts might apprear within their neighborhood.

5.4.2 Scenario 2. Three hidden influences on nodes with highest degrees (3HIHD)

As mentioned earlier, influences are defined as as individuals who collectively select a unique solution to the particular network under consideration, assume the colors representative of that solution and never change their color during the experiment. A hidden influence is defined as a node whose neighbors do not know that their color is fixed. In this scenario we chose 3 of the nodes of each network with the highest number of connections to be the influences. Figure 5.3 shows the placement of influences.

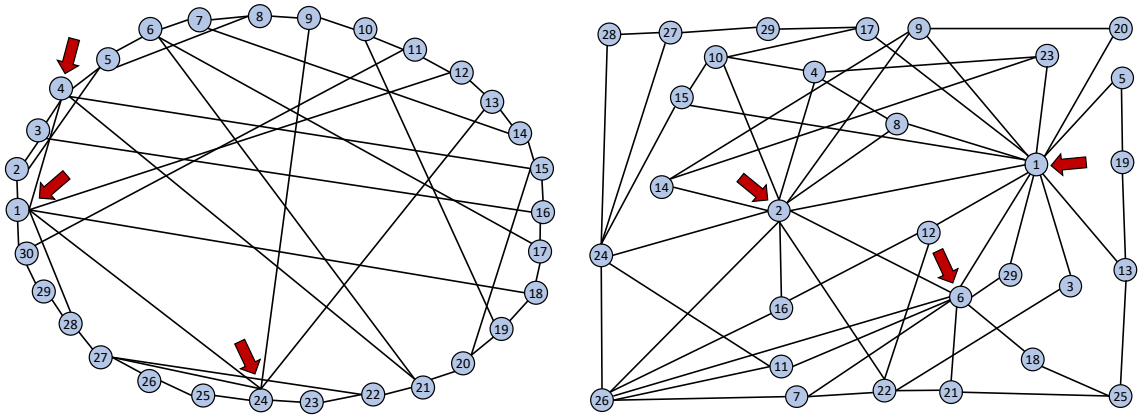

(a) Small World Network (b) Scale Free Network

Figure 5.3: Location of three hidden influences

The results of the experiment show clear changes in the behavioral dynamics of participants. The small world network is solved 6 times and with a shorter AST. Also, the scale free networked is solved 5 times with a much shorter AST, Fig. 5.4. This drastic change in the dynamics is in part because three nodes do not change colors during the experiments, so there are 27 nodes left to color, and in part because the problematic nodes from the benchmark experiments are already solved by the influences.

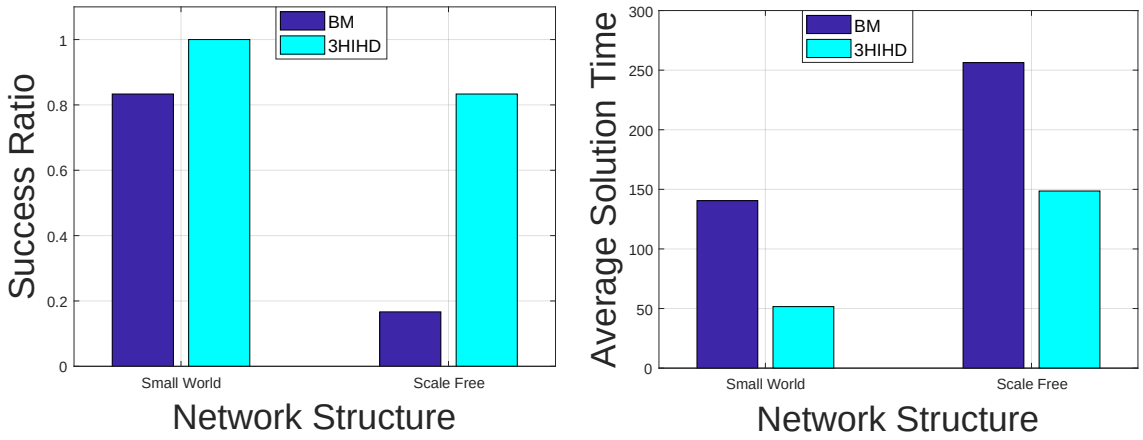

(a) Success Ratio

(b) Average Solution Time

Figure 5.4: Effect of hidden influences (3HIHD) on the dynamic compared to the benchmark (BM)

5.4.3 Scenario 3. Three known influences on nodes with highest degrees (3KIHD)

In [97], researchers studied the effect of providing extra information to the participants on the collective behavior of the group by giving them the global view of the experiment. In our experiments, we provide extra information to the participants by informing them whether they are attached to influences; the influences were in the shape of a triangle. We also inform the participants that the influences do not change colors by writing "Fixed" inside the triangles; we also instruct the participants to expect their neighbors to not change colors when they see that their neighbor is a triangle with the word "Fixed" on them. Figure 5.5 illustrates the presentation of known influences to the participants (if connected) in the user interface. We have chosen the same nodes from 3HIHD to be influences.

The results illustrate that in presence of known influences the success rate is 100%, and the AST is even shorter than those of the hidden influences in both networks, Fig. 5.6. This is because of the fact that most people are connected to influences; when an agent knows one of it's neighbors will never change colors, the size of the decision space for them reduces to 1 dimension in the small world network, and to 2 or 1 in the scale free network. This makes it easier for the participents to make decisions and choose colors.

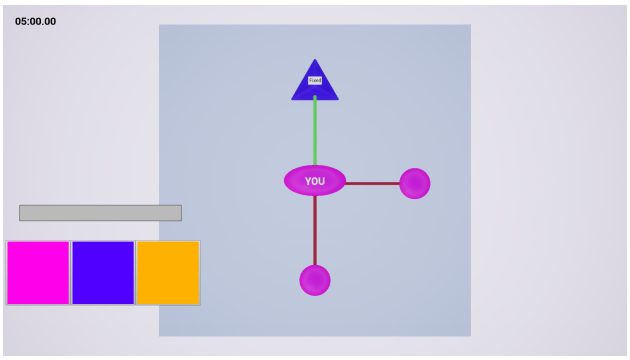

Figure 5.5: User interface when the participant is connected to a known influence

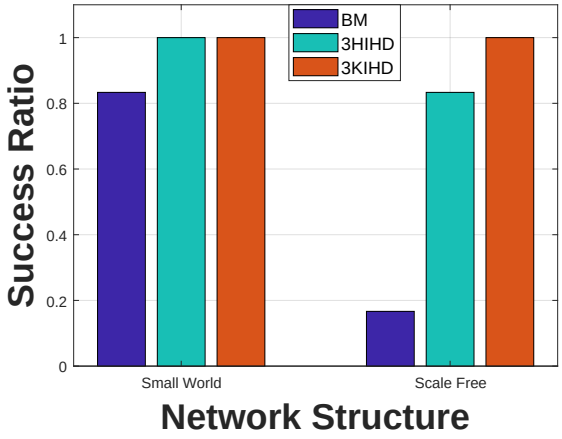

(a) Success Ratio

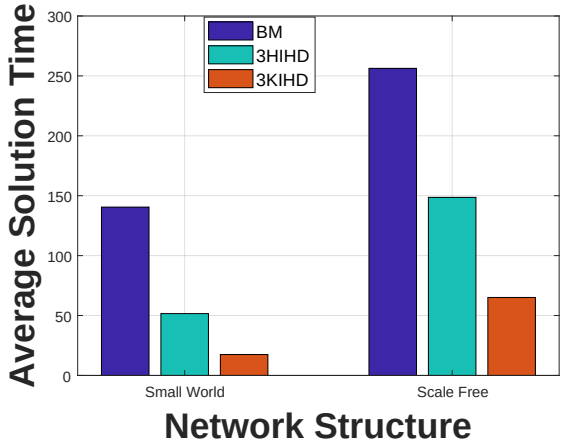

(b) Average Solution Time

Figure 5.6: Effect of Known influences (3KIHD) compared to the effect of hidden influences (3HIHD) and the benchmark (BM)

5.4.4 Scenario 4. One hidden influence on the node with the highest degree (1HIHD)

The results from previous experiments indicate that having three influences does affect the dynamics of the collective behavior. In this scenario, we want to investigate the effect of number of influences on the dynamics. We use only one influence on the node with the highest number of connections.

Results of the experiments depict that for the small world network, the success frequency is 6/6 which is better than that of the benchmark, and the AST is also shorter than AST of the benchmark. However, when comparing these results to the scenario with three hidden influences, it is observed that AST increases, Fig. 5.7.

Conversely, in the scale-free network, acquired data reveals that one hidden influence is not capable of changing the dynamics compared to the benchmark neither in the frequency of success, nor in shortening the AST, Fig. 5.7. This phenomenon happens because the chromatic number of the scale free network is 3, and adding only one influence does not reduce the size of the solution space to 1. As a results, there is no difference between a system with one influence and a system without influences. In this case, it would have been better to have two influences to limit the size of the solution space to 1.

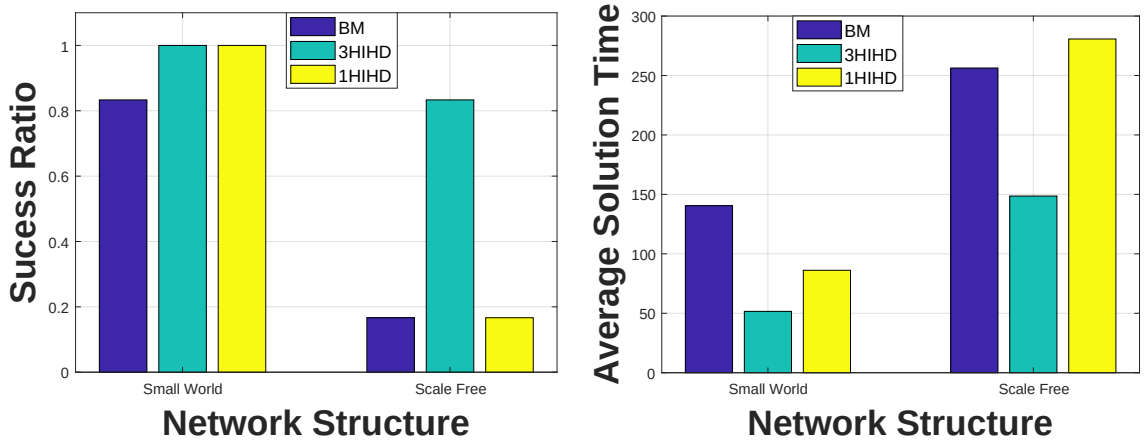

(a) Success Ratio (b) Average Solution Time

Figure 5.7: Effect of one hidden influence (1HIHD) compared to the Effect of three hidden influences (3HIHD) and the benchmark (BM)

5.4.5 Scenario 5. One known influence on the node with the highest degree (1KIHD)

In this scenario, we repeat the experiment from 1HIHD with a known influence. In the scale free network, the performance gets slightly better than the hidden scenario both in frequency of success, and AST. However, in the small world network, only five experiments are successful, and the AST is longer. This finding is in contrast with the previous findings that known influences have better performance than the hidden types. We believe the only unsuccessful experiment could be because of human errors during the game. If the unsuccessful experiment is removed from the analyses, then the AST is much shorter than that from 1HIHD, Fig. 5.8.

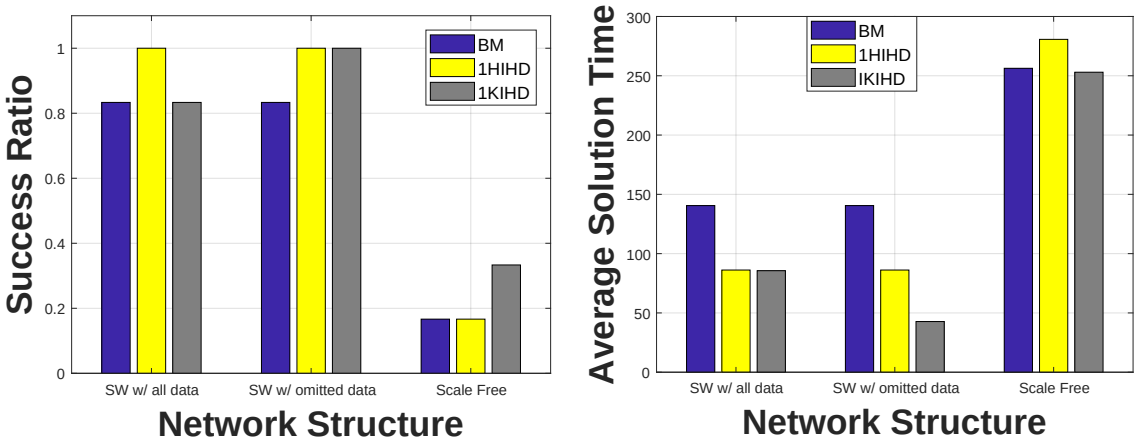

(a) Success Ratio

(b) Average Solution Time

Figure 5.8: Effect of one known influence (1KIHD) compared to the Effect of one hidden influence (1HIHD) and the benchmark (BM)

5.4.6 Scenario 6. Three known influences on the nodes with the lowest degrees (3KILD)

So far, to expose most of the nodes in both networks to influences, we have been choosing the nodes with the highest degrees to be influences. In this scenario, we want to study the effect of influence placement on the dynamics on the collective behavior. We choose three of the nodes with the lowest connections to be the influences. We also argue that since six or

seven nodes will be exposed to influences, it would be better to have only known influences. Figure 5.9 shows the placement of influences for this scenario.

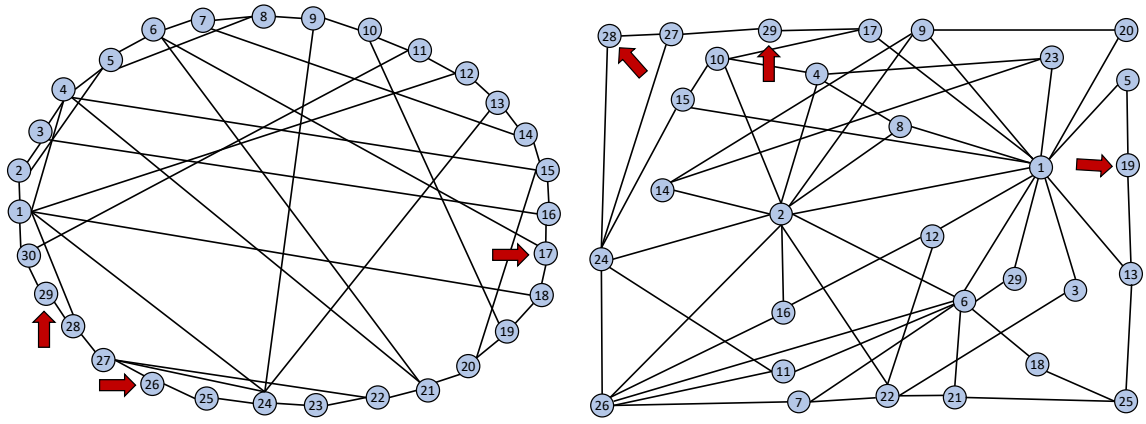

(a) Small World (b) Scale Free

Figure 5.9: Location of the three known influences on the nodes with the lowes degrees

Results of the experiments illustrate that even though placed on the nodes with the lowest degrees, having influences in the network changes the dynamics in both networks in comparison to the benchmark; the success frequencies are higher and the AST is shorter. However, this type of influence placement is not as effective as placing influences on the nodes with the highest degrees, Fig. 5.10.

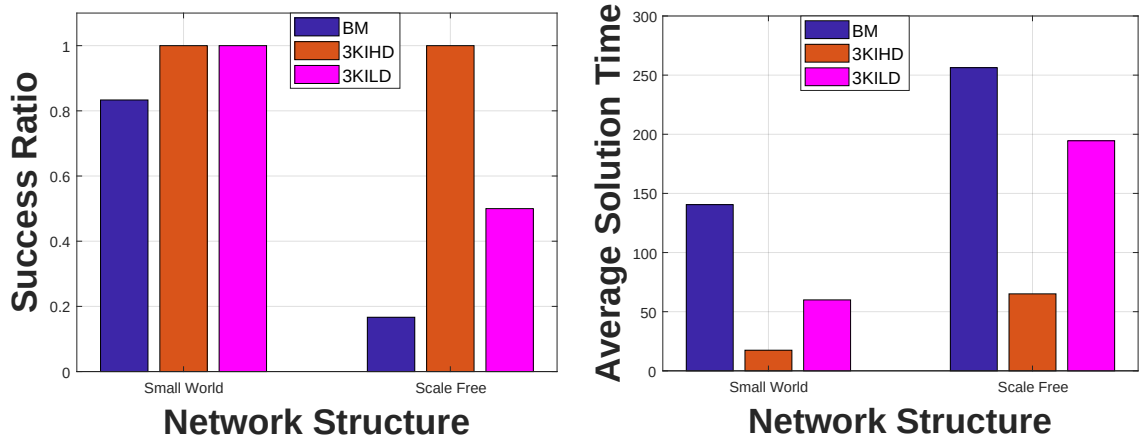

(a) Success Ratio (b) Average Solution Time

Figure 5.10: Effect of placing 3 known influences on the nodes with the lowest degrees

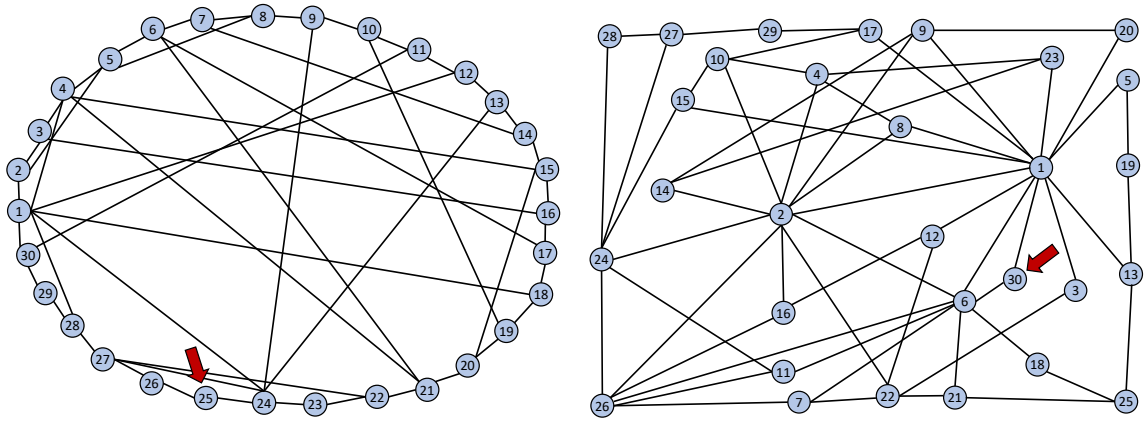

(a) Small World (b) Scale Free

Figure 5.11: Location of the influence on the node with lowest degree but connected to nodes with high degrees

5.4.7 Scenario 7. One known influence on the node with the lowest degree adjacent to high degree nodes (1KILD)

We already learned that location of the influences is very important in the dynamics of the system. In this scenario, the purpose is to study whether choosing the node with the highest degree is the best option to maximize influence. We will repeat the experiment 1KIHD with a different placement in both networks. In the scale free network, we have chosen a node with two connections which is connected to nodes with high degrees. In the small world network, again, we have chosen a node with two neighbors one of whom had the highest number of connections and the other one did not, Fig. 5.11.

Results of the experiments depict that in the scale-free network this placement enhances both frequency of success and AST compared to 1KIHD scenario. Conversely, a negative effect on the collective behavior is observed in the small world network, Fig. 5.12. This proves that having high number of connections does not necessarily result in the optimized influence on the collective behavior; i.e. first degree exposure to influences is not the determining factor in influence maximization.

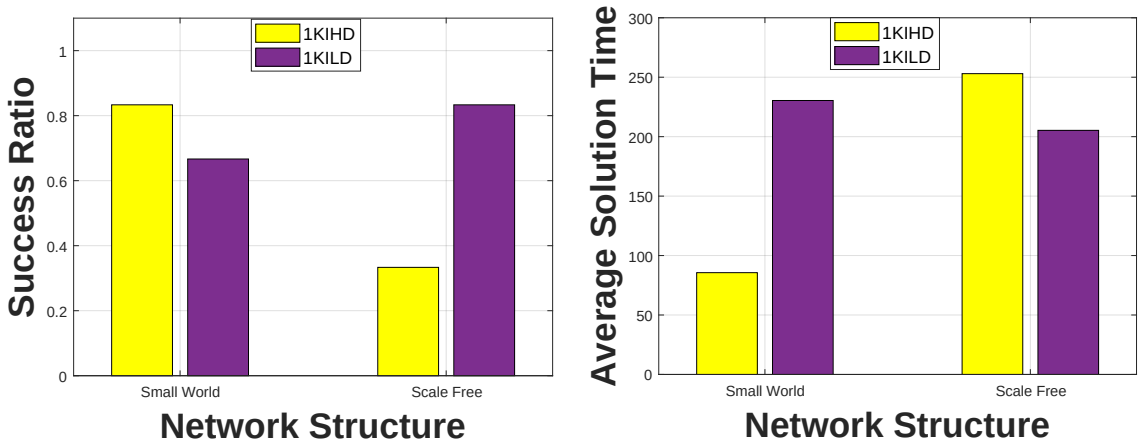

(a) Success Ratio

(b) Average Solution Time

Figure 5.12: Effect of placement of influences on low degree nodes adjacent to high degree nodes

5.5 Chapter Summary

In this chapter, effects of influences on the collective behavior of a group of connected individuals has been experimentally studied. To do so, we have extended on a series of experiments by Kearns et al. [97] by adding the concept of influences. We have presented the details of the experiment setup, and then we have explained how the experiments are conducted. We have designed different scenarios to investigate different phenomena such as effect of adding hidden influences, effect of adding known influences, effect of number of influences, and effect of placement of influences.

We found out that having influences does enhance the performance of participants, and between hidden and known influences, the known influences performed even better. We also showed that placement of influences is of great importance to optimize the performance control. Additionally, we proved that having high number of first degree neighbors for a node does not necessarily make it a better candidate for influence placement for optimized influence.

Chapter 6

Conclusion

6.1 Research Overview

The overarching goal of this thesis is to further our understanding about opinion evolution in networked societies. Such insights can be used in a variety of fields such as economy, marketing, transportation, egress, etc. Three main subjects build up this interdisciplinary research: Sociology, Statistical Mechanics, and Network Sciences. In this thesis, firstly, techniques from statistical mechanics have been borrowed to mathematically model opinion dynamics on different network topologies based on different interaction models (macro-level or society-level analyses). Controllability of such dynamics have been investigated both mathematically and with simulations. Secondly, to incorporate individual-level parameters in opinion dynamics of a group of people, Individual Decision Making Algorithms (IDMA) have been designed. Finally, extensive experimentation in presence of actual humans have been performed to study the conrollability of collective human behaviors in a group of connected individuals. The common theme among the above-mentioned goals is to understand dynamics of opinion propagation in networked socities and whether such dynamics can be controlled.

6.1.1 Contributions

Objective 1 (*addressing Gap 1*). **Mathematical modeling of opinion evolution (DE-Models).** In this section of the thesis, mathematical modeling of various combinations of interaction models and network topologies will be performed in the framework of the Master Equation (ME). ME is a stochastic differential equation describing how the population is distributed over the opinion space and how such distribution changes with time. All the analyses will be performed, which accounts for the presence of influences (control inputs) in the society. Analytical solutions are expected to cast light on different aspects of the system such as convergence time, equilibrium state opinion distribution, progression of the opinion dynamics, controllability of the system, etc.

- Mathematically modelled the Influenced Sznajd model on a Complete Graph and assessed the controllability of the dynamics (Chapter 2)
- Introduced a new interaction model called "The Repulsive Voter Model", modelled it with/without influences on different network topologies e.g. Complete Graph, Random Graph, and a lattice; assessed the controllability of the derived dynamics (Chapter 3)

Objective 2 (*addressing Gap 1*). **Numerical simulations of the systems from *Objective 1*.** This section will be devoted to extensive Monte Carlo simulations of the indicated systems in Objective 1. These simulations will be used to validate the precision of modeling procedures and accuracy of analytical solutions. Also, these simulations will serve as a guide towards appropriate time scaling procedures of the systems. Effects of control inputs on the final state of the society can be investigated with such simulations.

- Developed a Monte-Carlo simulation in presence of influences and studied the controllability of the influenced Sznajd model, proved the existance of convergence zones, proved the linear scalibility property of the system, and performed entropy analyses (Chapter 2)
- Developed a Monte-Carlo simulation in presence of influences and studied the controllability of the repulsive voter model, studied the equilibrium density and expected magnetization of the system (Chapter 3)

Objective 3 (*addressing Gap 2*). **Decision making (AB-Models).** This section of the thesis will concentrate on the decision making processes of individuals (designed in the framework of a Probabilistic Finite State Automata (PFSA)). The decision making algorithm will be able to model the behavior of agents when they are exposed to external events, and also when they interact with other people. This part of the study combines micro-level and macro-level parameters of opinion evolution. Such combination can be instrumental in understanding the mutual effects that the society and the individual have on each other; or, how influences can alter an individual's decisions and cognitive states.

- Developed an Individual Decision Making Algorithm in the frame of the Probabilistic Finite State Automata and incorporated the effect of interactions in it (Chapter **??**)
- Developed a Monte-Carlo simulation in presence of influences and studied the controllability of the groups collective decision making patterns (Chapter **??**)
- Performed a thorough parametric study and provided the results and discussions (Chapter **??**)

Objective 4 (*addressing Gap 3*). **Assessing controllability of collective human behaviors in presence of actual humans.** This part of the thesis will be devoted to studying the controllability of collective behavior of people in an experimental setup in presence of actual humans. Different influence scenarios will be developed with the purpose of maximizing the influence of control inputs. Optimality, and time-effectiveness of these algorithms are the important design parameters.

- Developed a multi-player game on UnrealEngine4 and tested it (Chapter 5)
- Designed different experiment scenarios to investigate the effect of presence of influences in a system, number of influences in the system, and the placement of influences in the network (Chapter 5)
- Conducted the experiments in two different sessions (Summer and Fall of 2018) and acquired data (Chapter 5)

- Performed extensive analyses on the collected data and provided results and comprehensive discussions (Chapter 5)

6.2 Future Directions

The research line of this thesis can be continued in different directions. Expanding on the mathematical modeling of different interaction models is one of the avenues to take on. Influenced bounded confidence is a clear example. Or, new models need to be developed to capture the effect of agents' movements (Chapters 2 and 3). The individual decision making aspect of this research could be followed by incorporating real world data into the development of algorithms, or by further involving psychological concepts in the simulations (Chapter 4). The experimental study presented in this thesis has the potential to be used for numerous studies regarding collective behaviors. Behavioral anomaly detection, behavioral classification, study of gate keepers, autonomous vehicle platoon formation, building evacuation, roadway crossings, etc. are a few of the avenues for which researchers can further utilize this experimental setup (Chapter 5).

Bibliography

[1] James J Binney et al. *The theory of critical phenomena: an introduction to the renormalization group*. Oxford University Press, Inc., 1992.

[2] Dirk Helbing. *Quantitative sociodynamics: stochastic methods and models of social interaction processes*. Springer Science & Business Media, 2010.

[3] David P Landau and Kurt Binder. *A guide to Monte Carlo simulations in statistical physics*. Cambridge university press, 2014.

[4] Fa-Yueh Wu. "The potts model". In: *Reviews of modern physics* 54.1 (1982), p. 235.

[5] Tsung-Dao Lee and Chen-Ning Yang. "Statistical theory of equations of state and phase transitions. II. Lattice gas and Ising model". In: *Physical Review* 87.3 (1952), p. 410.

[6] A Martınez et al. "Combining qualitative evaluation and social network analysis for the study of classroom social interactions". In: *Computers & Education* 41.4 (2003), pp. 353–368.

[7] Charles F Manski. *Economic analysis of social interactions*. Tech. rep. National bureau of economic research, 2000.

[8] Subhadeep Chakraborty. "Analytical methods to investigate the effects of external influence on socio-cultural opinion evolution". In: *International Conference on Social Computing, Behavioral-Cultural Modeling, and Prediction*. Springer. 2013, pp. 386–393.

[9] Claudio Castellano, Santo Fortunato, and Vittorio Loreto. "Statistical physics of social dynamics". In: *Reviews of modern physics* 81.2 (2009), p. 591.

[10] John Von Neumann and Oskar Morgenstern. *Theory of games and economic behavior*. Princeton university press, 2007.

[11] Milton Friedman and Leonard J Savage. "The utility analysis of choices involving risk". In: *Journal of political Economy* 56.4 (1948), pp. 279–304.

[12] Leonard J Savage. *The foundations of statistics*. Courier Corporation, 1972.

[13] Martin Fishbein and Icek Ajzen. "Belief, attitude, intention, and behavior: An introduction to theory and research". In: (1977).

[14] Howard Rachlin. "Behavior and learning." In: (1976).

[15] Herbert Blumer. "What is wrong with social theory?" In: *American sociological review* 19.1 (1954), pp. 3–10.

[16] Michael A Hogg. "Social identity theory". In: *Understanding Peace and Conflict Through Social Identity Theory*. Springer, 2016, pp. 3–17.

[17] John T Jost, Mahzarin R Banaji, and Brian A Nosek. "A decade of system justification theory: Accumulated evidence of conscious and unconscious bolstering of the status quo". In: *Political psychology* 25.6 (2004), pp. 881–919.

[18] Lars Kai Hansen et al. "Good friends, bad news-affect and virality in twitter". In: *Future information technology* (2011), pp. 34–43.

[19] Tina Balke and Nigel Gilbert. "How do agents make decisions? A survey". In: *Journal of Artificial Societies and Social Simulation* 17.4 (2014), p. 13.

[20] Gerald Häubl and Valerie Trifts. "Consumer decision making in online shopping environments: The effects of interactive decision aids". In: *Marketing science* 19.1 (2000), pp. 4–21.

[21] Thomas M Jones. "Ethical decision making by individuals in organizations: An issue-contingent model". In: *Academy of management review* 16.2 (1991), pp. 366–395.

[22] BJ Alder and TEf Wainwright. "Phase transition for a hard sphere system". In: *The Journal of chemical physics* 27.5 (1957), pp. 1208–1209.

[23] Berni J Alder and TâĂŇ E Wainwright. "Studies in molecular dynamics. I. General method". In: *The Journal of Chemical Physics* 31.2 (1959), pp. 459–466.

[24] Stanislaw M Ulam. *A collection of mathematical problems*. Vol. 8. Interscience Publishers, 1960.

[25] Hirotsugu Matsuda et al. "Statistical mechanics of population: the lattice Lotka-Volterra model". In: *Progress of theoretical Physics* 88.6 (1992), pp. 1035–1049.

[26] Aravinda R Srinivasan and Subhadeep Chakraborty. "Effect of network topology on the controllability of voter model dynamics using biased nodes". In: *2014 American Control Conference*. IEEE. 2014, pp. 2096–2101.

[27] Frantisek Slanina and Hynek Lavicka. "Analytical results for the Sznajd model of opinion formation". In: *The European Physical Journal B-Condensed Matter and Complex Systems* 35.2 (2003), pp. 279–288.

[28] Claudio Castellano et al. "Comparison of voter and Glauber ordering dynamics on networks". In: *Physical review E* 71.6 (2005), p. 066107.

[29] Vishal Sood and Sidney Redner. "Voter model on heterogeneous graphs". In: *Physical review letters* 94.17 (2005), p. 178701.

[30] Katarzyna Sznajd-Weron. "Sznajd model and its applications". In: *arXiv preprint physics/0503239* (2005).

[31] Americo T Bernardes, Dietrich Stauffer, and Janos Kertész. "Election results and the Sznajd model on Barabasi network". In: *The European Physical Journal B-Condensed Matter and Complex Systems* 25.1 (2002), pp. 123–127.

[32] Gerard Weisbuch. "Bounded confidence and social networks". In: *The European Physical Journal B-Condensed Matter and Complex Systems* 38.2 (2004), pp. 339–343.

[33] Rainer Hegselmann, Ulrich Krause, et al. "Opinion dynamics and bounded confidence models, analysis, and simulation". In: *Journal of artificial societies and social simulation* 5.3 (2002).

[34] Manfred Scheucher and Herbert Spohn. "A soluble kinetic model for spinodal decomposition". In: *Journal of statistical physics* 53.1 (1988), pp. 279–294.

[35] Duncan J Watts and Steven H Strogatz. "Collective dynamics of'small-world'networks". In: *nature* 393.6684 (1998), p. 440.

[36] Dietrich Stauffer. "Monte Carlo simulations of Sznajd models". In: *Journal of Artificial Societies and Social Simulation* 5.1 (2001).

[37] AS Elgazzar. "Applications of small-world networks to some socio-economic systems". In: *Physica A: Statistical Mechanics and its Applications* 324.1 (2003), pp. 402–407.

[38] Christian Schulze. "Long-range interactions in Sznajd consensus model". In: *Physica A: Statistical Mechanics and its Applications* 324.3 (2003), pp. 717–722.

[39] Santo Fortunato. "Universality of the Threshold for Complete Consensus for the Opinion Dynamics of Deffuant et al." In: *International Journal of Modern Physics C* 15.09 (2004), pp. 1301–1307.

[40] Eli Ben-Naim, Paul L Krapivsky, and Sidney Redner. "Bifurcations and patterns in compromise processes". In: *Physica D: Nonlinear Phenomena* 183.3 (2003), pp. 190–204.

[41] M Porfiri, EM Bollt, and DJ Stilwell. "Decline of minorities in stubborn societies". In: *The European Physical Journal B-Condensed Matter and Complex Systems* 57.4 (2007), pp. 481–486.

[42] MF Laguna, Guillermo Abramson, and Damián H Zanette. "Minorities in a model for opinion formation". In: *Complexity* 9.4 (2004), pp. 31–36.

[43] Kathleen M Carley, Michael J Prietula, Zhiang Lin, et al. "Design versus cognition: The interaction of agent cognition and organizational design on organizational performance". In: *Journal of Artificial Societies and Social Simulation* 1.3 (1998), pp. 1–19.

[44] Nigel Gilbert. "Agent-based social simulation: dealing with complexity". In: *The Complex Systems Network of Excellence* 9.25 (2004), pp. 1–14.

[45] Johannes J Schneider. "The influence of contrarians and opportunists on the stability of a democracy in the Sznajd model". In: *International Journal of Modern Physics C* 15.05 (2004), pp. 659–674.

[46] AT Bernardes et al. "Damage spreading, coarsening dynamics and distribution of political votes in Sznajd model on square lattice". In: *International Journal of Modern Physics C* 12.02 (2001), pp. 159–167.

[47] Russell F Settle and Buron A Abrams. "The determinants of voter participation: A more general model". In: *Public Choice* 27.1 (1976), pp. 81–89.

[48] Serge Galam and Frans Jacobs. "The role of inflexible minorities in the breaking of democratic opinion dynamics". In: *Physica A: Statistical Mechanics and its Applications* 381 (2007), pp. 366–376.

[49] Mauro Mobilia, A Petersen, and Sidney Redner. "On the role of zealotry in the voter model". In: *Journal of Statistical Mechanics: Theory and Experiment* 2007.08 (2007), P08029.

[50] Jierui Xie et al. "Evolution of opinions on social networks in the presence of competing committed groups". In: *PLoS One* 7.3 (2012), e33215.

[51] Jierui Xie et al. "Social consensus through the influence of committed minorities". In: *Physical Review E* 84.1 (2011), p. 011130.

[52] Ercan Yildiz et al. "Binary opinion dynamics with stubborn agents". In: *ACM Transactions on Economics and Computation* 1.4 (2013), p. 19.

[53] David Knoke and Song Yang. *Social network analysis*. Vol. 154. Sage, 2008.

[54] Garry Robins, Peter Elliott, and Philippa Pattison. "Network models for social selection processes". In: *Social networks* 23.1 (2001), pp. 1–30.

[55] Réka Albert and Albert László Barabási. "Statistical mechanics of complex networks". In: *Reviews of modern physics* 74.1 (2002), p. 47.

[56] Jeffrey Travers and Stanley Milgram. "An experimental study of the small world problem". In: *Sociometry* (1969), pp. 425–443.

[57] Albert-László Barabási and Réka Albert. "Emergence of scaling in random networks". In: *science* 286.5439 (1999), pp. 509–512.

[58] Petter Holme and Beom Jun Kim. "Growing scale-free networks with tunable clustering". In: *Physical review E* 65.2 (2002), p. 026107.

[59] Aravinda R Srinivasan and Subhadeep Chakraborty. "Effect of network topology on the controllability of voter model dynamics using biased nodes". In: *American Control Conference (ACC), 2014*. IEEE. 2014, pp. 2096–2101.

[60] Piotr Nyczka, Jerzy Cisło, and Katarzyna Sznajd-Weron. "Opinion dynamics as a movement in a bistable potential". In: *Physica A: Statistical Mechanics and its Applications* 391.1 (2012), pp. 317–327.

[61] Piotr Nyczka, Katarzyna Sznajd-Weron, and Jerzy Cisło. "Phase transitions in the q-voter model with two types of stochastic driving". In: *Physical Review E* 86.1 (2012), p. 011105.

[62] Arkadiusz Jędrzejewski. "Pair approximation for the q-voter model with independence on complex networks". In: *Physical Review E* 95.1 (2017), p. 012307.

[63] Mauro Mobilia. "Nonlinear q-voter model with inflexible zealots". In: *Physical Review E* 92.1 (2015), p. 012803.

[64] F. S. Naneh Karan and S. Chakraborty. "Dynamics of a Repulsive Voter Model". In: *IEEE Transactions on Computational Social Systems* 3.1 (2016), pp. 13–22. ISSN: 2329-924X. DOI: 10.1109/TCSS.2016.2560627.

[65] Katarzyna Sznajd-Weron and Jozef Sznajd. "Opinion evolution in closed community". In: *International Journal of Modern Physics C* 11.06 (2000), pp. 1157–1165.

[66] Farshad Salimi Naneh Karan and Subhadeep Chakraborty. "Dynamics of a Repulsive Voter Model". In: *Social Computing, Behavioral-Cultural Modeling, and Prediction: 8th International Conference, SBP 2015, Washington, DC, USA, March 31-April 3, 2015. Proceedings*. Ed. by Nitin Agarwal, Kevin Xu, and Nathaniel Osgood. Cham: Springer International Publishing, 2015, pp. 428–433. ISBN: 978-3-319-16268-3. DOI: 10.1007/978-3-319-16268-3_54. URL: http://dx.doi.org/10.1007/978-3-319-16268-3_54.

[67] Robin Dunbar. *How many friends does one person need?: Dunbar's number and other evolutionary quirks*. Faber & Faber, 2010.

[68] Aaron Smith. *6 new facts about Facebook*. Pew Research Center, Washington, D.C., http://pewrsr.ch/1dm5NmJ. 2013. URL: http://pewrsr.ch/1dm5NmJ.

[69] Renaud Lambiotte and Sidney Redner. "Dynamics of non-conservative voters". In: *EPL (Europhysics Letters)* 82.1 (2008), p. 18007.

[70] Kingo Kobayashi et al. *Mathematics of information and coding*. Vol. 203. American Mathematical Soc., 2007.

[71] W. Wang et al. "Learning patch-dependent kernel forest for person re-identification". In: *2016 IEEE Winter Conference on Applications of Computer Vision (WACV)*. 2016, pp. 1–9. DOI: 10.1109/WACV.2016.7477578.

[72] Samantha Holland. *Alternative femininities: Body, age and identity*. Berg Publishers, 2004.

[73] Thomas K Greenfield, Lorraine T Midanik, and John D Rogers. "A 10-year national trend study of alcohol consumption, 1984-1995: is the period of declining drinking over?" In: *American Journal of Public Health* 90.1 (2000), p. 47.

[74] H Naseri, A Nahvi, and F Salimi Naneh Karan. "A new psychological methodology for modeling real-time car following maneuvers". In: *Travel behaviour and society* 2.2 (2015), pp. 124–130.

[75] H Naseri, A Nahvi, and F Salimi Naneh Karan. "A real-time lane changing and line changing algorithm for driving simulators based on virtual driver behavior". In: *Journal of simulation* 11.4 (2017), pp. 357–368.

[76] Pavel L Krapivsky, Sidney Redner, and Eli Ben-Naim. *A kinetic view of statistical physics*. Cambridge University Press, 2010.

[77] Federico Vazquez et al. "Analytical solution of the voter model on uncorrelated networks". In: *New Journal of Physics* 10.6 (2008), p. 063011.

[78] Guillaume Deffuant et al. "Mixing beliefs among interacting agents". In: *Advances in Complex Systems* 3.01n04 (2000), pp. 87–98.

[79] Jan Lorenz. "Continuous opinion dynamics under bounded confidence: A survey". In: *International Journal of Modern Physics C* 18.12 (2007), pp. 1819–1838.

[80] C. Castellano, D. Vilone, and A. Vespignani. "Incomplete ordering of the voter model on small-world networks". In: *EPL (Europhysics Letters)* 63.1 (2003), p. 153. URL: http://stacks.iop.org/0295-5075/63/i=1/a=153.

[81] Daniele Vilone and Claudio Castellano. "Solution of voter model dynamics on annealed small-world networks". In: *Physical Review E* 69.1 (2004), p. 016109.

[82] Krzysztof Suchecki, Víctor M Eguíluz, and Maxi San Miguel. "Voter model dynamics in complex networks: Role of dimensionality, disorder, and degree distribution". In: *Physical Review E* 72.3 (2005), p. 036132.

[83] Ward Edwards. "The theory of decision making." In: *Psychological bulletin* 51.4 (1954), p. 380.

[84] Martin L Puterman. *Markov decision processes: discrete stochastic dynamic programming*. John Wiley & Sons, 2014.

[85] Robert Axelrod. "The dissemination of culture a model with local convergence and global polarization". In: *Journal of conflict resolution* 41.2 (1997), pp. 203–226.

[86] Dirk Jacobmeier. "Multidimensional consensus model on a Barabási–Albert network". In: *International Journal of Modern Physics C* 16.04 (2005), pp. 633–646.

[87] Santo Fortunato et al. "Vector opinion dynamics in a bounded confidence consensus model". In: *International Journal of Modern Physics C* 16.10 (2005), pp. 1535–1551.

[88] Subhadeep Chakraborty and Matthew M Mench. "Socio-cultural evolution of opinion dynamics in networked societies". In: *Social Computing, Behavioral-Cultural Modeling and Prediction*. Springer, 2012, pp. 78–86.

[89] Xi Wang and Asok Ray. "A language measure for performance evaluation of discrete-event supervisory control systems". In: *Applied Mathematical Modelling* 28.9 (2004), pp. 817–833.

[90] Aravinda Ramakrishnan Srinivasan, Farshad Salimi Naneh Karan, and Subhadeep Chakraborty. "A Study of How Opinion Sharing Affects Emergency Evacuation". In: *International Conference on Social Computing, Behavioral-Cultural Modeling and Prediction and Behavior Representation in Modeling and Simulation*. Springer. 2018, pp. 176–182.

[91] Aravinda Ramakrishnan Srinivasan, Farshad Salimi Naneh Karan, and Subhadeep Chakraborty. "Pedestrian dynamics with explicit sharing of exit choice during egress through a long corridor". In: *Physica A: Statistical Mechanics and its Applications* 468 (2017), pp. 770–782.

[92] NANEH KARAN, FARSHAD SALIMI, and SUBHADEEP CHAKRABORTY. "EFFECT OF ZEALOTS ON THE OPINION DYNAMICS OF RATIONAL AGENTS WITH BOUNDED CONFIDENCE." In: *Acta Physica Polonica B* 49.1 (2018).

[93] George C Homans. "Social behavior as exchange". In: *American journal of sociology* (1958), pp. 597–606.

[94] Karen S Cook et al. "Social exchange theory". In: *Handbook of social psychology*. Springer, 2013, pp. 61–88.

[95] Farshad Salimi Naneh Karan, Aravinda Ramakrishnan Srinivasan, and Subhadeep Chakraborty. "Modeling and numerical simulations of the influenced Sznajd model". In: *Physical Review E* 96.2 (2017), p. 022310.

[96] Farshad Salimi Naneh Karan and Subhadeep Chakraborty. "A Parametric Study of Opinion Progression in a Divided Society". In: *International Conference on Social Computing, Behavioral-Cultural Modeling and Prediction and Behavior Representation in Modeling and Simulation*. Springer, Cham. 2017, pp. 182–192.

[97] Michael Kearns, Siddharth Suri, and Nick Montfort. "An experimental study of the coloring problem on human subject networks". In: *Science* 313.5788 (2006), pp. 824–827.

[98] Michael R Garey. "DS Johnson Computers and intractability". In: *A Guide to the Theory of NP-Completeness* (1979).

[99] Lada A Adamic and Natalie Glance. "The political blogosphere and the 2004 US election: divided they blog". In: *Proceedings of the 3rd international workshop on Link discovery*. ACM. 2005, pp. 36–43.

[100] Ingrid Erickson. "Geography and community: New forms of interaction among people and places". In: *American Behavioral Scientist* 53.8 (2010), pp. 1194–1207.

[101] Shade T Shutters. "Cultural polarization and the role of extremist agents: A simple simulation model". In: *International Conference on Social Computing, Behavioral-Cultural Modeling, and Prediction*. Springer. 2013, pp. 93–101.

[102] A Ray*. "Signed real measure of regular languages for discrete event supervisory control". In: *International Journal of Control* 78.12 (2005), pp. 949–967.

[103] Vladimir Batagelj and Andrej Mrvar. "Pajek: Program for analysis and visualization of large networks". In: *Timeshift-The World in Twenty-Five Years: Ars Electronica* (2004), pp. 242–251.

[104] Sushil Bikhchandani, David Hirshleifer, and Ivo Welch. "A theory of fads, fashion, custom, and cultural change as informational cascades". In: *Journal of political Economy* (1992), pp. 992–1026.

[105] Duncan J Watts. "A simple model of global cascades on random networks". In: *Proceedings of the National Academy of Sciences* 99.9 (2002), pp. 5766–5771.

[106] Sergey N Dorogovtsev, Alexander V Goltsev, and José Fernando F Mendes. "Ising model on networks with an arbitrary distribution of connections". In: *Physical Review E* 66.1 (2002), p. 016104.

[107] Konstantin Klemm et al. "Nonequilibrium transitions in complex networks: A model of social interaction". In: *Physical Review E* 67.2 (2003), p. 026120.

[108] David Kempe, Jon Kleinberg, and Éva Tardos. "Maximizing the spread of influence through a social network". In: *Proceedings of the ninth ACM SIGKDD international conference on Knowledge discovery and data mining*. ACM. 2003, pp. 137–146.

[109] Farshad Salimi Naneh Karan and Subhadeep Chakraborty. "Detecting behavioral anomaly in social networks using symbolic dynamic filtering". In: *ASME 2015 Dynamic Systems and Control Conference*. American Society of Mechanical Engineers. 2015, V003T37A001–V003T37A001.

[110] Vladimir Batagelj and Andrej Mrvar. *Pajek - analysis and visualization of large networks*. Springer, 2004.

[111] A. Ray. "Symbolic Dynamic Analysis of Complex Systems for Anomaly Detection". In: *Signal Processing* 84.7 (2004), pp. 1115–1130.

[112] R. Badii and A. Politi. *Complexity hierarchical structures and scaling in physics*. Cambridge University Press, United Kingdom, 1997.

[113] D. Lind and M. Marcus. *An Introduction to Symbolic Dynamics and Coding.* Cambridge University Press, United Kingdom, 1995.

[114] H.E. Hopcroft, R. Motwani, and J.D. Ullman. *Introduction to Automata Theory, Languages, and Computation, 2nd ed.* Addison Wesley, Boston, 2001.

[115] R. Duda, P. Hart, and D. Stork. *Pattern Classification.* John Wiley & Sons Inc., 2001.

[116] M.F. Møller. "A scaled conjugate gradient algorithm for fast supervised learning". In: *Neural Networks* 6.4 (1993), pp. 525 –533.

Appendices

Appendix A

A Parametric Study of Opinion Progression in a Divided Society

In chapter 4, it was assumed that all the agents shared the same normative perspective, and the agents did not have specific biases. However, in reality, people carry preconceptions and biases. These preconceptions play a prominent role in their decision making. This chapter is an effort to address this problem. In this chapter, we simulate a society which includes three groups with different pre-biases.

A.1 Introduction

While the extremity of the current (2017) political rhetoric may feel unprecedented, confrontation has always focused on the singular goal of winning over the other side. As an entire population becomes consumed by this mindset, we reenact partisan patterns of conflict that may comfort our fears, promote strong clustering between like-minded people, but undermine cooperation across society and the chance of ever achieving unity and consensus.

Studies suggest that the operation of homophily, i.e. the tendency to follow like-minded individuals and to shun those with opposing opinions, is strongly prevalent in social media applications [99]. Furthermore, shared geo-locality and communal bonds are strengthened via Twitter posts, permitting forms of "peripheral awareness and ambient community" [100]. To model these findings, several non-linear interaction models among individuals, have been

studied which illustrate polarized decision, the self-organization of behavioral conventions, and the transition from individual to mass behavior. In one such study by Shutters [101], the cultural polarization phenomenon has been studied on different network structures in the presence of extremists in the framework of bounded confidence. In this study, the change of opinion after each interaction is guaranteed for non-extremists, rendering the imitation and simulation of human decision making rather unrealistic.

This chapter is an attempt to construct a parametric study that can address at least a portion of these ideas within a mathematically tractable agent-based modeling (ABM) framework. The Probabilistic Finite State Automata (PFSA) based discrete choice model, proposed and studied in [88] has been modified with one key difference. The scenario under discussion and its key difference are explained in the next section. Also, the PFSA framework and its assumptions are briefly explained. Next, we discuss how the Bounded Confidence interaction model is applied in the simualtions. Then the results of simulations for different scenarios are presented and discussed. In the end, all findings of this chapter are summarized and concluded.

A.2 Simulation Setup

A.2.1 Probabilistic Finite state Automata

This framework has already been explained in chapter 4. However, because another problem is addressed in this chapter, some changes have been made to the assumptions. In this framework, it is assumed that every agent has the same *finite set of discrete choices (or states)* at each time instant. Also, we assume that agents subscribe to the normative perspective of the group they belong to; social norms of groups can differ from each other, but inside a group the same social norm is shared with everybody.

Assumption. Different normative perspective for different groups

In this chapter, it is assumed that the society is divided in three groups: the Independent group, the group with preexisting bias towards Revolution (R-Leaning), and the group biased

towards the government (G-Leaning). The way each group perceives the actions of the government is different. Members of the Independent group perceive the popular actions as good and the unpopular actions as bad. However, members of the R-Leaning group perceive all actions of the government as bad. On the other hand, members of the G-Leaning group perceive all actions of the government as good. This assumption results in having three different normative perspectives in the population, Fig. A.1.

Figure A.1a gives a schematic of the assumed normative perspective encoded as a PFSA for the Independent group . It may be noticed that transitions such as $g : G \rightarrow R$ or $g : I \rightarrow R$ are unauthorized since it is assumed that a favorable act by the government should not make anyone decide to join the opposing group. Also, the same event can cause alternate transitions from the same state; the actual transition will depend probabilistically on the measure of attractiveness of the possible target states. In Fig. A.1b, all actions of the government are clubbed together and recognized as good for the G-Leaning group. The elimination of some transitions between states in Figs. A.1b, c is rooted in the biased views that the G-Leaning and R-Leaning groups have. For example, the only way the transition $G \rightarrow R$ can be authorized is when an unpopular action by the government, $\tilde{g}$, happens. Since unpopular actions are perceived as good by the G-Leaning group, $G \rightarrow R$ can never happen for this group and must be eliminated.

In the PFSA framework, the probability of transitioning to a different state is dependent on the reachability of that state from the current state, the current event (external or internal), and also the relative degree of attractiveness of the target state. The state

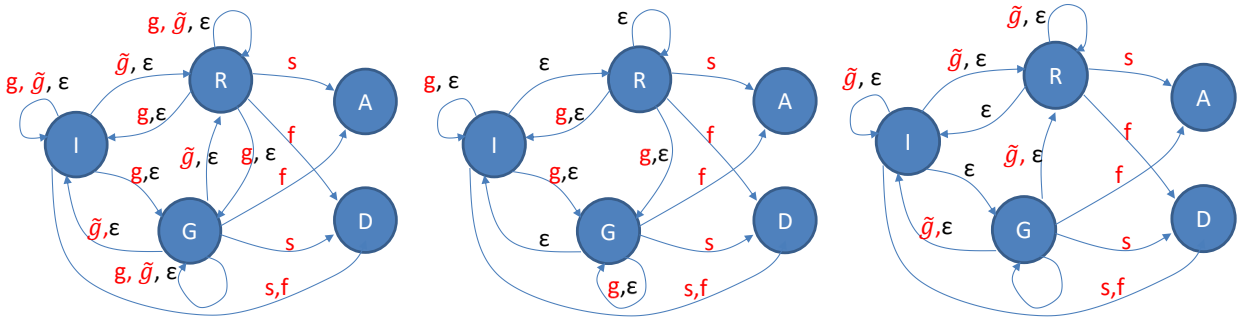

(a) Independent (b) G-Leaning (c) R-Leaning

Figure A.1: Normative perspective of different groups

attractiveness measure is calculated using the concept of positive real measure attributed to a string of events [102]. It depends on the reward from each state (χ), the state transition matrix (Π), and the distribution of states ($\bar{v}_i$). A real measure ν_θ^i for state i is defined as:

$$\nu_\theta^i = \sum_{\tau=0}^{\infty} \theta\,(1-\theta)^\tau\, \bar{v}^i \Pi^\tau \bar{\chi} \tag{A.1}$$

where $\theta \in (0, 1]$ is a user-specified parameter. Mathematical structure of the mentioned parameters are available in chapter 4.

It should be noted at this point that the premise for these assumptions are the authors' hypotheses and conjectures based on observations from the political sphere, but these are as of now unsubstantiated by studies or data analytics. The basic observation is that in response to the SAME political event two groups of people respond in diametrically opposite manners (strongly in favor, or strongly against) - each group with the same passion and conviction that they are correct. Thus, although within their own logical construct, the two groups are not dissimilar, but the perturbation that drives the two groups manifest itself in two completely different ways; to the G-leaning group, each action by the government seems perfect, while to the R-leaning group, the same actions are detestable.

The other interesting dynamic in these composite groups is the possibility of gradual drift of opinion due to interaction and inter/intra-group communications. It seems that the KH bounded confidence model of interactions is appropriate since this model predicates that two nodes only communicate if they are not too dissimilar. A BA-extended model network created by the Pajek software program is used [103]. Table A.1 presents the parameters of the network. In addition, one of the experiments is repeated on a complete graph topology for comparing the results related to different networks.

Table A.1: List of parameters used for BA scale-free network

Network Parameter	Quantity
Number of vertices	100
Number of initial disconnected nodes	3
Number of added/rewired edges at a time	2
Probability to add new lines	0.3333
Probability to rewire edges	0.33335

Influence Model: the influences are treated as indistinguishable except for the fact that they never update or change their $\bar{\chi}$ values; moreover, they do not make decisions, and stay in the same state of mind during the entire simulation. Also, it is typical that the influences are serving a certain agenda, in this case, trying to mobilize forces to join the Revolution. But, this influence is exerted very passively, by advertising a higher value for $\chi(R)$ and lower value for all other states.

$$\chi^I(q_j) = \begin{cases} \chi_m(q_j) - \Delta & \text{if } j = 1, 3, 4, 5, \\ \chi_m(q_j) + \Delta & \text{if } j = 2. \end{cases} \tag{A.2}$$

in which $\chi^I(q_j)$ represents the reward associated with state q_j for influence nodes, and $\bar{\chi}_m$ is an estimate of the reward values expressed by the whole society on an average. Δ is a parameter adjusting the strength of influences (control input).

Simulation Process: a population of 100 people are divided in three groups with specific ratios (G_i, R_i, I_i where $G_i + R_i + I_i = 1$). Each group is initialized and given the respective normative perspective. All agents are assigned a random number drawn from a uniform distribution $U(0, 1)$, representing the time remaining before that person makes a decision. This imposes an ordering on the list of people in the network. As soon as someone makes a decision, the time to his next decision, drawn from $U(0, 1)$, is assigned and the list is updated. Additionally, external events g and $\tilde{g}$ are also associated with a random time drawn from $U(a, b)$.

At the time epoch t_k, when it is the i^{th} person's turn to make a decision, he updates his personal estimate of the reward vector according to the Bounded Confidence model. Then, he calculates the degree of attractiveness of the states based on the normalized measure, using Eqn. A.1. The only difference in the case of an external event such as $g, \tilde{g}, s$ or f is that everyone simultaneously updates their states rather than asynchronously, as in the case of internal events. Each simulation is run 50 times and the average of all the runs is analyzed.

A.3 Simulation Scenarios and Results

A.3.1 Effect of Global Events

This experiment studies the effect of the ratio of good to bad external events, or equivalently $r = \frac{P(g)}{P(\bar{g})}$, on the opinion dynamic of the population. First, we consider equal initial distributions for G-Leaning and R-Leaning groups ($G_i = R_i = 0.25$). The first row of Fig. A.2 provides the results of this type of initial distribution. In all three cases, as soon as events happen, members of the Independent group change their opinions.

In Fig. A.2a, the same probability of good and bad external events causes the Independent group to equally divide between the G-Leaning and R-Leaning groups. However, in Fig. A.2b, because of the higher probability of bad events, people from the Independent group lean towards the Revolution group. The exact same reasoning can be used for Fig. A.2c where good actions by the government outnumber the bad ones causing people from the Independent group to support the Government. It can be concluded that in the absence of

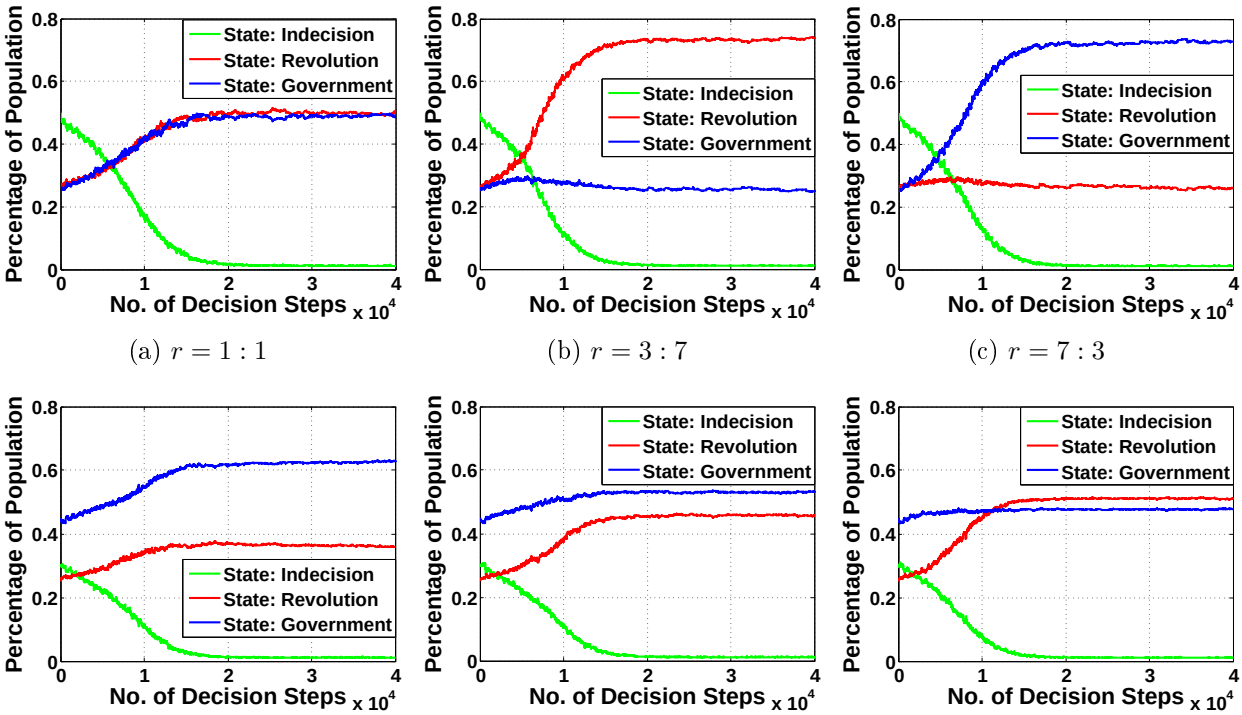

(a) $r = 1:1$ (b) $r = 3:7$ (c) $r = 7:3$

(d) $r = 1:1$ (e) $r = 4:6$ (f) $r = 3:7$

Figure A.2: Effect of external events on population opinion without influence group

influences, for equal initial distribution, r is the determining factor of the state distribution of the population at equilibrium.

In a second set of experiments, we consider unequal initial distributions for G-Leaning and R-Leaning groups ($G_i = 0.45, R_i = 0.25$). Similar to the previous experiment, when equal number of good and bad events happen, the Independent group leans towards either groups somewhat equally, Fig. A.2d.

In Fig. A.2e, when bad events slightly outnumber the good events, the Revolution state starts to increase, but it is not the dominant opinion of the population as it was in Fig. A.2b. The reason is that a high percentage of the population is initially in the G-Leaning group. As a result, Independent members have a higher chance of interacting with G-Leaning members in their network, and consequently, changing their opinions to G. Nonetheless, when bad policies outnumber the good policies significantly, the Revolution state rises to the top and becomes the dominant opinion of the population, Fig. A.2f. The slight increase in the G state in the beginning of the simulation is because of this phenomenon. In conclusion, in absence of influences, for unequal initial distribution both initial distribution and r are important in the steady state opinion distribution of the population.

A.3.2 Effect of Influences

This experiment investigates the effects of presence of influences and their quantity on the steady state behavior of the population. In order to specifically observe the effect of influences, they are activated at decision step 10000, and they are biased towards the Revolution state. The influences randomly choose people to form links with where the probability of forming a link is 0.25. Figure A.3 presents the results of this experiment for $G_i = R_i = 0.3$.

In the first experiment, only one influence is available in the society, Figs. A.3a, b, c. When $r = 1 : 1$, as discussed earlier, Independent members start joining the R or G state equally, Fig. A.3a. However, as soon as the influence is activated, the percentage of people in the R state starts rising drastically because of the interactions which happen among the population. The interesting point is that there is a slight increase in the state of Indecision too. The reason can be found in the normative perspective of the G-Leaning group, Fig. A.1b.

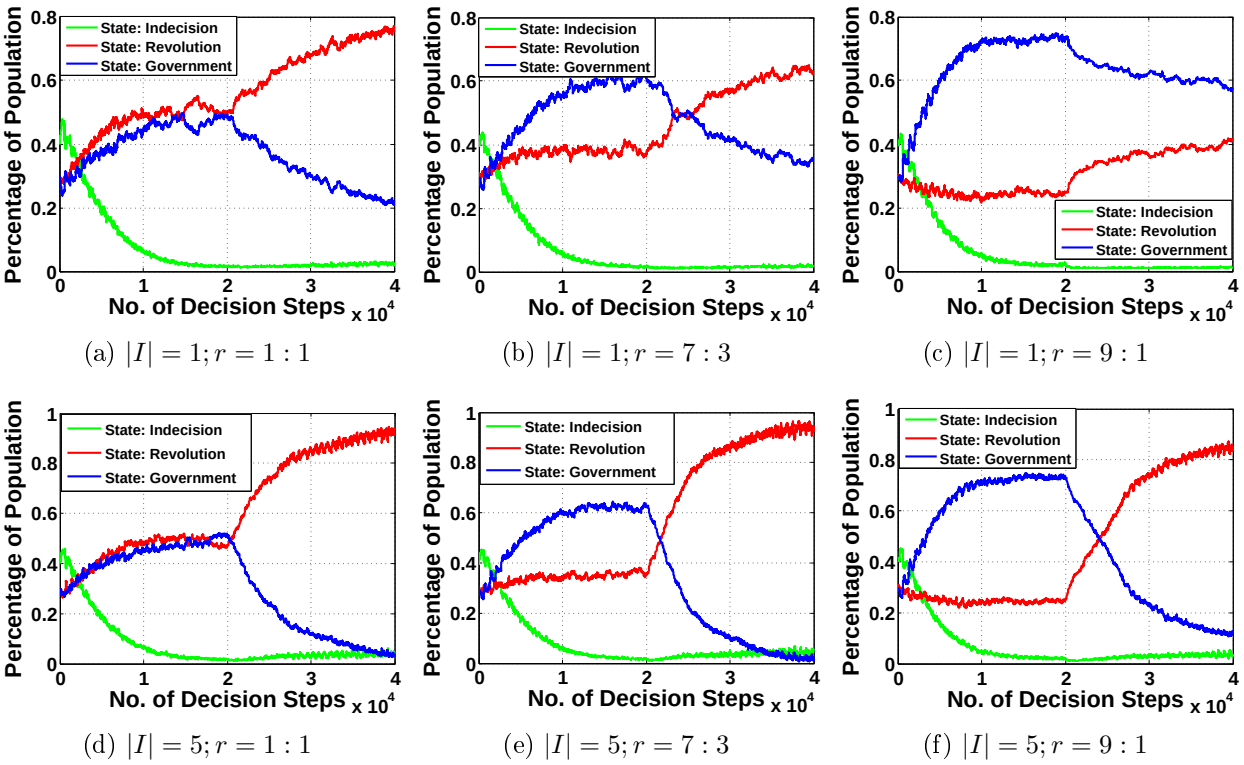

(a) $|I| = 1; r = 1:1$ (b) $|I| = 1; r = 7:3$ (c) $|I| = 1; r = 9:1$

(d) $|I| = 5; r = 1:1$ (e) $|I| = 5; r = 7:3$ (f) $|I| = 5; r = 9:1$

Figure A.3: Effect of external events on population opinion in presence of influences

As a result of continuous interactions with influences, even a G-Leaning member might change her/his opinion to R, and the only path s/he can change her/his opinion from the G state is through state I. This causes a slight increase in the number of agents in the state of Indecision.

As the number of popular acts by the government increases, in the first phase of the simulation, the Independent members join the G state making it the dominant opinion of the whole population, Fig. A.3b. However, the presence of the influence affects people's opinions through interactions causing the R state to be the dominant opinion of the society although there are more popular acts by the government. In this scenario, higher probability of the good actions just makes the transition to the R state slower. The same reasoning is applicable for Fig. A.3c with the only exception that presence of one influence is not able to overcome the effect of significantly higher probability of the popular acts, to destabilize the society.

In another set of experiments, higher number of influences were added to the population, Figs. A.3d, e, f. It is observed that with more influences present, the transition is faster, and almost all the populations joins the R state. Also, higher number of popular act by the government cannot prevent the destabilization of the society. This raises the question that "Can high number of Influences guide the population towards destabilization under any condition?"

To answer this question, we consider an extreme case where the initial distribution is highly in favor of the G-Leaning group ($G_i = 0.45, R_i = 0.1$), and the probability of popular actions by the government is significantly higher. Figure A.4 represents the results of simulation for such a case with varying number of influences. As number of influences increases, the percentage of population in the R state increases. Moreover, this transition is faster. However, the influences are not able to dominate the majority opinion. Both the dominant initial G-Leaning distribution and the high number of popular acts by the government cause this behavior. So, a large group of influences is not a guarantee for guiding a population towards a predetermined state under all conditions.

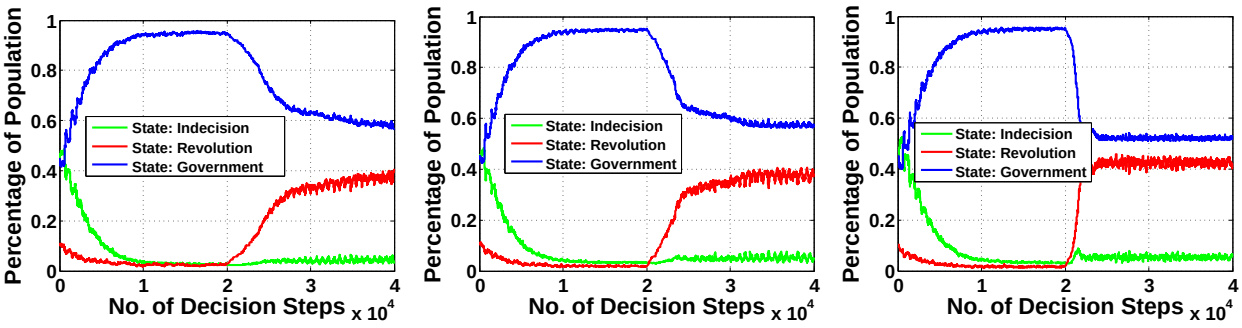

(a) $|I| = 5$ (b) $|I| = 10$ (c) $|I| = 50$

Figure A.4: Effect of number of influences on a G-dominant society with $r = 9 : 1$

A.3.3 Effect of Distance Parameter (d)

Influences deliberately advertise biased reward values in an attempt to pull the population slowly towards the state of their choice (R, in this study). Nonetheless, they would be successful in doing so if they are reachable for agents in the society. The parameter which controls reachability is the distance parameter d. In this section, we study the effect of

the distance parameter on the steady state behavior of the population. Figure A.5 presents the behavior of a society with two values of d. In Fig. A.5a, because of the low distance parameter, most of the agents are not able to interact with influences. As a result the change in the population behavior is not significant. However, in Fig. A.5b, the distance parameter is higher, more agents are affected by the influences as a result of interacting with them, and the change in the behavior of the society is significant.

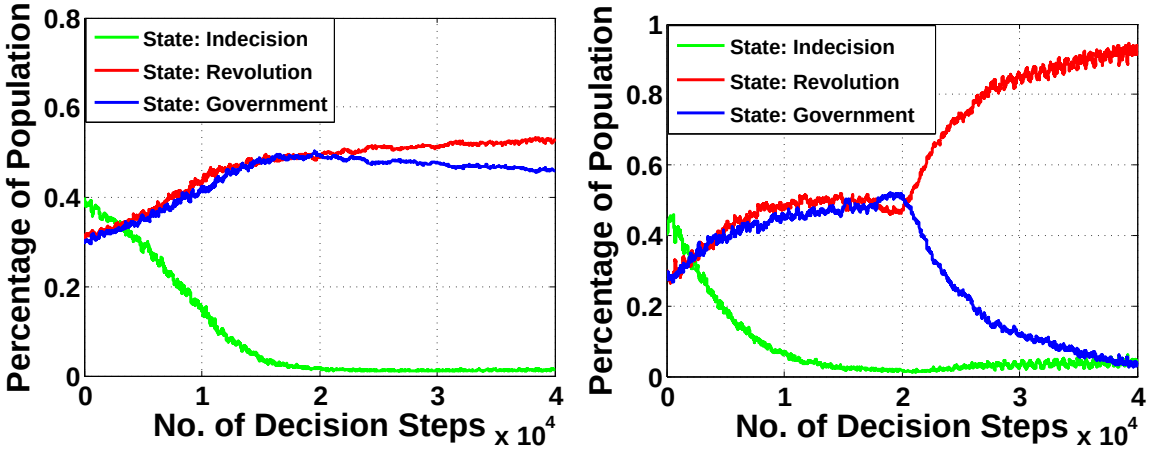

(a) $d = 0.5$ (b) $d = 1$

Figure A.5: Effect of distance parameter, $|I| = 5$, $r = 1 : 1$

A.4 Chapter Summary

This chapter studies the temporal evolution of opinions of individuals in an ideologically divided society by incorporation a PFSA framework along with the KH Bounded Confidence model. Three ideological groups called Independent, G-Leaning and R-Leaning, form a population in which people are connected. Indistinguishable influences are also present in some experiments. There are two motives for individuals to change their decisions: popular/unpopular acts by the government, and interactions between people.

Results show that, in absence of influences, ratio is the determining parameter in the equilibrium state of the population unless one of the groups includes a significantly higher number of members. The results also reveal that although very small in number, influences are capable of creating drastic changes in the opinion dynamic of the society. Higher number

of influences result in faster transitions and attracting more people to the target state. It is shown that in the presence of a major group, there are situations where influences, although very high in number, are not able to push the population's opinion towards the opinion of the minor group. Finally, it is presented that with a low distance parameter, the societies behavior is not greatly affected by the influences.

Appendix B

Detecting Behavioral Anomaly in Social Networks Using Symbolic Dynamic Filtering

B.1 Introduction

Humans have always existed in social groups and hence have likely always been attuned to the preferences and positions of others. At the same time, we have evolved sophisticated sensory systems and brains capable of reaching independent conclusions about the world. Therefore, in our efforts to function effectively, we have likely had to balance our own experiences, ideas, and beliefs with those of close and powerful others. This fulcrum between maintaining one's idiosyncratically-derived views and acquiescing to consensus has been the focus of several social influence researches in psychology.

As insightful as this largely individual- and laboratory-based approach has been, it was not designed to explain social influence at a broader, mass-scale and has rarely been employed to explain social influence at the societal level. At the same time, undeniable and radical change in the availability of consensus information is likely to have affected that fulcrum of influence between the self and others. The rapid dissemination of consensus information via social media has placed such information literally at the fingertips of billions. Although

speculative, it has been proposed that the accessibility of such information has facilitated social movements and rapid mass opinion change, including, perhaps, the recent Arab Spring that spanned several nations and continents simultaneously, and the rapid rise of ISIS in Syria and Northern Iraq.

Such events demonstrate a crucial need for better tools to understand the underlying decision mechanisms that mobilize sudden transitions from indifference to passive crowd support of fringe social movements to active political violence. These cultural, political and social *snowballing* effects are called *information cascades* [104]. The impact of these information cascades are felt in many aspects of the social experience, from emergence of viral videos to large untraceable fluctuations in the stock market. From a process-control perspective, social networks have changed the time scale of the cascading effect.

The concept of *information cascades*, based on *observational learning theory* was formally introduced in a 1992 article by Bikhchandani S. et.al. [104]. Watts D.J. [105] has studied the origin of rare cascades in terms of a sparse, random network of interacting agents using *generating functions*. Statistical mechanics tools, such as the Ising model [106] as well as non-equilibrium statistical models [107] has been used extensively to model the spread of influence in a networked society. *Influence maximization*, deals with finding the optimal set of people in a society to start an information cascade. Approximate solutions to this problem have been studied by Kempe [108] using *submodular functions*. However, in all these models, individual decision logic is largely overlooked.

In a previous work, using an Agent-Based model, the authors have shown [88] that a handful of influences (extremists) can cause rapid destabilization. At the same time, the effectiveness of this radical group can be enhanced by repeated imposition of unpopular policies by the existing government. This has also been borne out by analytical modeling [8, 26] and real world studies implying that being able to estimate the quantity and mechanism of influence in a society has become vital to our well being and security. In this chapter, we try to estimate the size of the extremist population in a society by monitoring global responses to relevant external impetus. We are using a stochastic signal processing tool called Symbolic Dynamic Filtering (SDF) for generating and clustering behavioral patterns in networks corresponding to different levels of influence. Further, we use neural networks

to classify and distinguish patterns that characterize two distinct behaviors; one influenced by extremist nodes, and the other which is a cumulative response to continued government unpopularity.

The organization and flow of the research described in this chapter is best described by the figure shown in Fig. B.1, [109]. In Block 1, we generate data from an agent-based discrete choice model which relies on a Markov Decision Process (MDP) framework for stochastic simulation of decision-making in a social setting where choices and decisions by individuals are influenced by social interactions. We show that such collective imitative behavior, based on local interaction between nodes, (described in Block 2) leads to rapid unstable fluctuations in the society, the fluctuation statistics being a weak function of the number of extremist nodes (influences/bigots in our example) present in the network as well as the ratio of popular vs. unpopular policies enacted by the government. The global response is then passed through SDF (Block 3) which captures the essential characteristics of the data in the form of statistical patterns. We investigate the effectiveness of SDF in estimating the number of influences in the network using a time-trace of opinions in the society. Also, we use a trained neural net to classify the patterns corresponding to the two types of responses described above. A short description of each of these blocks are included next.

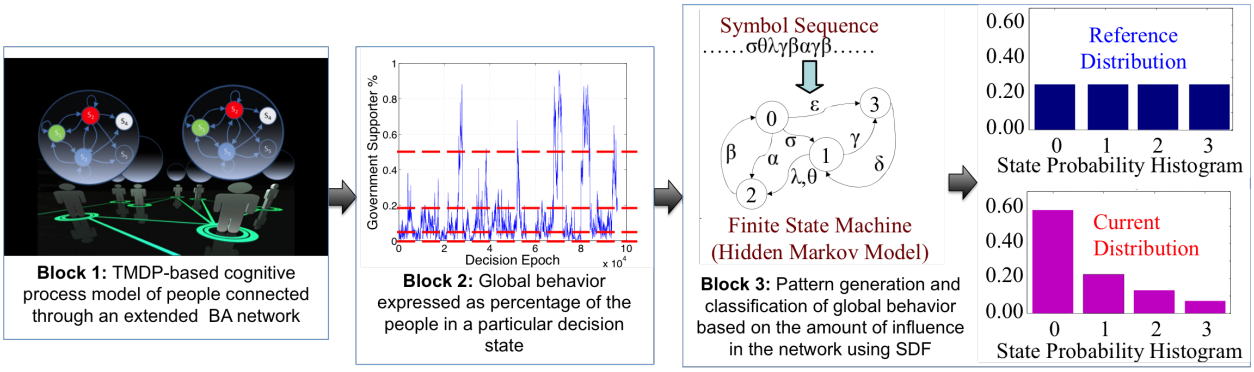

Figure B.1: Organization of the data flow and enumeration of the afferent blocks used in this chapter

B.2 Block 1: The MDP Framework

The assumption of normative perspective allows rational behavior to be encoded as an MDP. The Markov Decision Process is conceived as an abstract mathematical construct that consists of a finite number of states (a set of cognitive states S relevant to the decision problem). For example, in a society in the cusp of seeing a revolution, for an individual, the set S may denote the discrete states of supporting either the government, the revolution, or remaining neutral. The probabilistic automaton generalizes the concept of a Markov chain.

In this chapter, we have modelled the discrete choice behavior as a discrete-time MDP: $G_i = (S, A, T, \chi, \gamma)$ where $S = \{s_1, s_2, ..., s_n\}$ is defined as before, $A = \{a_1, a_2, ..., a_m\}$ is a (finite) set of actions, and the (possibly partial) function $T : S \times A \times S \to [0, 1]$ represents probabilities of transitions from one state to another; also $\chi : A \times S \to \chi$ is the reward or payoff that a person expects to receive from each state. The payoff assigns a real weight to each state s_i, chosen based on the individual state's impact and the event occurrence probabilities. When serving as a simplistic Markov decision model for human cognition, the probability of choosing a particular action from the current state according to a policy $\pi : S \to A$ is dependent on:

- whether that action is available from the current state (for example, the action of attending a political rally organized by the government is available to the individuals who are already in a pro-government state),

- external trigger events (for example, news of atrocities by the government troops may trigger an instantaneous change in some people), and

- the estimated payoff from choosing that action, the expected discounted payoff from possible future actions, and the estimated external political, economic and strategic event occurrence probabilities. Depending on the context, the payoff may be financial, personal security, social approval, etc.

The value of a state $V^\pi(s, \chi)$ is the weighted expected reward over all time-steps in the future for the Markov process that begins in state s and adopts policy π. $V^\pi(s, \chi)$ is defined

as:

$$V^{\pi}(s,\chi) = \chi(s) + \gamma\Sigma_{s'}T(s,\pi(s),s')V^{\pi}(s',\chi). \tag{B.1}$$

The parameter γ controls the rate at which the weights decrease with time. Large values of γ force the weights to decay rapidly, thereby placing more importance to states reachable in the near future from the current state. Thus, γ is the parameter which describes the balance between long-term and short-term objectives.

In our example, each individual in th society is either in a state of supporting the existing government, the revolutionary group, or in a state of neutrality. Additionally, the individual can reach a state of political advantage or disadvantage, but the uncontrollable transition to these two states can only occur through an *external* event, namely, the success or failure of the revolution. The five MDP states and events are described in Table B.1.

Figure B.2 gives a schematic of the assumed normative perspective encoded as a triggered MDP. It may be noticed that transitions such as $g : G \to R$ or $g : I \to R$ are unauthorized, since it is assumed that a favorable act by the government should not make anyone decide to join the opposing group. Also, the same event can cause alternate transitions from the same state; the actual transition will depend probabilistically on the value of the possible target states.

B.3 Block 2: Interaction and Social Feedback Algorithms

One of the most interesting facets of a networked society is the strong interdependence between rewards and popularity of choices. For example, the reward from joining the

Table B.1: List of MDP States and Events

States	Description	Events	Description
I	State of indecision	g	A popular act by the government
R	State of supporting the revolution	$\tilde{g}$	An unpopular government act
G	State of supporting the government	ε	An internal decision
A	State of political advantage	s	Success of the revolution
D	State of political disadvantage	f	Failure of the revolution

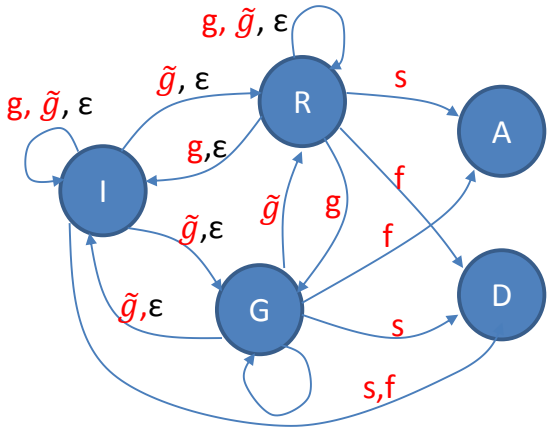

Figure B.2: Schematic of normative perspective coded as a PFSA

revolutionary group ($\chi(R)$) may be small at the initial stages, but as more and more people join, the estimate of $\chi(R)$ as well as the probability of success of the revolution $P(s)$ increases. Thus, in our modified MDP, the reward $\chi(s)$ of a node is a function of the reward values for adjoining nodes.

In this chapter, it is thus assumed that the influence is entirely through the reward $\chi(s)$ of the states. This assumption is based on the physical insight that the anticipated reward from a state is the most well-discussed and well-broadcast quantity in a social network. In addition, influence of mass media can be accounted for by assuming that an unbiased reporter reports the mass opinion in the form of a unified reward for the different choices averaged over the entire population. The interaction dynamics may be mathematically expressed as:

$$\bar{\chi}^i(t+1) = f_i \bar{\chi}^i(t) + g_i \frac{1}{|\mathcal{N}_i|} \sum_{j \in \mathcal{N}_i} \bar{R}^j(t) + h_i \frac{1}{N} \sum_{j=1}^{N} \bar{\chi}^j(t) \tag{B.2}$$

where N is the size of the network, $\mathcal{N}_i$ is the set of first order neighbors of node i, f_i is that fraction of the i^{th} individual's opinion about potential value of the available states that is based on his past beliefs, g_i is the fraction derived from the opinion of his acquaintances (network neighbors), and h_i=1-f_i-g_i is the fraction formed due to the influence of mass media such as newspapers, television, etc.

B.4 Simulation Results and Symbolic Dynamic Filtering

For simulations, the scale free BA extended model network created with the Pajek [110] software, Fig. B.3 has been used to model the connectivity structure since many of the real-world networks are conjectured to be scale free, including the World Wide Web, biological networks, and social networks [57]. The mechanism of preferential attachment and the fitness model have been proposed as a mechanisms to explain conjectured power law degree distributions in real networks. The parameters are listed in Table B.2.

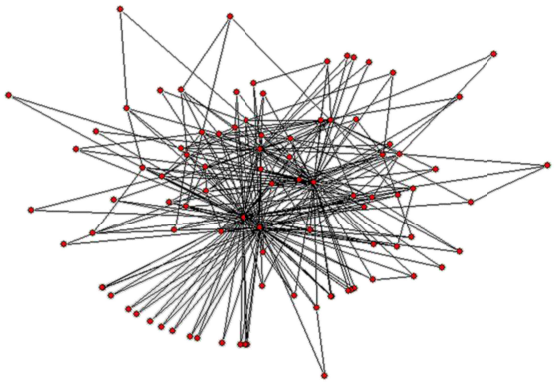

Figure B.3: A 100 node network created with the Pajek software [110]

Before the start of the simulation, the list of nodes in the society is sorted randomly indicating the order in which individuals will make decisions. As soon as someone makes a decision, he is reinserted into the list at a new random location, and the list is updated. Additionally, external events g and $\tilde{g}$ are also interspersed in the list. At t_0, all individuals are initialized at state I. Initial values of the true reward vector $\bar{\chi}$ and the true event probabilities are fixed. Individuals receive a noisy estimate of the true probabilities and the

Table B.2: Parameters for the scale free extended BA network

Network Parameter	Quantity
Number of vertices: (N)	100
Number of initial, disconnected nodes: (m_0)	3
Number of edges to add/rewire at a time: $(m \leq m_0)$	2
Probability to add new lines: (p)	0.3333
Probability to rewire edges: $(0 \leq q \leq 1-p)$	0.33335

rewards. At the time epoch t_k, when it is the i^{th} person's turn to make a decision, s/he updates her/his personal estimate of the reward vector according to the influence equation (Eqn. B.2). Then s/he calculates the degree of attractiveness of the states based on the normalized value $V^{\pi}(S,\chi)$ by solving the Bellman equation (Eqn. B.1). The transition probabilities are calculated as $P(s_{t_{k+1}} = s'|s_{t_k} = s, \sigma = \sigma') = V_{norm}(s')R(q,\sigma',q')$ where $R(s,\sigma',s') = 1$ if $\sigma' : q \to q'$ exists, otherwise 0. The only difference in the case of an external event such as $g, \tilde{g}, s$ or f is that everyone simultaneously updates their states rather than asynchronously as in the case of internal events.

B.5 Block 3: Pattern Extraction with Symbolic Dynamic Filtering (SDF)

An independent observer can estimate the global opinion state of the society by calculating the percentage of people in the individual states. In practice, this data (here generated using the interacting MDP framework described above) can be obtained by conducting opinion polls, monitoring social network contents, etc. This global observation is passed to the next block where it is processed using a stochastic signal processing tool called symbolic dynamic filtering (SDF) [111] for extraction of characteristic pattern vectors. While the details are reported in different publications [111], the essential concepts of space partitioning[112], symbol sequence generation [113], construction of a finite-state machine [114] and pattern recognition [115] are consolidated here and succinctly described for self-sufficiency and clarity.

B.5.1 Symbolic Dynamic Encoding

Let $\Omega \in \mathbb{R}^n$ be the compact (i.e. closed and bounded) region within which the global opinion trajectory is circumscribed. The region Ω is partitioned into a finite number of (mutually exclusive and exhaustive) cells so as to obtain a coordinate grid. Let the cell visited by the trajectory at a time instant be denoted as a random variable taking a symbol value from the alphabet Σ. A trajectory of the opinion dynamics is described by the time series data as $\{x_0, x_1, \cdots, x_k, \cdots\}$ with $x_i \in \Omega$, which passes through or touches one of the cells of the

partition. Each initial state $x_0 \in \Omega$ generates a sequence of symbols defined by a mapping from the opinion space into the symbol space as:

$$x_0 \rightarrow s_0 s_1 s_2 \cdots s_k \cdots \tag{B.3}$$

where each $s_i,\ i = 0, 1, \cdots$ takes a symbol from the alphabet Σ. The mapping in Eq. (B.3) is called *Symbolic Dynamics* as it attributes a legal (i.e. physically admissible) sequence of symbols to the system dynamics starting from an initial state.

Figure B.1 pictorially elucidates the concepts of partitioning a finite region of the phase space and the mapping from the partitioned space into the symbol alphabet. This represents a spatial and temporal discretization of the system dynamics defined by the trajectories. Fig. B.1 also shows conversion of the symbol sequence into a finite-state machine and generation of the state probability vectors as explained in the following subsections.

The time series data set of selected observable outputs such as the global opinion data or percentage of supporters can be used for partitioning and symbolic dynamic encoding.

B.5.2 Probabilistic Finite State Machine Construction

Using the discrete-time discrete-valued stochastic sequence created by partitioning, the state machine is constructed on the principle of sliding block codes [113]. A window of length D on the symbol sequence $\mathbb{S} = \cdots, s_{-2}, s_{-1}, s_0, s_1, s_2, \cdots$ is shifted to the right by one symbol such that it retains the last $(D-1)$ symbols of the previous state and appends it with the new symbol at the end. The states of the machine are represented by blocks $s_i s_{i+1} s_{i+2} ... s_{i+D-1}$ in the symbol sequence. Each state belongs to an equivalence class of strings characterized by a specific word of length D at the leading edge. Thus, with cardinality $|\Sigma|$ of the alphabet and depth D of a symbol string of a state, the total maximum number of states in the D-Markov machine is given by $|\Sigma|^D$. The state machine moves from one state to another upon occurrence of a symbol. All symbol sequences that have the same last D symbols represent the same state. The machine constructed in this fashion is called the D-Markov machine [111] because of its Markov properties.

Definition. $\mathbb{S} = \cdots, s_{-2}, s_{-1}, s_0, s_1, s_2, \cdots$ is called D^{th} order Markov process if the probability of the next symbol depends only on the previous (at most) D symbols, i.e.:

$$P\left(s_i|s_{i-1}s_{i-2}\cdots s_{i-D}\cdots\right) = P\left(s_i|s_{i-1}s_{i-2}\cdots s_{i-D}\right)$$

The finite state machine constructed above has D-Markov properties because the probability of occurrence of symbol σ_{i_ℓ} on a particular state depends only on the configuration of that state, i.e. the previous D symbols. The states of the machine are marked with the corresponding symbolic word permutation and the edges joining the states indicate the occurrence of a symbol σ_{i_ℓ}. The occurrence of a symbol at a state may keep the machine in the same state or move it to a new state.

Definition. The probability of transitions from state q_j to state q_k belonging to the set Q of states under a transition $\delta : Q \times \Sigma \to Q$ is defined as [111]:

$$\pi_{jk} = P\left(\sigma \in \Sigma \mid \delta(q_j, \sigma) \to q_k\right); \sum_k \pi_{jk} = 1; \tag{B.4}$$

Thus, for D-Markov machines, the irreducible stochastic matrix $\Pi \equiv [\pi_{ij}]$ describes all transition probabilities between states with at most $|\Sigma|^{D+1}$ nonzero entries.

The time series data at the reference uninfluenced condition, set as a benchmark, generates the *state transition matrix* Π which, in turn, is used to obtain the *state probability vector* $\mathbf{p}$ whose elements are the stationary probabilities of the state vector where $\mathbf{p}$ is the left eigenvector of Π corresponding to the (unique) unit eigenvalue. The state probability vector $\mathbf{q}$ is obtained from time series data at a condition where one or more influencing agents are present. The partitioning of time series data and the state machine structure should be the same in both cases but the respective state transition matrices could be different.

Pattern changes take place in the global opinion condition due to variations in the number of influences. These variations are a result of passive or active propaganda, word of mouth persuasion, etc. The probability distributions obtained by analyzing the opinion data for different influenced conditions serve as low-dimensional feature vectors which are unique to that particular condition of the society.

Behavioral pattern changes may take place in dynamical systems due to incorporation of external influences such as fake reviewers, political party canvassers, etc. The pattern changes are quantified as deviations from the nominal pattern (i.e. the probability distribution at the nominal condition). The resulting anomalies (i.e., deviations of the evolving patterns from the nominal pattern) are characterized by a scalar-valued function called *Influence Measure* μ. The influence measures at respective influence conditions $\{f_1, f_2, \ldots, f_k, \cdots\}$ are obtained as:

$$\mu_k \equiv d\left(\mathbf{p}^k, \mathbf{p}^0\right) \tag{B.5}$$

where the $d(\bullet, \bullet)$ is an appropriately defined distance function.

B.6 Data Analysis - Part I

In our experiment, to assess the resolving capability of SDF, we have studied the effect of low numbers of influences in the society. As a preliminary study, $1, 2, 3, 5$ and 10 person groups of external agents have been added to a total networked group of 100. This group randomly forms links with people in the network; the probability of forming a link is 0.25. At a certain time, this influence group is activated all at once with all external agents initialized to state R. Themselves being in state R and broadcasting a high reward value for R, this group indirectly starts convincing its first order neighbors to increase their personal estimate of the payoff $\chi(R)$ from state R. Furthermore, in this particular setting, probability of success of the revolution $P(s)$ being linked to the percentage of the population in R, individuals develop a higher estimate of $P(s)$ as a result of being associated with these influence group members. Even though the effect of adding influences is easily understandable in principle, for a particular case, the time series data denoting the opinion dynamics is remarkably noisy and characterized by rapid unstable fluctuations in the society. It is evident that the fluctuation statistics is a function of the number of extremist nodes present in the network.

Time series data for both nominal and influenced conditions have been analyzed using symbolic dynamic filtering (SDF) method for generation of statistical patterns of evolving trends. For symbol sequence generation, maximum entropy partitioning has been used. The

symbol alphabet size for partitioning is chosen to be $|\Sigma| = 6$ and the depth $D = 1$ for construction of the finite state machine. Hence, the number of states in the finite state machine is $n = |\Sigma|^D = 6$.

Figure B.4 shows the results of SDF-based analysis of the time series data sets. The top row of Fig. B.4 shows the time trace of fluctuations in the percentage of government followers for four different influenced conditions of the society: a) uninfluenced i.e. size of influence group $|Inf| = 0$, b) $|Inf| = 1$, c) $|Inf| = 3$, d) $|Inf| = 5$, and e) $|Inf| = 10$. In order to generate statistically stationary data, the test data is generated for sufficiently large number of decision epochs; sufficiency of data length is governed by a stopping rule and has been discussed in [111]. The bottom row of Fig. B.4 shows the histograms of probability distribution that are generated from the SDF analysis of corresponding opinion data sets. The histograms represent the statistical patterns at the above four different influence conditions. As more and more influence nodes are active in the network, the statistical patterns gradually evolve from the nominal pattern of uniform distribution as seen in plots Fig. B.4a-e.

Figure B.5 shows the profile of influence measure with gradual increment in the number of influences. Influence measure is quantitatively expressed as a (scalar) distance (e.g. the Euclidean norm) between the statistical patterns (i.e. probability distributions) corresponding to an influenced condition and the nominal condition that are generated using

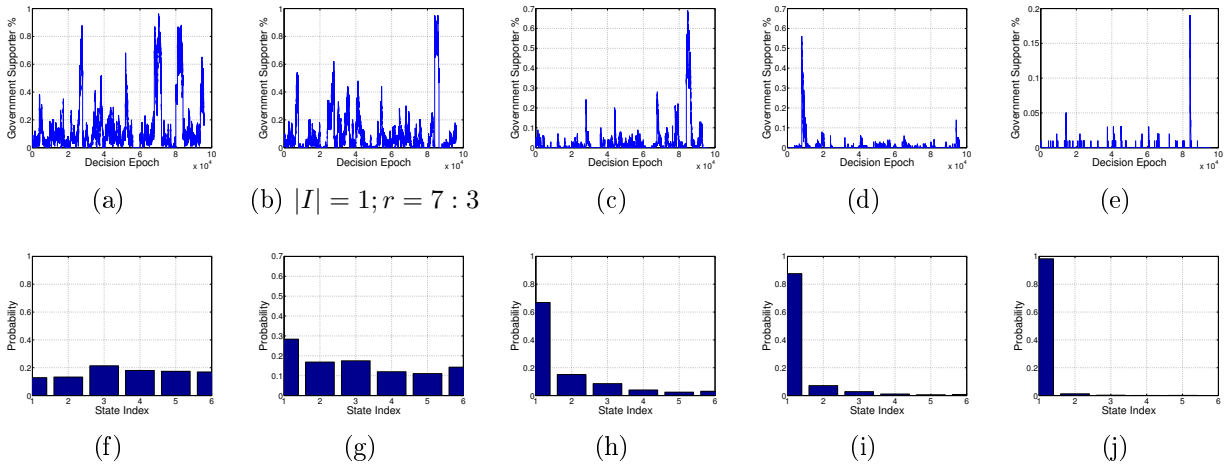

Figure B.4: Evolution of statistical patterns with increasing influence group size

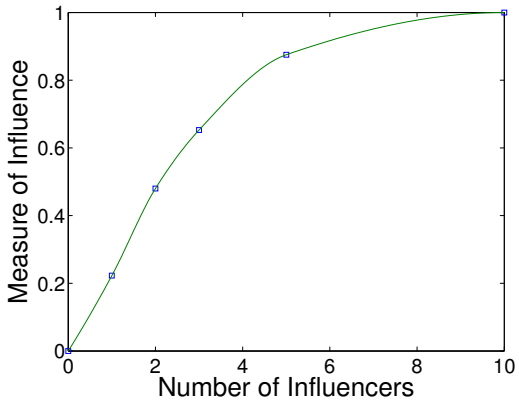

Figure B.5: Measure of the amount of Influence estimated by SDF

SDF of global opinion data. The distance function is chosen to be the Euclidean norm of the difference between the two patterns (see Eqn. B.5). A non-zero value of anomaly measure indicates deviation from the nominal condition and therefore provides a warning of anomalous behavior trends. It is seen in Fig. B.5 that the anomaly measure profile grows as the size of the influence group increases, but more interestingly, even small influence ($|Inf| = 1$ or $|Inf| = 2$) can be observed in the presence of random fluctuations using this technique.

B.7 Data Analysis - Part II

In the last section, we presented results demonstrating the effectiveness of SDF in distinguishing the effect of small influencing groups in large population opinion dynamics. In this section, we report the use of the SDF generated patterns in distinguishing the effect of influencing groups from the other source of perturbation in the global opinion - government policies. In this series of numerical simulations, we modify the ratio of popular vs. unpopular policies ($g/\tilde{g}$) imposed by the government and generate the global opinion dynamics data for each case. The influence group size for all these cases are kept constant at $|Inf| = 3$.

The patterns generated for all 11 cases are used to train and test a two-layer feed-forward neural network with sigmoid hidden and output neurons. Such networks can classify vectors arbitrarily well given enough neurons in its hidden layer. The network was trained with scaled conjugate gradient back- propagation [116]. Once trained, the performance of the

neural net is evaluated on a total of 22 separate data sets, 2 sets for each class as defined in Table B.3.

Table B.3: Membership indicators for the 11 classes

Classes	1	2	3	4	5	6	7	8	9	10	11
$g/\tilde{g}$	1/9	3/7	5/5	7/3	9/1	5/5	5/5	5/5	5/5	5/5	5/5
$\|Inf\|$	3	3	3	3	3	0	1	2	3	5	10

Figure B.6 demonstrates the resolving capability of the SDF generated patterns in the form of a confusion matrix. The algorithm shows an overall success rate of 81.8%, but even when the data is misclassified, the estimated class is not wrong by much, in fact adjacent to the true class in both cases. Specifically, the 2 datasets belonging to Class 3 are misclassified as Class 2 and Class 4, respectively. In other words, the government policy ratio $g/\tilde{g}$ is estimated to be 3/7 and 7/3 instead of the correct value 5/5. The only other misclassification occurred when the number of influences is wrongly estimated as 3 in one case and 10 in another, while the true value was $|Inf| = 5$.

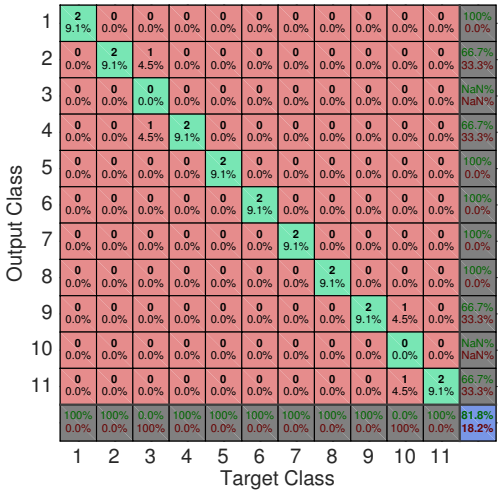

Figure B.6: Confusion matrix demonstrating the classification efficiency of the SDF generated patterns processed by a two-layer feed-forward neural network

B.8 Chapter Summary and Future Work

In this chapter, some of the critical and practical issues regarding the problem of monitoring opinion trends in societies have been discussed, and a data-driven algorithm has been investigated. The two primary features of this proposed concept are: (i) an MDP architecture for simulating cognitive processes, (ii) local interaction by exchange of reward information between nodes connected through an extended BA topology, and (iii) a stochastic signal processing approach for generating patterns from global information.

The reported work is a step toward building a real-time data-driven tool for estimation of parametric conditions in nonlinear dynamical systems. Spread of influence and "recruiting" by extremist groups through social networks has become an important political issue in recent years. This study is a step in the direction of building tools to preempt and intervene such efforts. Further theoretical, computational, and experimental work is necessary before the SDF-based trend detection tool can be considered for incorporation into decision guidance tools. For example, an important issue in trend detection is the unavailability of data in a convenient form. Often, the current state is not always directly observable, rather a set of observations about the behavior may be available which provides an estimate of what state the system is in. For example, even though an individual may not publicly proclaim allegiance to a party, Twitter updates from that person may contain clues to his political inclinations. The observations are probabilistic, so the observation model also needs to be specified. These issues are currently under investigation using a Partially Observable MDP.

Vita

Farshad Salimi Naneh Karan was born in January of 1987 in Ardebil, Ardebil, Iran. He attended the National Organization for Development of Exceptional Talents (NODET) for his high school. Then, he got admitted to the undergraduate program in the Urmia University (Urmia, West Azerbaijan, Iran) in Mechanical Engineering in August of 2005. During his studies at Urmia University, he worked for different faculty members including Dr. Rasoul Shabani. Next, he chose Khadje Nasir Toosi University of Technology (KNTU) to continue his education in a Master's program. At KNTU, he conducted research under Dr. Shahram Azadi's supervision. His dissertation title was "Active Control of Hydraulic Engine Mounts in Passenger Cars" for which he mathematically modelled and also simulated an engine mounted on three actively controlled hydraulic engine mounts.

In December 2013, he moved to Knoxville, Tennessee to start his PhD program (starting January 2014) in Mechanical Engineering under Dr. Subhadeep Chakraborty's supervision. During his studies at the University of Tennessee, he worked on different interesting projects related to multi-body complex systems. His PhD dissertation focuses on opinion dynamics and control in networked societies; his dissertation title is "Analysis and Control of Socio-Cultural Opinion Evolution in Complex Social Systems". His line of research has resulted in several journal and conference publications. Besides research, Mr. Karan has had different volunteer roles such as science judge for the Tennessee Science Bowl, or judge for the Tennessee Science Olympiad. His hobbies include going to the gym, hicking in the Smokey Mountains, playing Backgammon, Pool and Snooker.